

PH.D. DISSERTATION DEFENSE ON

# First Principles Investigations of Electrolyte Materials in All-Solid-State Batteries

---

**Yan Li**

*In partial fulfillment of the requirements for the award of the degree of*

**DOCTOR OF PHILOSOPHY IN PHYSICS**

### **Committee Members**

Natalie Holzwarth, Ph.D., Advisor

Abdessadek Lachgar, Ph.D., Chair

William C. Kerr, Ph.D.

Oana Jurchescu, Ph.D.

Timo Thonhauser, Ph.D.

October 21, 2021

- **Research background: General motivation and theoretical tools**
- **Finished/ongoing projects: Inputs and outcomes**

## **$\text{Na}_4\text{P}_2\text{S}_6$ , $\text{Li}_4\text{P}_2\text{S}_6$ , and possible alloy**

Yan Li, Zachary D. Hood, and N. A. W. Holzwarth  
**Phys. Rev. Mater. 4, 045406 (2020)**

## **Phonon dispersion**

Yan Li, W. C. Kerr, and N. A. W. Holzwarth  
**J. Condens. Matter Phys. 32, 055402 (2020)**

## **$\text{Li}_3\text{BO}_3$ and $\text{Li}_3\text{BN}_2$ (I & II)**

Yan Li, Zachary D. Hood, and N. A. W. Holzwarth  
**Phys. Rev. Mater. 5, 085402 & 085403 (2021)**

## **$\text{Li}_{4+x}\text{B}_7\text{O}_{12+x/2}\text{Cl}$ ( $x = 0, 1$ ) and related**

**$\text{Li}_{7.5}\text{B}_{10}\text{O}_{18}\text{X}_{1.5}$  ( $\text{X} = \text{Cl, Br, and I}$ )**

- ❑ **Research background: General motivation and theoretical tools**
- ❑ **Finished/ongoing projects: Inputs and outcomes**

## **$\text{Na}_4\text{P}_2\text{S}_6$ , $\text{Li}_4\text{P}_2\text{S}_6$ , and possible alloy**

Yan Li, Zachary D. Hood, and N. A. W. Holzwarth  
Phys. Rev. Mater. 4, 045406 (2020)

## **Phonon dispersion**

Yan Li, W. C. Kerr, and N. A. W. Holzwarth  
J. Condens. Matter Phys. 32, 055402 (2020)

## **$\text{Li}_3\text{BO}_3$ and $\text{Li}_3\text{BN}_2$ (I & II)**

Yan Li, Zachary D. Hood, and N. A. W. Holzwarth  
Phys. Rev. Mater. 5, 085402 & 085403 (2021)

## **$\text{Li}_{4+x}\text{B}_7\text{O}_{12+x/2}\text{Cl}$ ( $x = 0, 1$ ) and related**

**$\text{Li}_{7.5}\text{B}_{10}\text{O}_{18}\text{X}_{1.5}$  ( $\text{X} = \text{Cl}, \text{Br}, \text{and I}$ )**

## The Nobel Prize in Chemistry 2019

rewards the development of lithium ion battery

### ❑ Nobel prize recognition

*"The Lithium ion batteries have laid the foundation of a wireless, fossil fuel-free society and are of the greatest benefit to humankind"* (words of the Nobel committee)

### ❑ Continuous challenges

- More demanding applications
- **New materials and recipes for battery components**
- Balance of capacity, cost, size, and weight



**John B. Goodenough**



**M. Stanley Whittingham**



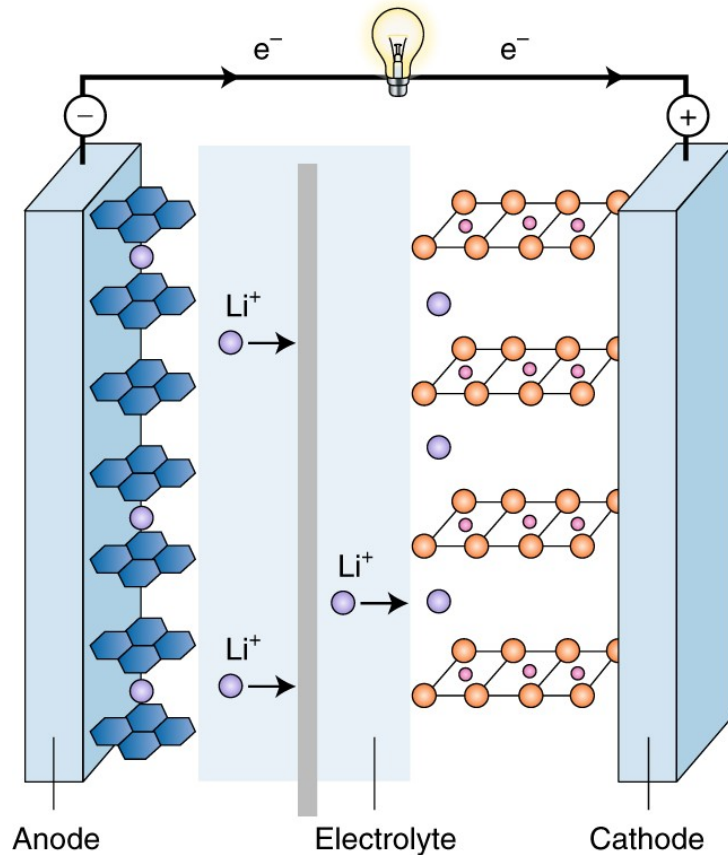
**Akira Yoshino**

Whittingham: developed the first functional lithium battery in the early 1970s

Goodenough: doubled the battery's potential in the following decade

Yoshino: eliminated pure lithium from the battery, making it much safer to use

Photo from <https://www.nobelprize.org>



## Discharge mode

### Role of the electrolyte:

Allow for the transport of Li ions, excluding electrons from the battery and forcing them through the external circuit.

### Why solid-state electrolyte?

- Superior safety due to the absence of flammable liquid content
- Excellent physical and chemical stability
- Compatible and stable with Li metal anodes
- Acceptable ionic conductivity

Figure used with permission from J.B. Goodenough. *Nat Electron* **1**, 204 (2018). Copyright @ 2018 Springer Nature

## **For known and theoretically predicted Li or Na ion solid electrolyte materials (electronically insulating & operate in ground electronic states)**

### ❑ Structures and stabilities

- Construct models for various forms of ideal crystals
- Simulate the static and vibrational properties
- Identify stable and metastable configurations

### ❑ Electrolyte properties

- Mechanisms: vacancy migration, interstitial migration
- Quantitative analysis: defect formation energy, migration energy barrier, ionic conductivity
- Model ideal electrolyte interfaces with anodes

Exact time-independent Schrödinger equation for a system of  $N$  electrons with coordinates  $\{\mathbf{r}_i\}$  ( $i = 1, 2, \dots, N$ ) and  $M$  nuclei with coordinates  $\{\mathbf{R}_I\}$  ( $I = 1, 2, \dots, M$ )

$$i \frac{\partial}{\partial t} \Psi(\{\mathbf{r}_i\}, \{\mathbf{R}_I\}) = \hat{H}_{\text{tot}} \Psi(\{\mathbf{r}_i\}, \{\mathbf{R}_I\})$$

where  $\hat{H}_{\text{tot}} = - \sum_I \frac{\hbar^2}{2M_I} \nabla_I^2 + \frac{e^2}{2} \sum_{I \neq J} \frac{Z_I Z_J}{|\mathbf{R}_I - \mathbf{R}_J|}$  
 $\hat{T}_N(\mathbf{R}) + \hat{V}_{NN}(\mathbf{R})$   
Nuclear

$- \frac{\hbar^2}{2m} \sum_i \nabla_i^2 + \frac{e^2}{2} \sum_{i \neq j} \frac{1}{|\mathbf{r}_i - \mathbf{r}_j|}$  
 $\hat{T}_e(\mathbf{r}) + \hat{V}_{ee}(\mathbf{r})$   
Electronic

$- \sum_{i,I} \frac{Z_I e^2}{|\mathbf{r}_i - \mathbf{R}_I|}$  
 $\hat{V}_{eN}(\mathbf{r}, \mathbf{R})$   
Mixed

First principles methods: a series of well-established physical approximations



Born-Oppenheimer approximation ( $M_I \gg m$ )

$$\Psi(\{\mathbf{r}_i\}, \{\mathbf{R}_I\}) = \Psi_{\mathbf{R}}(\{\mathbf{r}_i\})\chi(\{\mathbf{R}_I\})$$

↓  
Electron part: treated  
quantum mechanically

↓  
Nuclei part: treated classically

Electronic Schrödinger equation:

$$\hat{H}_{\mathbf{R}}\Psi_{\mathbf{R}}(\{\mathbf{r}_i\}) = E_{\mathbf{R}}\Psi_{\mathbf{R}}(\{\mathbf{r}_i\})$$

$$\hat{H}_{\mathbf{R}} = -\frac{\hbar^2}{2m} \sum_i \nabla_i^2 - \sum_{i,I} \frac{Z_I e^2}{|\mathbf{r}_i - \mathbf{R}_I|} + \frac{e^2}{2} \sum_{i \neq j} \frac{1}{|\mathbf{r}_i - \mathbf{r}_j|}$$



Hohenberg-Kohn theorem:

$$E_{\mathbf{R}} = F[\rho(\mathbf{r})] \quad \text{Reduction of dimensionality (3N} \rightarrow \text{3)!}$$

Kohn-Sham equations:

$$E_{\mathbf{R}} = F[\rho(\mathbf{r})] = E_{\mathbf{T}} + E_{\text{ext}} + E_{\mathbf{H}} + E_{\text{xc}} \quad \text{unknown}$$

$$\left. \frac{\delta F[\rho]}{\delta \rho} \right|_{\rho_0} = 0 \quad \text{obtained from independent electrons approximation}$$

Hohenberg and Kohn, *Phys. Rev.* **136**, B864 (1964)

Kohn and Sham, *Phys. Rev.* **140**, A1133 (1965)

$$\left[ -\frac{\hbar^2}{2m} \nabla^2 + V_{\text{ext}}(\mathbf{r}) + V_{\mathbf{H}}(\mathbf{r}) + V_{\text{xc}}(\mathbf{r}) \right] \psi_i(\mathbf{r}) = \varepsilon_i \psi_i(\mathbf{r})$$

$$V_{\text{ext}}(\mathbf{r}) = -\sum_I \frac{Z_I e^2}{|\mathbf{r} - \mathbf{R}_I|}$$

$$\nabla^2 V_{\mathbf{H}}(\mathbf{r}) = -4\pi e^2 \rho(\mathbf{r})$$

$$V_{\text{xc}}(\mathbf{r}) = \left. \frac{\delta E_{\text{xc}}[\rho]}{\delta \rho} \right|_{\rho(\mathbf{r})}$$

$$\rho(\mathbf{r}) = \sum_i |\psi_i(\mathbf{r})|^2$$

LDA: Perdew and Wang, *Phys. Rev. B* **45**, 13244 (1992)

GGA: Perdew et al., *Phys. Rev. L* **77**, 3865 (1996)

...

To solve DFT equations: Planewave representations; Pseudopotential formulations

At equilibrium:

$$\mathbf{F}_I = -\frac{\partial U(\{\mathbf{R}_I\})}{\partial \mathbf{R}_I} = 0$$

- Optimized structural parameters
- Static lattice energy:  $U_{\text{SL}} = \min U(\{\mathbf{R}_I\})$
- Kohn-Sham orbitals and energies
- Interstitial-vacancy pair formation energy:  $E_f = U_{\text{SL}}^{\text{defect}} - U_{\text{SL}}^{\text{perfect}}$
- Ionic migration energies:  $E_m$

Near equilibrium (Harmonic approximation):

$$U(\{\mathbf{u}_s(l)\})_{\text{harm}} = U(\{\mathbf{u}_s(l)\} = 0) + \frac{1}{2} \sum_{ls\alpha} \sum_{mt\beta} C_{st}^{\alpha\beta}(l, m) u_{s\alpha}(l) u_{t\beta}(m) \quad \text{where} \quad C_{st}^{\alpha\beta}(l, m) = \left. \frac{\partial^2 U}{\partial u_s^\alpha(l) \partial u_t^\beta(m)} \right|_0$$

$$M_s(\omega^\nu)^2 u_{s\alpha}^\nu(\mathbf{q}) = \sum_{t\beta} \tilde{C}_{st}^{\alpha\beta}(\mathbf{q}) u_{t\beta}^\nu(\mathbf{q})$$

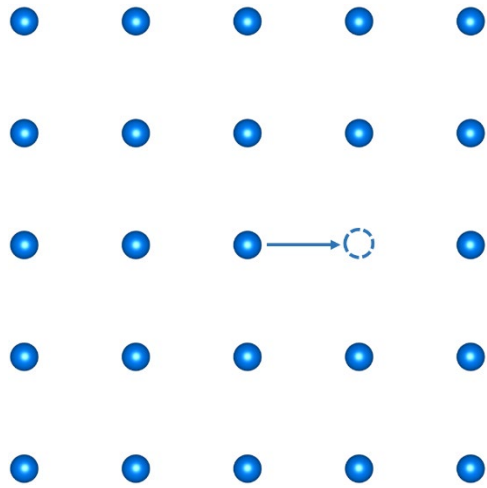
First principles phonon calculations:  
Density functional perturbation theory (DFPT)

- Phonon frequencies and eigenvectors at any wavevector
- Phonon dispersions:  $\omega^\nu \sim \mathbf{q}$  (by specifying a path of high symmetry points)
- Phonon density of states (PDOS):  $g(\omega) = \frac{V}{(2\pi)^3} \int d^3q \sum_{\nu=1}^{3N} \delta(\omega - \omega^\nu(\mathbf{q}))$
- Thermodynamic properties such as the vibrational energy:  $F_{\text{vib}}(T) = k_B T \int_0^\infty d\omega \ln \left( 2 \sinh \left( \frac{\hbar\omega}{2k_B T} \right) \right) g(\omega)$

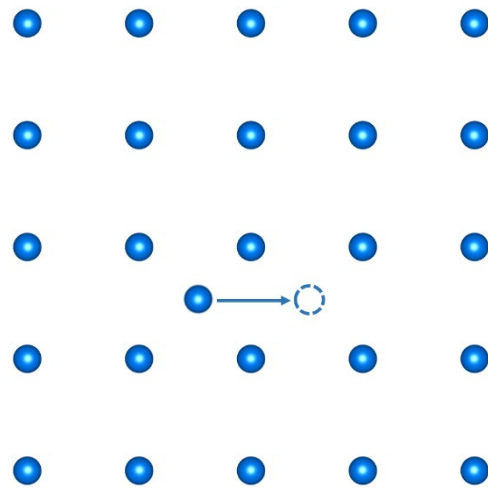
## Combined the DFT and DFPT energies

- The Helmholtz free energy:  $F(T) = F_{SL}(T) + F_{\text{vib}}(T) \approx U_{SL} + F_{\text{vib}}(T)$  Ordered system with constant volume

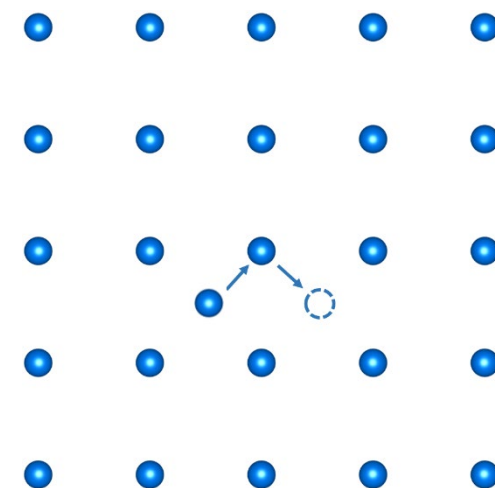




**Vacancy mechanism**



**Interstitial mechanism**



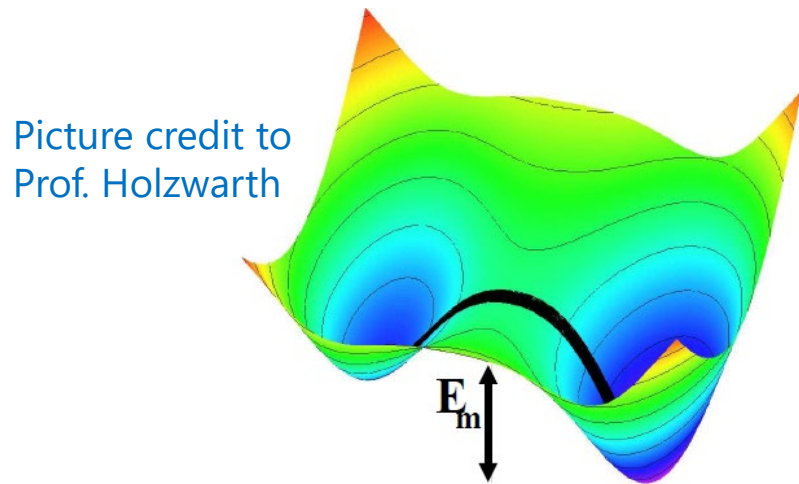
**Interstitialcy (kick-out) mechanism**

## High ionic diffusivity in solid conductors requires:

- Rigid framework and high concentration of mobile ions
- Sufficient number of available sites for the mobile ions to occupy
- Continuous channels with low migration barrier energies

## Nudged Elastic Band (NEB)

Requires a specific migration pathway as input  
Simple but limited



For perfect crystals:  $E_a^{\text{NEB}} = E_m^{\text{NEB}} + \frac{1}{2} E_f$

Arrhenius relation:  $\sigma(T) = \frac{A}{T} e^{-E_a^{\text{NEB}}/k_B T}$

## Ab Initio Molecular Dynamics (AIMD)

Statistical averaging over all diffusional events  
Large supercell & long simulation time

$$\text{MSD}(t, T) \equiv \frac{1}{N_a} \left\langle \sum_{i=1}^{N_a} |\mathbf{R}_i(t) - \mathbf{R}_i(0)|^2 \right\rangle$$

$$D_{\text{tr}}(T) = \frac{1}{6} \lim_{t \rightarrow \infty} \frac{1}{(t - t_{\text{eq}})} \text{MSD}(t - t_{\text{eq}}, T)$$

$$D_{\text{tr}}(T) = D_0 e^{-E_a^{\text{MD}}/k_B T}$$

Nernst-Einstein relation:

$$\sigma(T) = \frac{N}{V} \frac{q^2}{k_B T} D_{\text{all}} = \frac{1}{H_r} \frac{N}{V} \frac{q^2}{k_B T} D_{\text{tr}}$$

Haven ratio:  $H_r = D_{\text{tr}}/D_{\text{all}}$

measures effects of correlated motions

- ❑ Density Functional Theory (DFT) and Density Functional Perturbation Theory (DFPT) with the modified Perdew-Burke-Ernzerhof generalized gradient approximation (**PBEsol GGA**)  
*Perdew et al., PRL 100, 136406 (2008)*
- ❑ The projector augmented wave (PAW) formalism with atomic datasets generated by **ATOMPAW**  
code available at <http://pwpaw.wfu.edu>
- ❑ First principles electronic-structure calculations and materials modeling

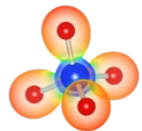


<https://www.quantum-espresso.org/>



<https://www.abinit.org/>

- ❑ Structural visualization, symmetry identification, X-ray patterns



<https://jp-minerals.org/vesta/>



<http://www.xcrysden.org/>

**FINDSYM**

Version 7.1.2, June 2021

<https://stokes.byu.edu/iso/findsym.php>



<https://www.ccdc.cam.ac.uk/solutions/csd-core/components/mercury/>

- Research background: General motivation and theoretical tools
- **Finished/ongoing projects: Inputs and outcomes**

## $\text{Na}_4\text{P}_2\text{S}_6$ , $\text{Li}_4\text{P}_2\text{S}_6$ , and possible alloy

Yan Li, Zachary D. Hood, and N. A. W. Holzwarth  
Phys. Rev. Mater. 4, 045406 (2020)

## Phonon dispersion

Yan Li, W. C. Kerr, and N. A. W. Holzwarth  
J. Condens. Matter Phys. 32, 055402 (2020)

## $\text{Li}_3\text{BO}_3$ and $\text{Li}_3\text{BN}_2$ (I & II)

Yan Li, Zachary D. Hood, and N. A. W. Holzwarth  
Phys. Rev. Mater. 5, 085402 & 085403 (2021)

## $\text{Li}_{4+x}\text{B}_7\text{O}_{12+x/2}\text{Cl}$ ( $x = 0, 1$ ) and related

$\text{Li}_{7.5}\text{B}_{10}\text{O}_{18}\text{X}_{1.5}$  ( $\text{X} = \text{Cl, Br, and I}$ )



□ Research background: General motivation and theoretical tools

□ **Finished/ongoing projects: Inputs and outcomes**

**$\text{Na}_4\text{P}_2\text{S}_6$ ,  $\text{Li}_4\text{P}_2\text{S}_6$ , and possible alloy**

Yan Li, Zachary D. Hood, and N. A. W. Holzwarth

**Phys. Rev. Mater. 4, 045406 (2020)**

**Phonon dispersion**

Yan Li, W. C. Kerr, and N. A. W. Holzwarth

**J. Condens. Matter Phys. 32, 055402 (2020)**

**$\text{Li}_3\text{BO}_3$  and  $\text{Li}_3\text{BN}_2$  (I & II)**

Yan Li, Zachary D. Hood, and N. A. W. Holzwarth

**Phys. Rev. Mater. 5, 085402 & 085403 (2021)**

**$\text{Li}_{4+x}\text{B}_7\text{O}_{12+x/2}\text{Cl}$  ( $x = 0, 1$ ) and related**

**$\text{Li}_{7.5}\text{B}_{10}\text{O}_{18}\text{X}_{1.5}$  ( $\text{X} = \text{Cl, Br, and I}$ )**



- Kuhn et al.<sup>1</sup> observed that  $\text{Na}_4\text{P}_2\text{S}_6$  crystallizes to form monoclinic space group **C2/m (#12)**
- Computations using LDA of Rush et al.<sup>2</sup>: **Kuhn structure is metastable**
- Recent experimental results of Hood et al.<sup>3</sup> also find the **C2/m** structure



**Structural and vibrational spectra simulation using PBEsol functional**

- Using combined approach of NMR and X-ray, the new experimental analysis<sup>4</sup> on  $\text{Li}_4\text{P}_2\text{S}_6$  concludes the structure to be ordered with space group **P321 (#150)**
- Theoretically,  $\text{Na}_4\text{P}_2\text{S}_6$  and  $\text{Li}_4\text{P}_2\text{S}_6$  are chemically and structurally related



**Property similarities (discrepancies) between  $\text{Na}_4\text{P}_2\text{S}_6$  and  $\text{Li}_4\text{P}_2\text{S}_6$**

- Structure and stability of the mixed ions material  $\text{Li}_2\text{Na}_2\text{P}_2\text{S}_6$



**Material prediction**

- Performance of  $\text{Li}_2\text{Na}_2\text{P}_2\text{S}_6$  in comparison with  $\text{Na}_4\text{P}_2\text{S}_6$  as solid electrolytes



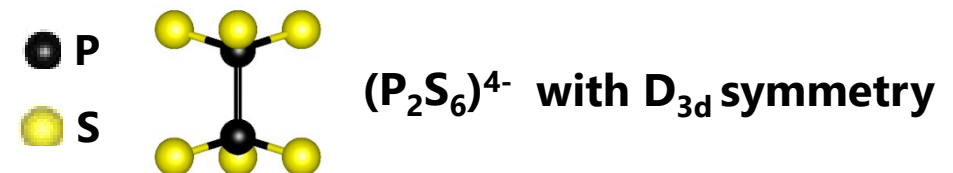
**Conductivity studies**

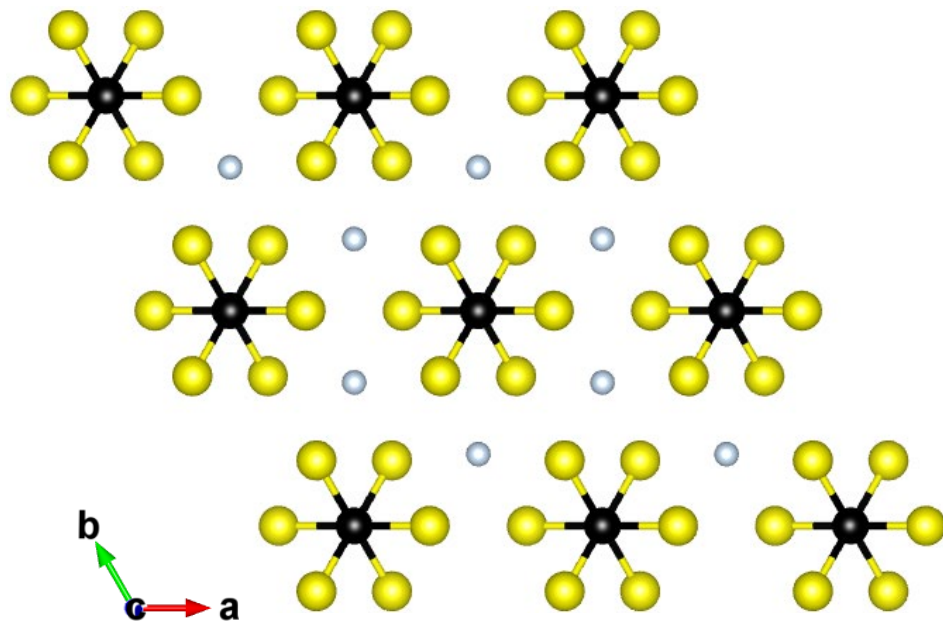
<sup>1</sup>Kuhn et al., *Z. Anorg. Allg. Chem.* **640**, 689-692 (2014)

<sup>2</sup>Rush et al., *Solid State Phys.* **286**, 45-50 (2016)

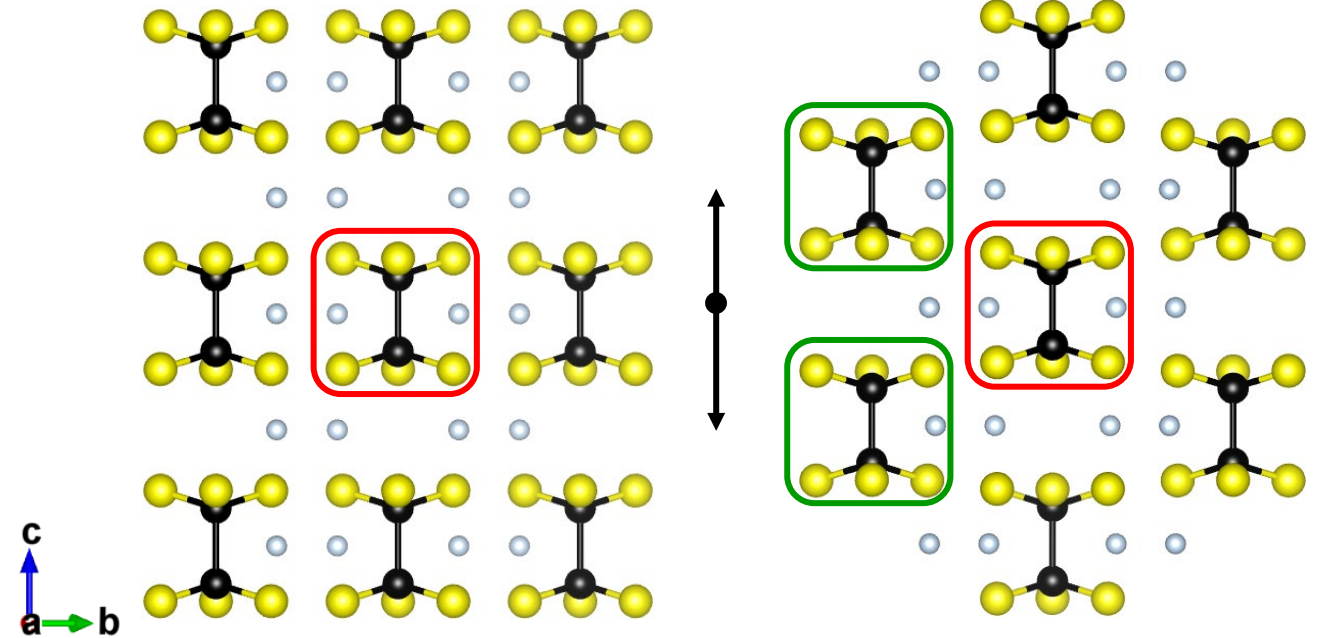
<sup>3</sup>Hood et al., Manuscript in preparation.

<sup>4</sup>Neuberger et al., *Dalton Trans.* **47**, 11691-11695 (2018)





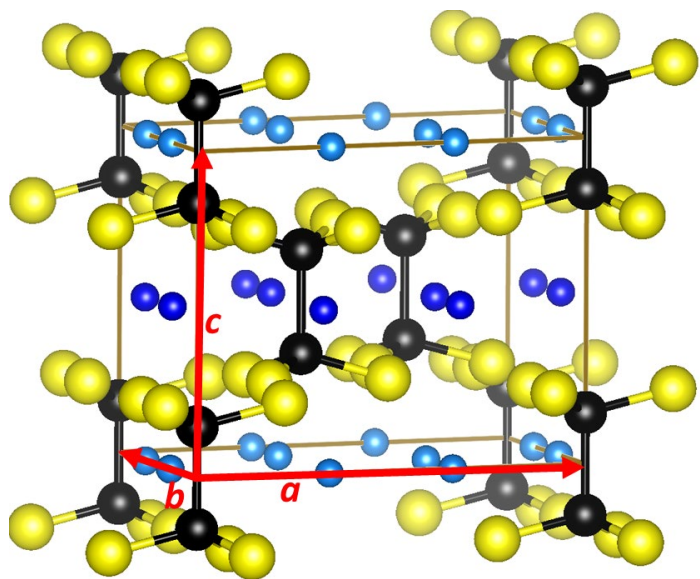
Projection of the basic structure of **Na<sub>4</sub>P<sub>2</sub>S<sub>6</sub>** and **Li<sub>4</sub>P<sub>2</sub>S<sub>6</sub>**



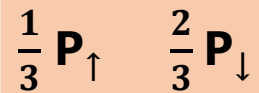
$$\mathbf{P}_{\uparrow} = \pm Z_P \vec{C}$$

$$\mathbf{P}_{\downarrow} = \pm \left( \frac{1}{2} - Z_P \right) \vec{C}$$

Hood et al., *J. Solid State Ionics* **284**, 61 (2016).

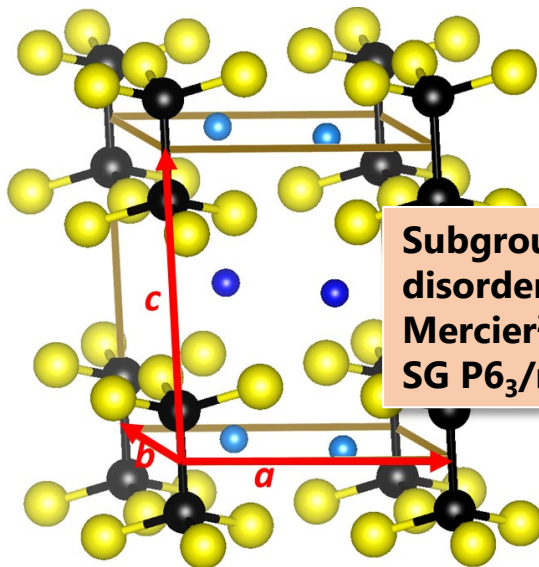


Hexagonal **P321** (#150)<sup>1</sup>  
3 formula units / unit cell



<sup>1</sup>Neuberger et al., *Dalton Trans.* **47**,  
11691-11695 (2018)

Our simulations  $\rightarrow$   **$P\bar{3}m1$**

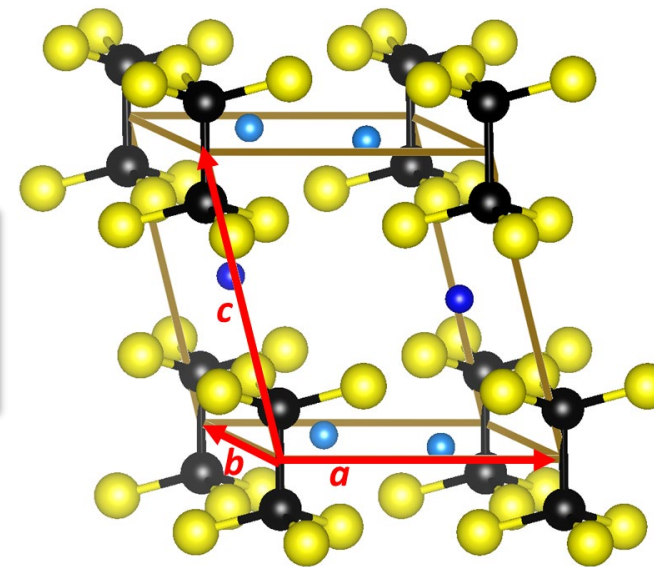


Hexagonal **P31m** (#162)<sup>3</sup>  
1 formula unit / primitive unit cell

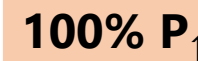


<sup>2</sup>Mercier et al., *J. Solid State Chem.* **43**,  
151-162 (1982)

<sup>3</sup>Hood et al., *J. Solid State Ionics*, **284**, 61  
(2016)



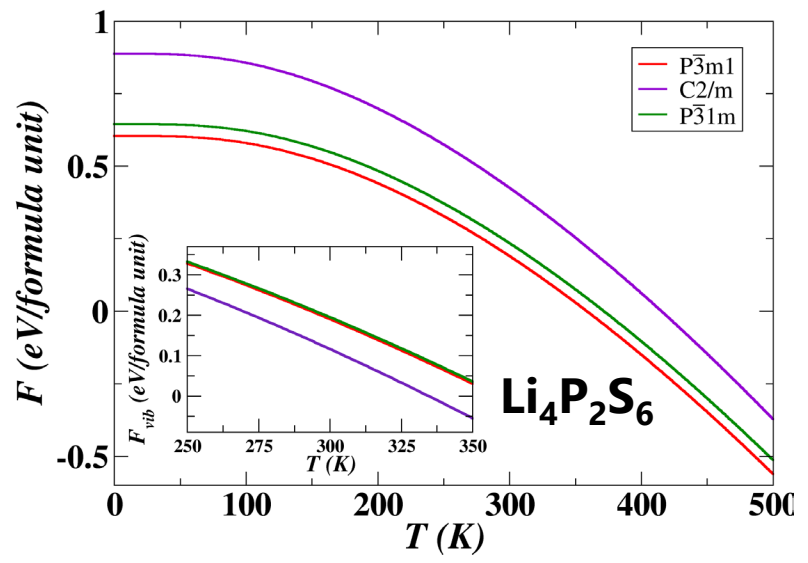
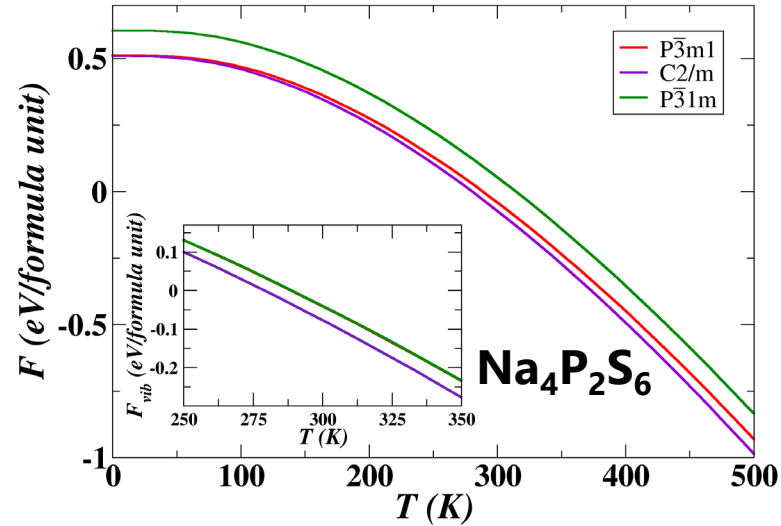
Monoclinic **C2/m** (#12)<sup>4</sup>  
1 formula unit / primitive unit cell



<sup>4</sup>Kuhn et al., *Z. Anorg. Allg. Chem.* **640**,  
689-692 (2014)



$$F(T) = U_{SL} + F_{vib}(T)$$



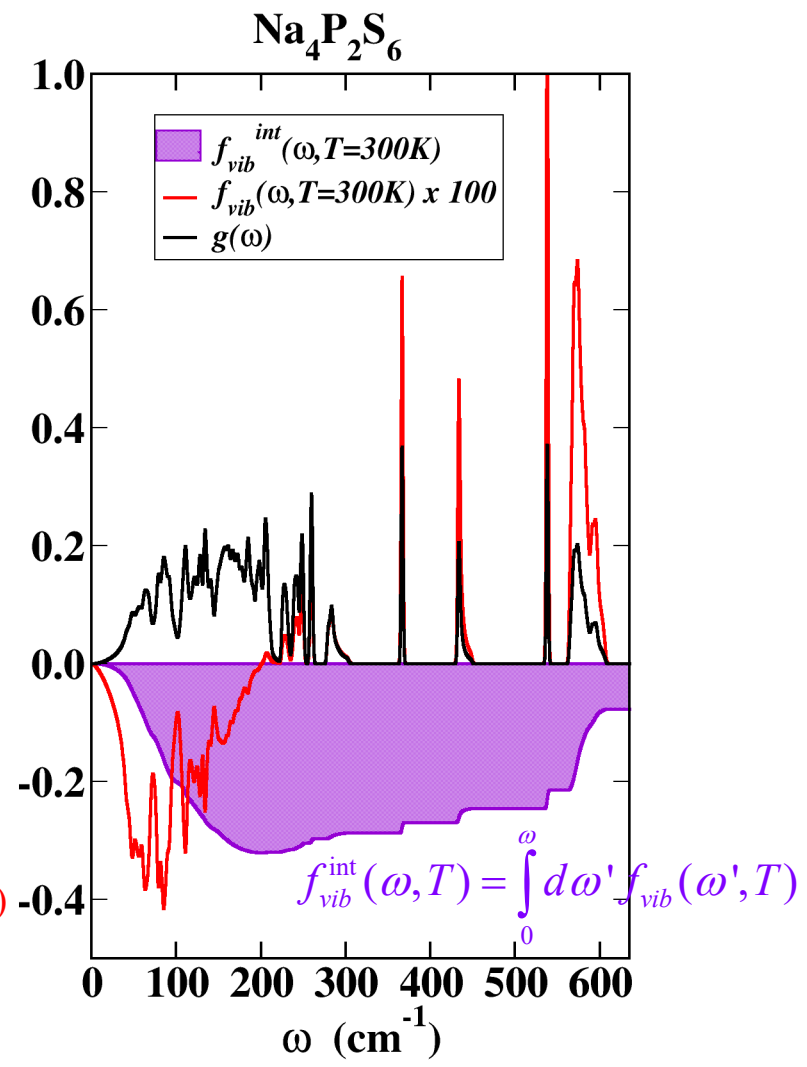
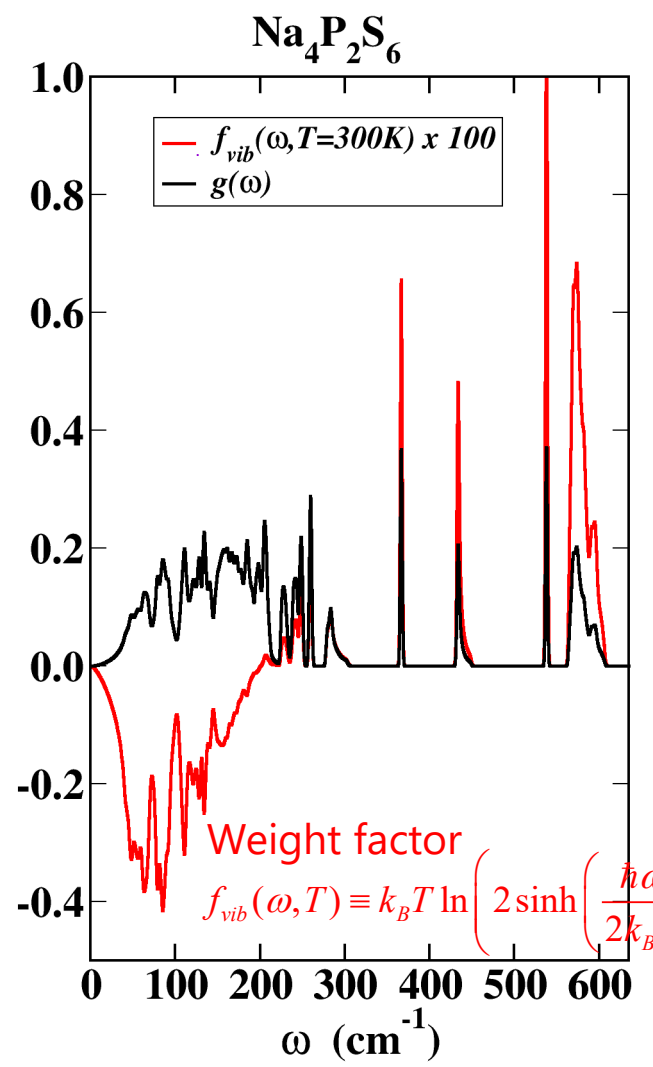
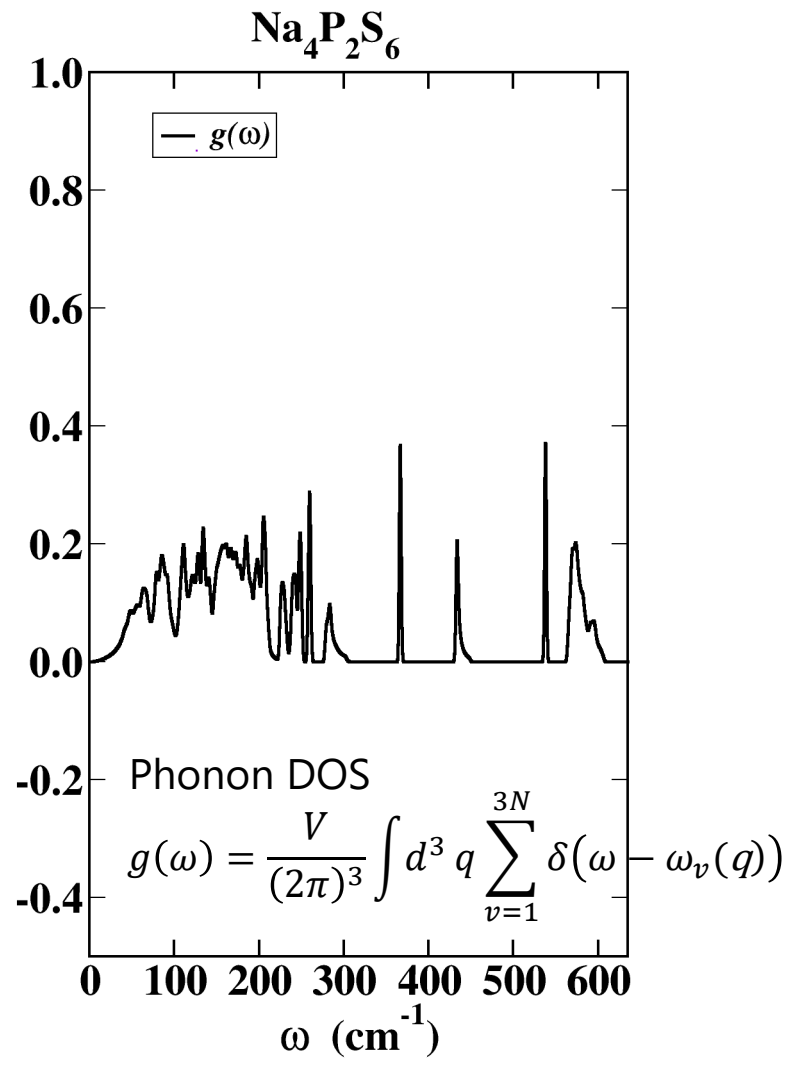
## Summary of simulation energies

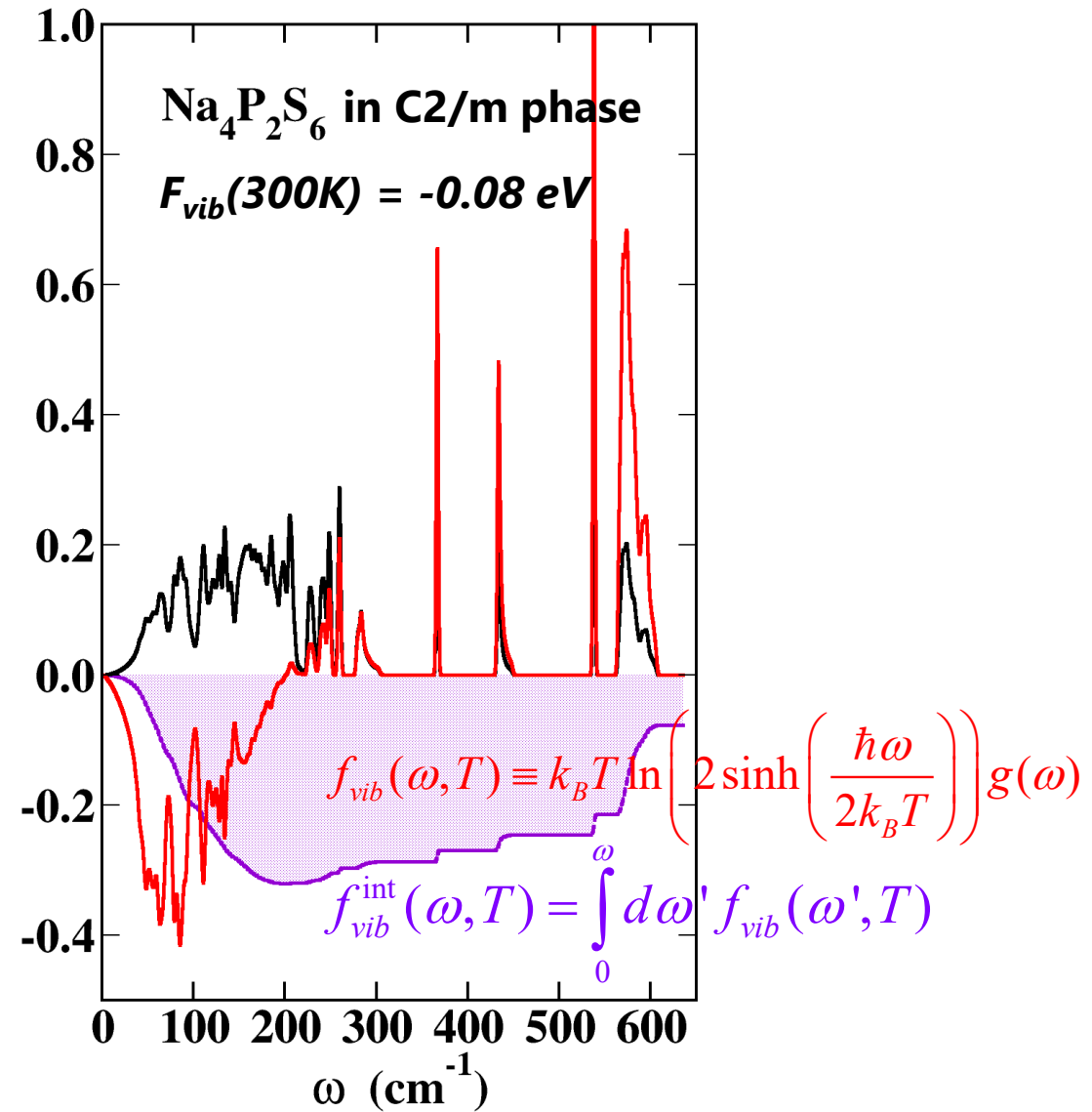
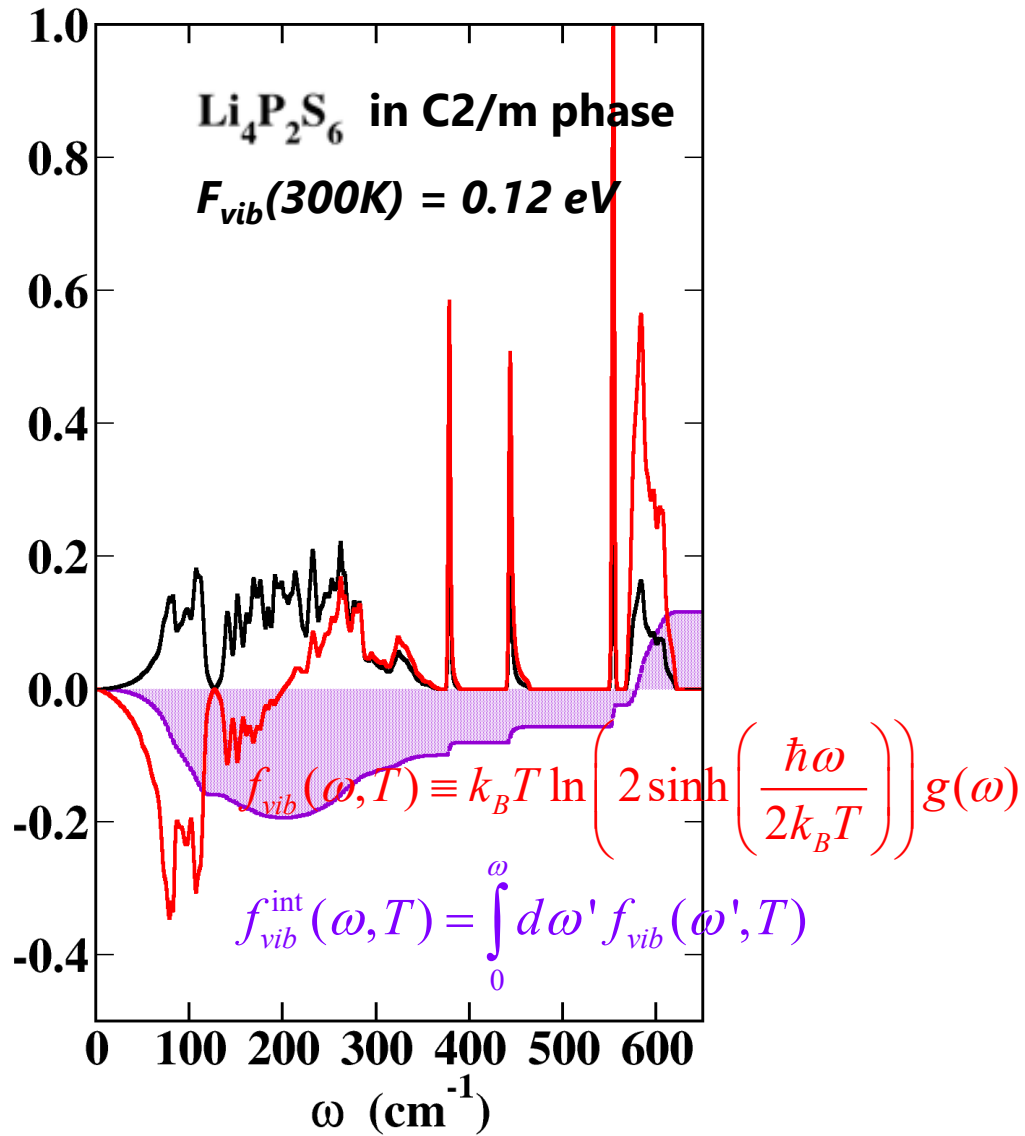
$\text{Na}_4\text{P}_2\text{S}_6$	$\Delta U_{SL}(\text{eV})$	$F_{vib}(300\text{K})(\text{eV})$	$F(300\text{K})(\text{eV})$
Neuberger structure ( $P\bar{3}m1$ )	0.00	-0.04	-0.04
Kuhn structure ( $C2/m$ )	0.00	-0.08	-0.08
Simple hex structure ( $P\bar{3}1m$ )	0.09	-0.04	0.05

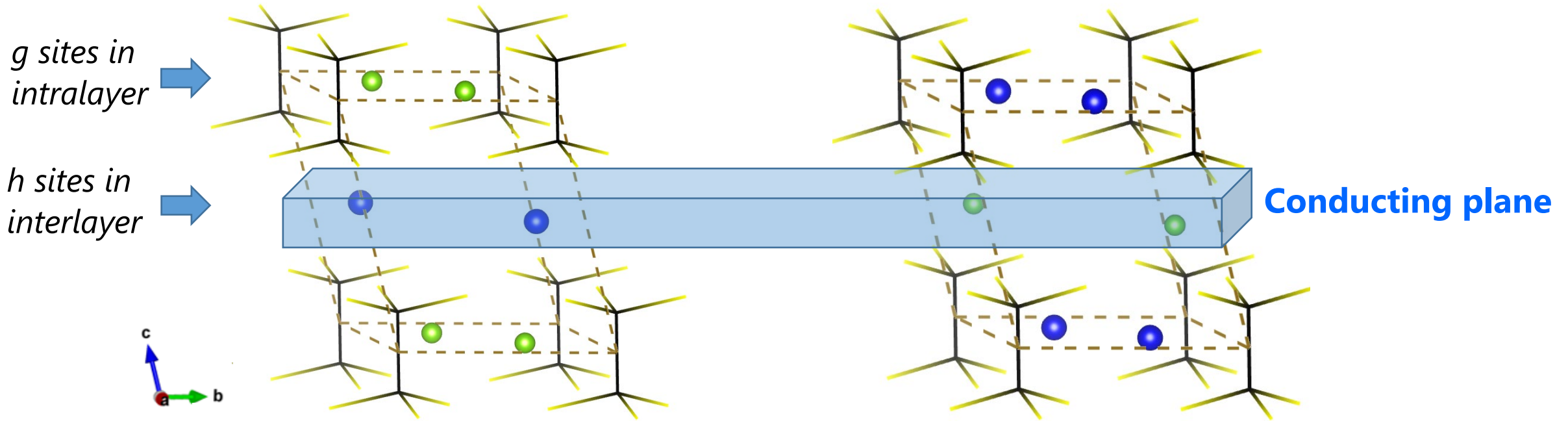
$\text{Li}_4\text{P}_2\text{S}_6$	$\Delta U_{SL}(\text{eV})$	$F_{vib}(300\text{K})(\text{eV})$	$F(300\text{K})(\text{eV})$
Neuberger structure ( $P\bar{3}m1$ )	0.00	0.19	0.19
Kuhn structure ( $C2/m$ )	0.31	0.12	0.43
Simple hex structure ( $P\bar{3}1m$ )	0.04	0.20	0.24

\*Energies given in units of eV/formula unit with zero set at the static lattice energy for the Neuberger structure.





Replace the (a) *g*-type or (b) *h*-type **Na** ions in the monoclinic  $\text{Na}_4\text{P}_2\text{S}_6$  with **Li** ions

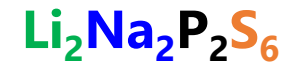


Monoclinic C2/m

$a = b = 6.18 \text{ \AA}, c = 7.50 \text{ \AA}$

$\alpha = \beta = 97.77^\circ, \gamma = 119.21^\circ$

$U_{\text{SL}} = -0.16 \text{ eV/FU}$  ✓



Monoclinic C2/m

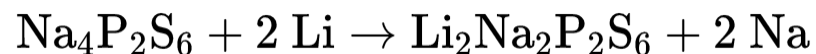
$a = b = 6.46 \text{ \AA}, c = 7.01 \text{ \AA}$

$\alpha = \beta = 97.88^\circ, \gamma = 118.43^\circ$

$U_{\text{SL}} = 0.00 \text{ eV/FU}$



## Possible reaction pathway:

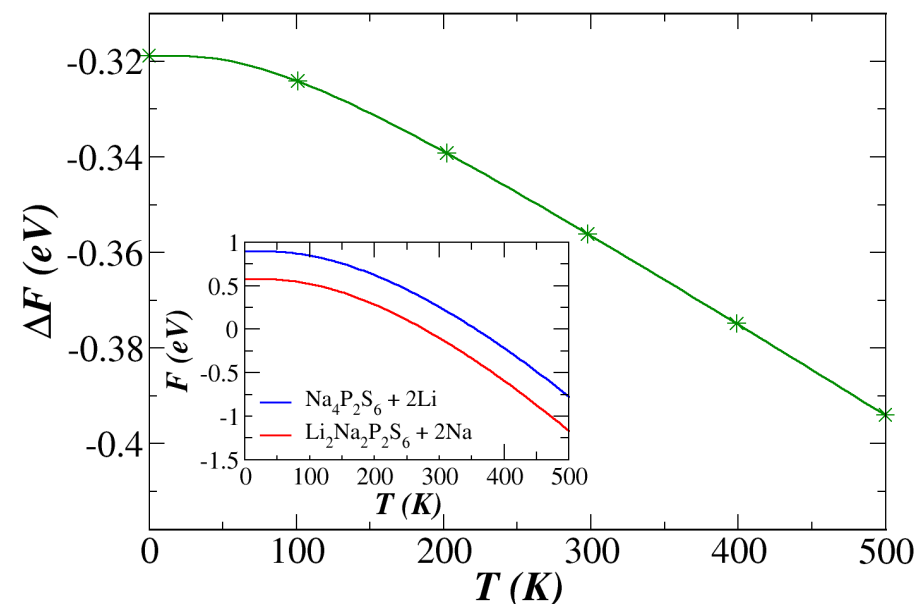


$$\Delta F(T) = \Delta U_{SL} + \Delta F_{vib}(T) + \Delta F_{elec}^{metal}(T)$$

$$\Delta = \Delta^{Products} - \Delta^{Reactants} \quad \text{trivial contribution (10}^{-3} \text{ eV)}$$

## Energy changes at T = 300 K in eV:

$$\begin{aligned} \Delta U_{SL} &= -0.29 \\ \Delta F_{vib} &= -0.06 \end{aligned} \quad \Rightarrow \quad \Delta F = -0.35$$

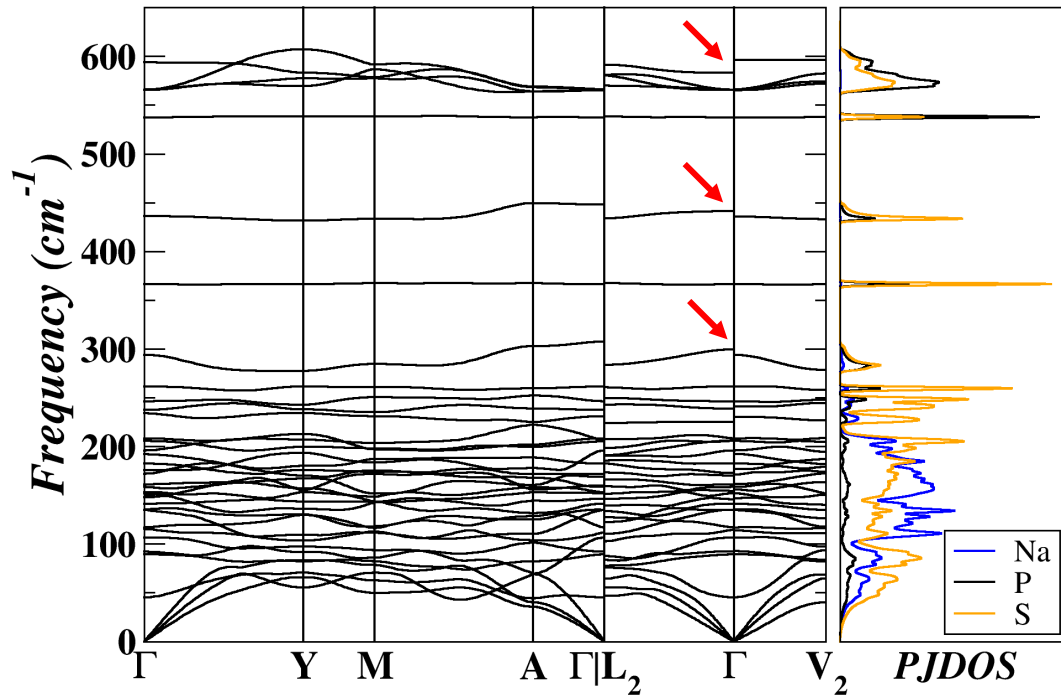


## More possible reaction pathways

No.	Reaction: $R \rightarrow P$	$\Delta U_{SL}$	$\Delta F_{vib}$	$\Delta F$
1	$\text{Na}_4\text{P}_2\text{S}_6 + 2 \text{Li} \rightarrow \text{Li}_2\text{Na}_2\text{P}_2\text{S}_6 + 2 \text{Na}$	-0.29	-0.06	-0.35
2	$2 \text{Li} + 2 \text{Na} + 2 \text{P}^a + 6 \text{S}^b \rightarrow \text{Li}_2\text{Na}_2\text{P}_2\text{S}_6$	-10.62	0.06	-10.56
3	$\frac{1}{2} \text{Na}_4\text{P}_2\text{S}_6 + \frac{1}{2} \text{Li}_4\text{P}_2\text{S}_6 \rightarrow \text{Li}_2\text{Na}_2\text{P}_2\text{S}_6$	0.13	-0.03	0.10
4	$\frac{1}{2} \text{Na}_4\text{P}_2\text{S}_6 + \frac{1}{2} \text{Li}_3\text{PS}_4^c + \frac{1}{12} \text{P}_4\text{S}_4^d \rightarrow \text{Li}_2\text{Na}_2\text{P}_2\text{S}_6$	-0.24	-0.02	-0.26
5	$\frac{1}{2} \text{Na}_4\text{P}_2\text{S}_6 + \frac{1}{2} \text{Li}_3\text{PS}_4^c + \frac{1}{6} \text{P}_4\text{S}_4^d \rightarrow \text{Li}_2\text{Na}_2\text{P}_2\text{S}_6$	-0.48	-0.00	-0.48
6	$\frac{1}{2} \text{Na}_4\text{P}_2\text{S}_6 + \frac{1}{3} \text{P}_4\text{S}_{10}^f + 2 \text{Li} \rightarrow \text{Li}_2\text{Na}_2\text{P}_2\text{S}_6$	-5.01	0.06	-4.95
7	$\frac{1}{2} \text{Na}_4\text{P}_2\text{S}_6 + \frac{1}{3} \text{P}_4\text{S}_{10}^f + 2 \text{Na} \rightarrow \text{Li}_2\text{Na}_2\text{P}_2\text{S}_6$	-4.70	0.07	-4.63

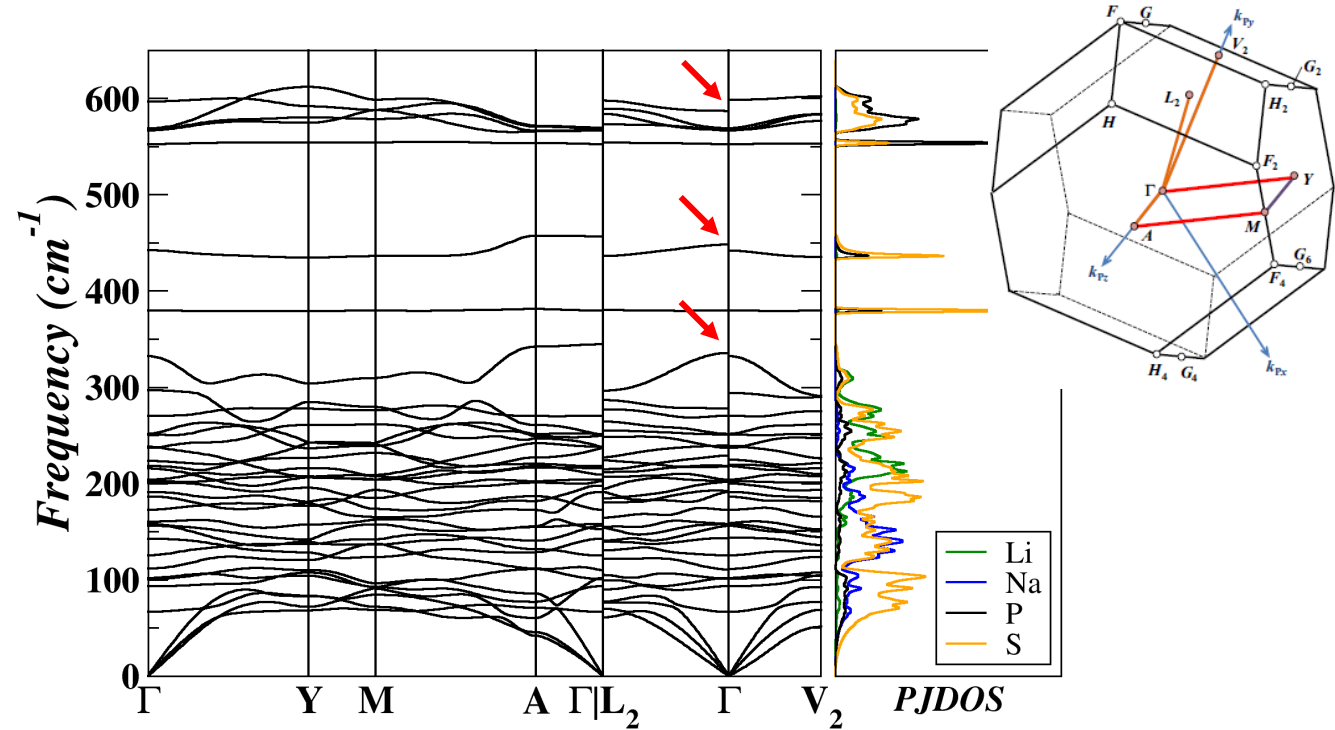


**Na<sub>4</sub>P<sub>2</sub>S<sub>6</sub> in the C2/m Structure (36 modes)**



Na<sup>+</sup> 0~300 cm<sup>-1</sup>  
(P<sub>2</sub>S<sub>6</sub>)<sup>4-</sup> 300~600 cm<sup>-1</sup>

**Li<sub>2</sub>Na<sub>2</sub>P<sub>2</sub>S<sub>6</sub> in the C2/m Structure (36 modes)**



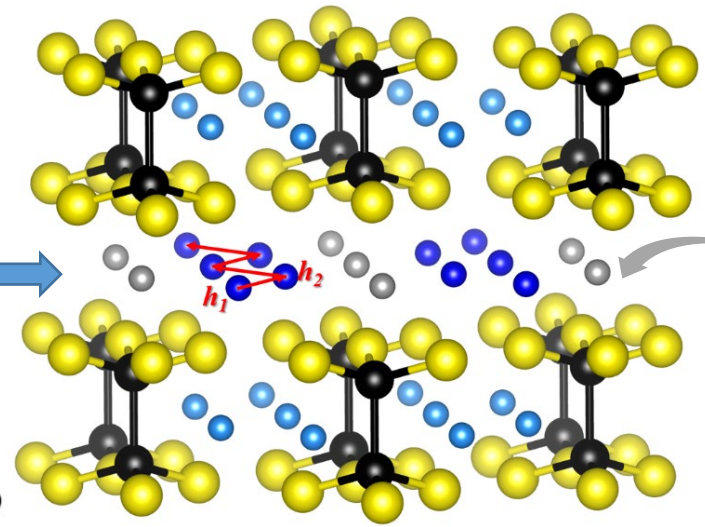
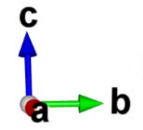
Li<sup>+</sup> 0~320 cm<sup>-1</sup>

Suggested path: Hinuma et al., *Comp. Mat. Sci.* **128**, 140-184 (2017)

Discontinuous branches at  $\Gamma$ : Li et al., *J. Phys. Condens. Matter*, **32**, 055402 (2020)

- Interstitial d site
- Na/Li (g)
- Na (h)
- P
- S

Vacancy process in interlayer *h* plane



*h* plane  
at  $\langle T \rangle = 1000$  K

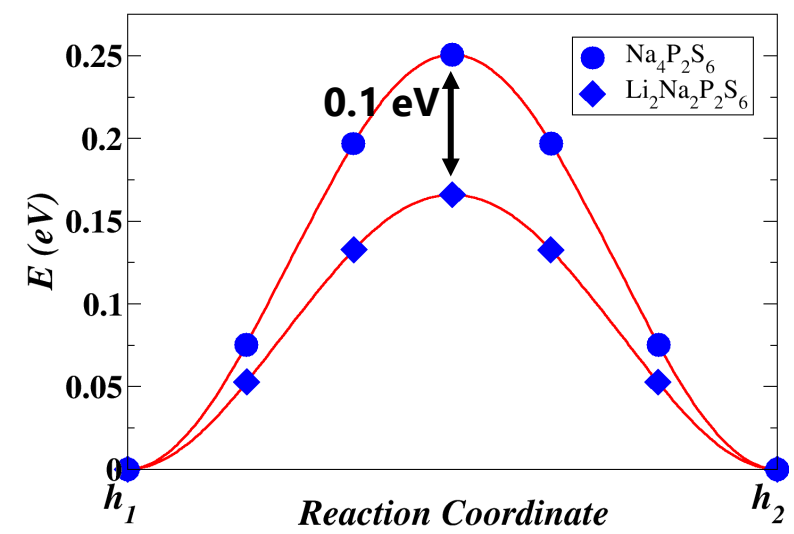
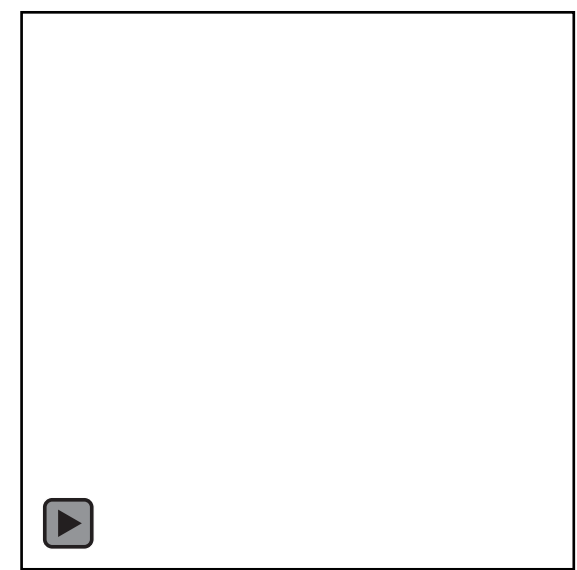
Host *h* site

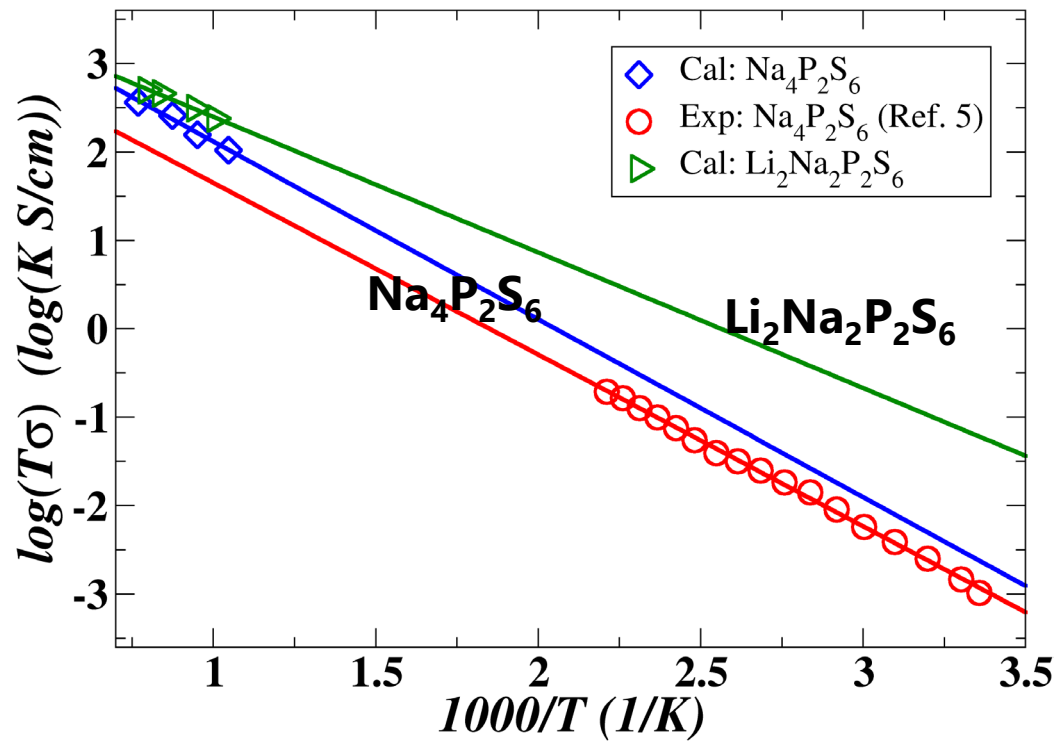
Extra interstitial *d* site

$a_4P_2S_6$



$2Na_2P_2S_6$





Molecular dynamics analysis of the ionic conductivity. The activation energy is obtained from the slope of the corresponding fit line.

Exp: Z. D. Hood, H. Wang, X. Liu, A. S. Pandian, R. Peng, J. K. Keum, and M. Chi (unpublished).

TABLE: NEB and MD results calculated with the PBEsol exchange-correlation functional, in comparison to those of previous work obtained using the LDA exchange-correlation functional and available experimental data. All energies are given in eV units.

Materials	Analysis	$E_m$	$E_f$	$E_a$
Na <sub>4</sub> P <sub>2</sub> S <sub>6</sub>	LDA + NEB <sup>1</sup>	0.30	0.24	0.42
	PBEsol + NEB	0.25	0.18	0.34
	PBEsol + MD	--	--	0.41
	Experiment <sup>2</sup>	--	--	0.39
Li <sub>2</sub> Na <sub>2</sub> P <sub>2</sub> S <sub>6</sub>	PBEsol + NEB	0.16	0.13	0.23
	PBEsol + MD	--	--	0.30

**Li<sub>2</sub>Na<sub>2</sub>P<sub>2</sub>S<sub>6</sub> presents better Na ion conductivity than Na<sub>4</sub>P<sub>2</sub>S<sub>6</sub>**



- ❑ DFT with PBEsol+harmonic phonon simulations agree with the experimental structures of  $\text{Na}_4\text{P}_2\text{S}_6$  (space group  $C2/m$  found by Kuhn and Hood) and  $\text{Li}_4\text{P}_2\text{S}_6$  (space group  $P\bar{3}m1$ , close to that found by Neuberger).
- ❑ For  $\text{Na}_4\text{P}_2\text{S}_6$  find Na ion migration to take place in planes with the  $h$ -sites via a vacancy mechanism, involving interstitial  $d$ -sites. Both simulations and experiment suggest that  $\text{Na}_4\text{P}_2\text{S}_6$  may be a viable solid electrolyte.
- ❑ Simulations predict  $\text{Li}_2\text{Na}_2\text{P}_2\text{S}_6$  to crystallize with the  $C2/m$  structure and to be stable relative to  $\text{Na}_4\text{P}_2\text{S}_6 + 2\text{Li} - 2\text{Na}$ . The mixed alkali electrolyte is predicted to substantially enhance Na ion conductivity.
- ❑ In addition to experimental verification (or otherwise) of the predictions for  $\text{Li}_2\text{Na}_2\text{P}_2\text{S}_6$ , further MD simulations for both  $\text{Na}_4\text{P}_2\text{S}_6$  and  $\text{Li}_2\text{Na}_2\text{P}_2\text{S}_6$  will help us better understand Na ion conductivity mechanisms.

**Phys. Rev. Mater. 4, 045406 (2020)**

- Research background: General motivation and theoretical tools
- **Finished/ongoing projects: Inputs and outcomes**

## **Na<sub>4</sub>P<sub>2</sub>S<sub>6</sub>, Li<sub>4</sub>P<sub>2</sub>S<sub>6</sub>, and possible alloy**

Yan Li, Zachary D. Hood, and N. A. W. Holzwarth  
*Phys. Rev. Mater.* **4**, 045406 (2020)

## **Phonon dispersion**

Yan Li, W. C. Kerr, and N. A. W. Holzwarth  
*J. Condens. Matter Phys.* **32**, 055402 (2020)

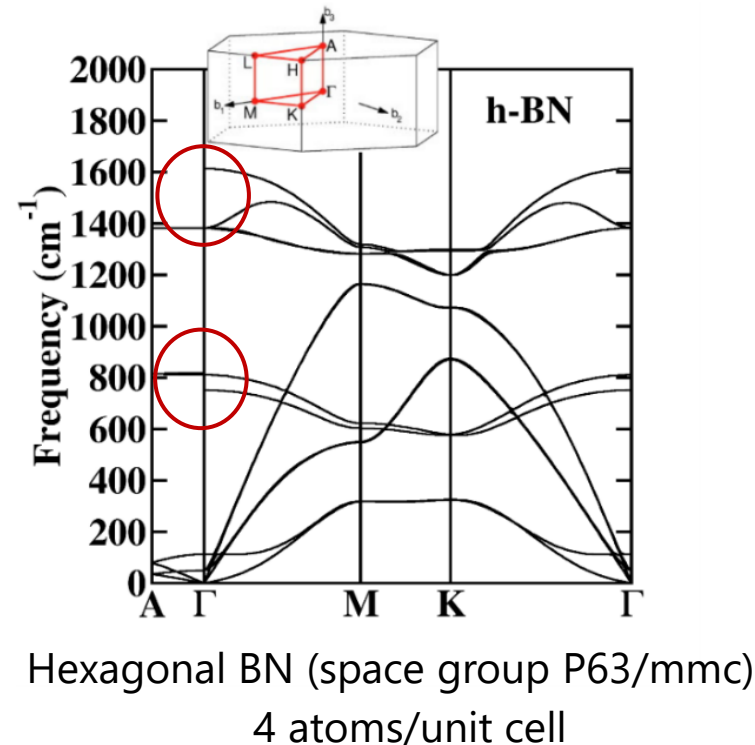
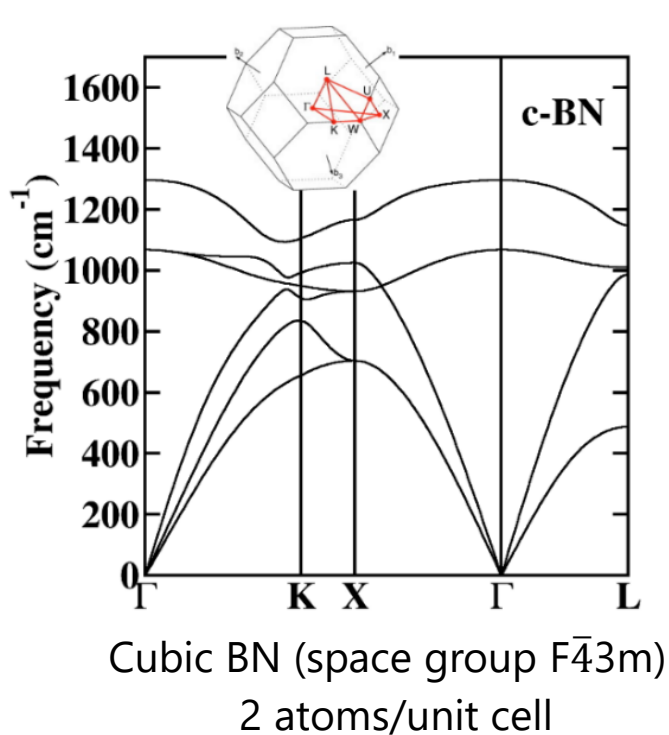
## **Li<sub>3</sub>BO<sub>3</sub> and Li<sub>3</sub>BN<sub>2</sub> (I & II)**

Yan Li, Zachary D. Hood, and N. A. W. Holzwarth  
*Phys. Rev. Mater.* **5**, 085402 & 085403 (2021)

## **Li<sub>4+x</sub>B<sub>7</sub>O<sub>12+x/2</sub>Cl (x = 0, 1) and related**

**Li<sub>7.5</sub>B<sub>10</sub>O<sub>18</sub>X<sub>1.5</sub> (X = Cl, Br, and I)**

**Q: Why do the phonon dispersion curves for ionic materials have mode “disappearances” near the center of the Brillouin zone?**



**Physical reasons:** Coupling between the vibrational modes and the electromagnetic waves in the long wavelength limit  $\mathbf{q} \rightarrow 0$ .

Born and Huang, *Dynamical Theory of Crystal Lattices*, Oxford (1954)



- Uncoupled equations of motion (EOM):

$$(\omega^\nu(\mathbf{q}))^2 M_s u_{s\alpha}^\nu(\mathbf{q}) = \sum_{t\beta} \tilde{C}_{s\alpha,t\beta}(\mathbf{q}) u_{t\beta}^\nu(\mathbf{q})$$

- Modified EOM at small  $\mathbf{q}$ :

$$M_s \frac{\partial^2 w_{s\alpha}(\mathbf{q})}{\partial t^2} = - \sum_{t\beta} \tilde{C}_{s\alpha,t\beta}(\mathbf{q}) w_{t\beta}(\mathbf{q}) + \sum_{\beta} e Z_{\alpha\beta}^{*s} E_{\beta}(\mathbf{q})$$

*Coupling of the lattice displacements to an electric field in the long wavelength range*

*coupled ionic displacements*

- Born effective charge tensor:

$$e Z_{\alpha\beta}^{*s} = - \left. \frac{\partial^2 U_{SL}}{\partial u_{s\alpha}(\mathbf{q} = 0) \partial E_{\beta}} \right|_{u_{s\alpha}=0, E_{\beta}=0}$$

- Define Born coupling parameters:

$$\mathcal{L}_{\beta}^{\nu} \equiv \sum_{s\alpha} (u_{s\alpha}^{\nu})^* Z_{\alpha\beta}^{*s}; \quad \mathcal{R}_{\alpha}^{\nu} \equiv \sum_{t\beta} Z_{\alpha\beta}^{*t} u_{t\beta}^{\nu}$$

- Trial solutions:

$$\mathbf{W}_s(l) \rightarrow \mathbf{W}_s^0(\mathbf{q}) e^{i\mathbf{q}\cdot\mathbf{r} - i\omega t} \quad \text{where} \quad \mathbf{w}_{s\alpha}^0(\mathbf{q}) = \sum_{\nu} U^{\nu}(\mathbf{q}) u_{s\alpha}^{\nu}(\mathbf{q})$$

$$\mathbf{E}(\mathbf{q}) = \mathbf{E}^0(\mathbf{q}) e^{i\mathbf{q}\cdot\mathbf{r} - i\omega t}$$

$$\rightarrow U^{\nu} = \frac{e}{((\omega^{\nu})^2 - \omega^2) M^{\nu}} \sum_{\beta} \mathcal{L}_{\beta}^{\nu} E_{\beta}^0$$

*pure vibrational modes*

- The electric displacement field:

$$D_\alpha(\mathbf{q}) = \sum_\beta \epsilon_{\alpha\beta}(\omega) E_\beta(\mathbf{q}) = \sum_\beta \epsilon_{\alpha\beta}^\infty E_\beta(\mathbf{q}) + \frac{4\pi e}{\Omega} \sum_{t\beta} Z_{\alpha\beta}^{*t} u_{t\beta}(\mathbf{q})$$

*Electronic response*
*Dipolar contributions due to the ionic displacements*

- Substituting the solutions for  $\mathbf{w}$  and  $\mathbf{E}$ , yields:

$$\epsilon_{\alpha\beta}(\omega) = \epsilon_{\alpha\beta}^\infty + \frac{4\pi e^2}{\Omega} \sum_\nu \frac{\mathcal{R}_\alpha^\nu \mathcal{L}_\beta^\nu}{((\omega^\nu)^2 - \omega^2) M^\nu}$$

$$\epsilon_{\alpha\beta}^0 \equiv \epsilon_{\alpha\beta}(\omega = 0) = \epsilon_{\alpha\beta}^\infty + \frac{4\pi e^2}{\Omega} \sum_\nu \frac{\mathcal{R}_\alpha^\nu \mathcal{L}_\beta^\nu}{(\omega^\nu)^2 M^\nu} \quad \text{-- static dielectric constant}$$

- Maxwell's equations in free space for non-magnetic materials:

$$\nabla \cdot \mathbf{D} = 0 \quad \text{produce longitudinal solutions}$$

$$\nabla \times (\nabla \times \mathbf{E}) + \frac{1}{c^2} \frac{\partial^2 \mathbf{D}}{\partial t^2} = 0 \quad \text{produce transverse solutions}$$



- For the case of longitudinal electric field:

➔ 
$$\epsilon_{LL} = \epsilon_{LL}^{\infty} + \frac{4\pi e^2}{\Omega} \sum_{\nu} \frac{\mathcal{R}_L^{\nu} \mathcal{L}_L^{\nu}}{((\omega^{\nu})^2 - \omega^2) M^{\nu}} = 0$$

$n_L = 1$  ➔  $\omega^2 \equiv \omega_L^2 = (\omega^{\nu})^2 + \frac{1}{\epsilon_{LL}^{\infty}} \frac{4\pi e^2}{\Omega M^{\nu}} \mathcal{R}_L^{\nu} \mathcal{L}_L^{\nu}$  (one coupled)



- General solutions for  $n_L > 1$ :

$$\sum_{\nu} \mathcal{G}_{\nu\nu}^L U^{\nu} = \omega_L^2 U^{\nu} \quad \text{where} \quad \mathcal{G}_{\nu\nu}^L = (\omega^{\nu})^2 \delta_{\nu\nu} + \frac{1}{\epsilon_{LL}^{\infty}} \frac{4\pi e^2}{\Omega M^{\nu}} \mathcal{L}_L^{\nu} \mathcal{R}_L^{\nu} \quad \text{No dispersion introduced}$$

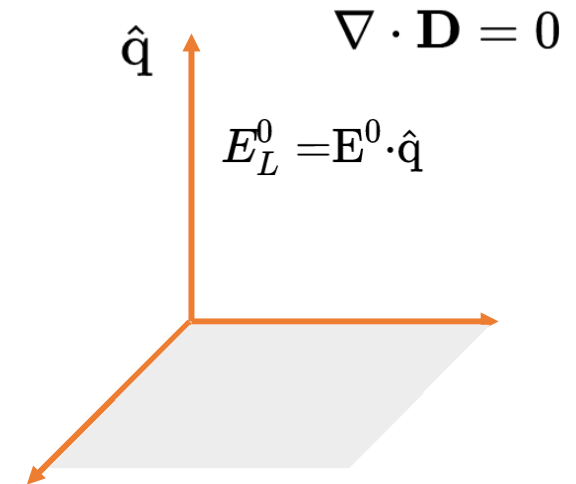
- Alternative approach

$$\omega^2 M_s w_{s\alpha}^0(\mathbf{q}) = \sum_{t\beta} \tilde{C}_{s\alpha,t\beta}^{\text{tot}}(\mathbf{q}) w_{t\beta}^0(\mathbf{q})$$

$$\tilde{C}_{s\alpha,t\beta}^{\text{tot}}(\mathbf{q}) = \tilde{C}_{s\alpha,t\beta}(\mathbf{q}) + \frac{4\pi e^2}{\Omega \epsilon_{LL}^{\infty}} Z_{L\alpha}^{*s} Z_{\beta L}^{*t}$$

 analytic
  non-analytic

QE/AB: one more step to correct the LO-TO (Longitudinal Optical-Transverse Optical) splitting





➤ For the case of transverse electric field:

$$\rightarrow \sum_{T_j} \left( q^2 c^2 \delta_{T_i T_j} - \omega_T^2 \left( \epsilon_{T_i T_j}^\infty + \frac{4\pi e^2}{\Omega} \sum_{\nu} \frac{\mathcal{R}_{T_i}^{\nu} \mathcal{L}_{T_j}^{\nu}}{((\omega^{\nu})^2 - \omega_T^2) M^{\nu}} \right) \right) E_{T_j}^0 = 0$$

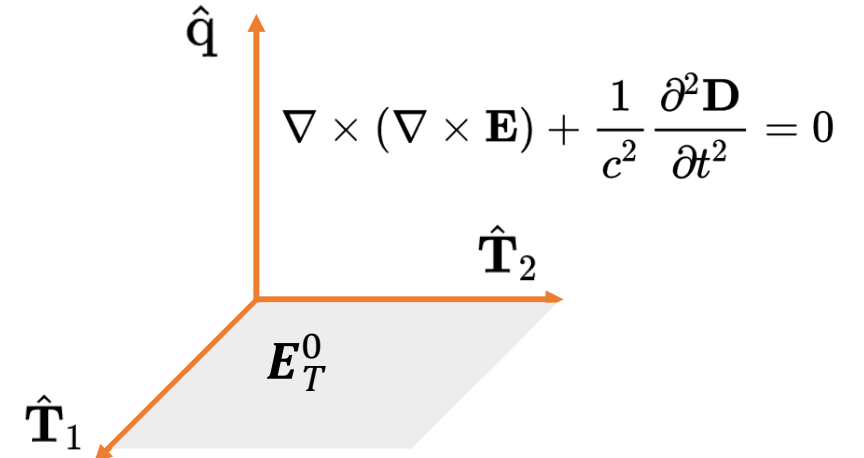
$$n_T = 1 \rightarrow \omega_{T_i \pm}^2(\mathbf{q}) = \frac{q^2 c^2 + (\omega^{\nu})^2 \epsilon_{T_i T_i}^\infty + \mathcal{A}^{\nu}}{2 \epsilon_{T_i T_i}^\infty} (1 \pm \mathcal{S}^{\nu}(\mathbf{q})) \quad (\text{one coupled})$$

$$\text{where } \mathcal{S}^{\nu}(\mathbf{q}) \equiv \sqrt{1 - \frac{4q^2 c^2 (\omega^{\nu})^2 \epsilon_{T_i T_i}^\infty}{(q^2 c^2 + (\omega^{\nu})^2 \epsilon_{T_i T_i}^\infty + \mathcal{A}^{\nu})^2}} ; \quad \mathcal{A}^{\nu} \equiv \frac{4\pi e^2}{\Omega M^{\nu}} \mathcal{R}_{T_i}^{\nu} \mathcal{L}_{T_i}^{\nu}$$

$$\rightarrow \omega_{T_i+}^2(\mathbf{q} \approx 0) = (\omega^{\nu})^2 + \frac{1}{\epsilon_{T_i T_i}^\infty} \frac{4\pi e^2}{\Omega M^{\nu}} \mathcal{R}_{T_i}^{\nu} \mathcal{L}_{T_i}^{\nu} + S q^2 c^2$$

➤ General solutions for  $n_T > 1$ :

$$\sum_{\nu'} \mathcal{G}_{\nu\nu'}^T U^{\nu'} = \omega_T^2 U^{\nu} \quad \text{where} \quad \mathcal{G}_{\nu\nu'}^T \equiv (\omega^{\nu})^2 \delta_{\nu\nu'} + \frac{4\pi e^2}{\Omega M^{\nu}} \sum_{T_i T_j} \left( \epsilon^\infty - \frac{q^2 c^2}{\omega_T^2} \mathbf{I} \right)_{T_i T_j}^{-1} \mathcal{L}_{T_i}^{\nu} \mathcal{R}_{T_j}^{\nu'}$$

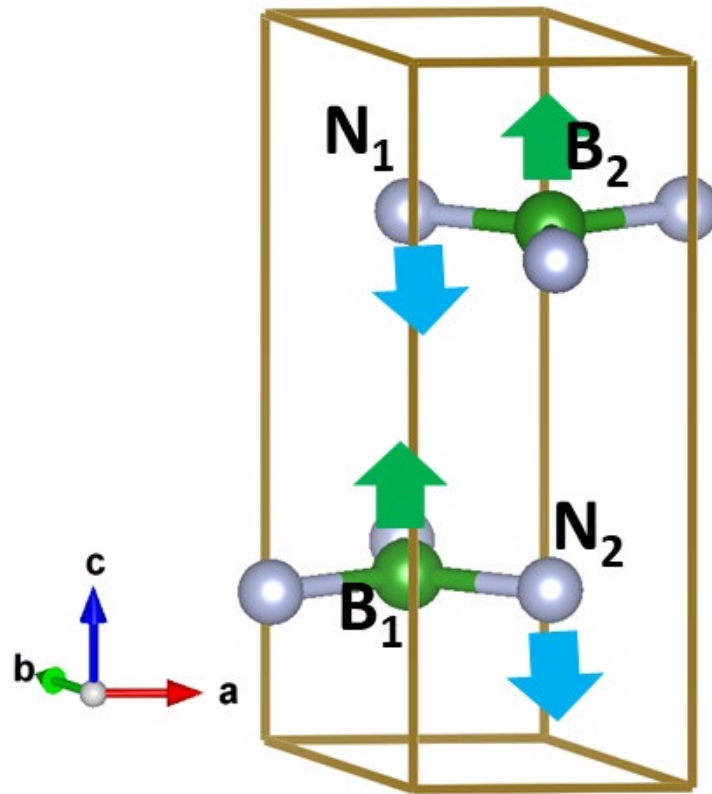




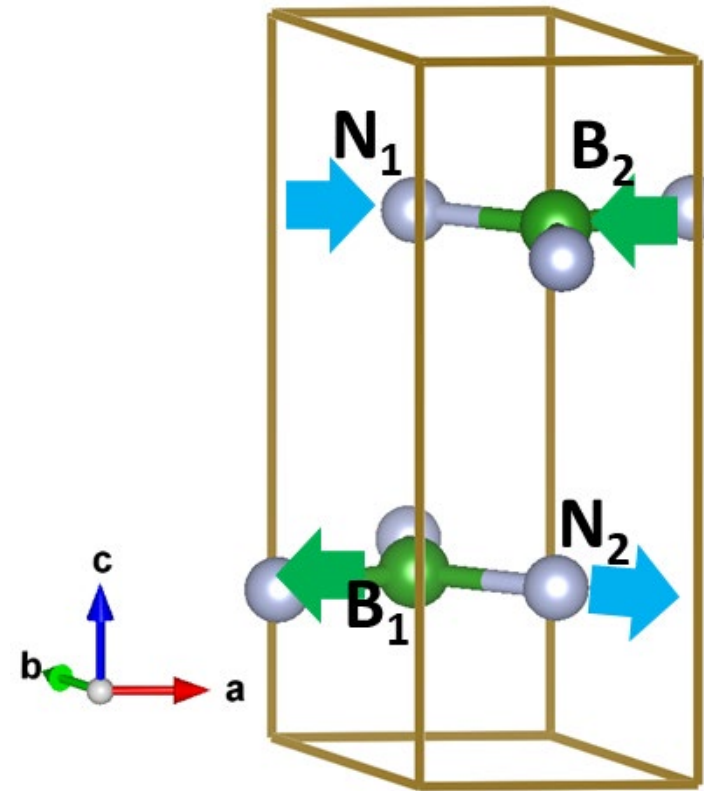
## Steps of finding all coupled modes along the high symmetry directions:

- Run ABINIT or QUANTUM ESPRESSO to obtain the pure phonon modes
- Calculate the Born coupling parameters  $\mathcal{L}_\beta^\nu \equiv \sum_{s\alpha} (u_{s\alpha}^\nu)^* Z_{\alpha\beta}^{*s}$  and  $\mathcal{R}_\alpha^\nu \equiv \sum_{t\beta} Z_{\alpha\beta}^{*t} u_{t\beta}^\nu$   
Note that for highly symmetric materials,  $\mathcal{R}_\alpha^\nu = (\mathcal{L}_\alpha^\nu)^*$   
Also note that for many modes  $\nu$ ,  $\mathcal{R}_\alpha^\nu = 0$  and  $\mathcal{L}_\alpha^\nu = 0$
- Identify the direction of the wavevector  $\hat{q}$  from the modes with non-trivial values of  $\mathcal{R}_\alpha^\nu$  and  $\mathcal{L}_\alpha^\nu$ , such modes are also the coupled LO modes
- Analyze the corresponding coupled TO modes

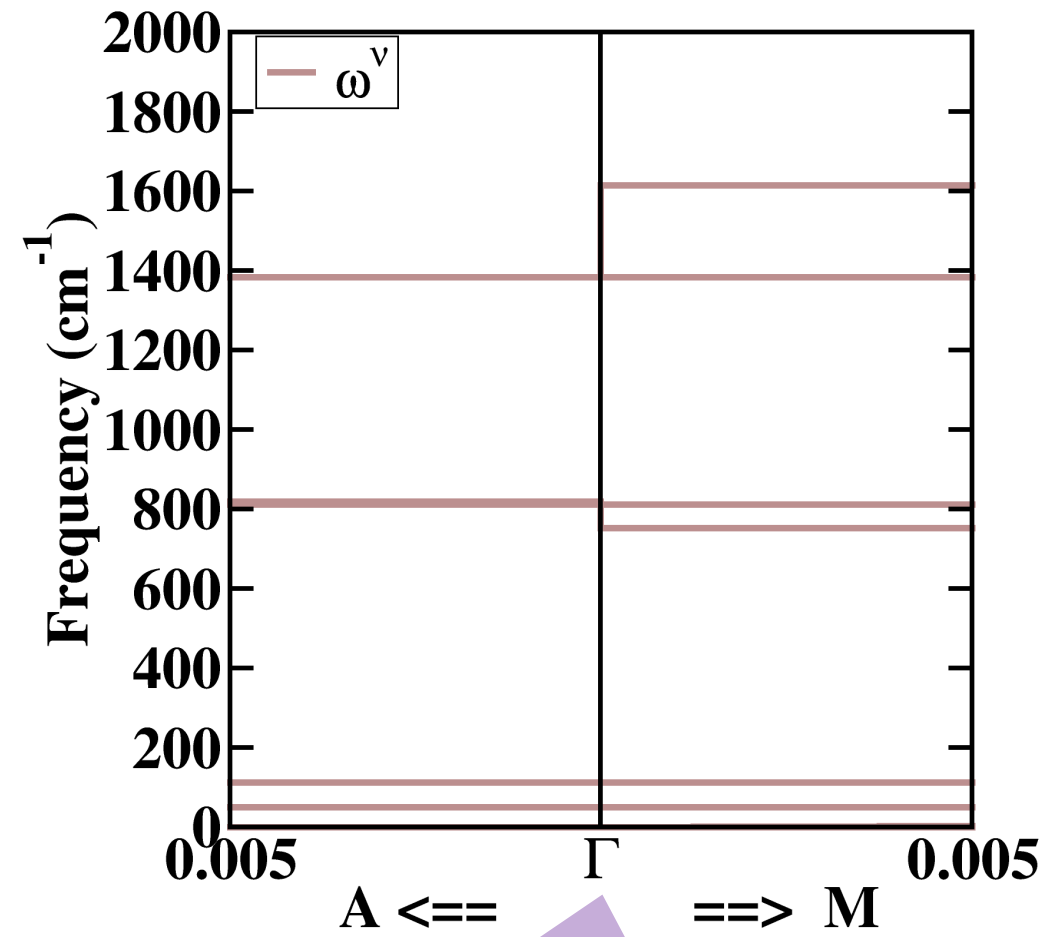
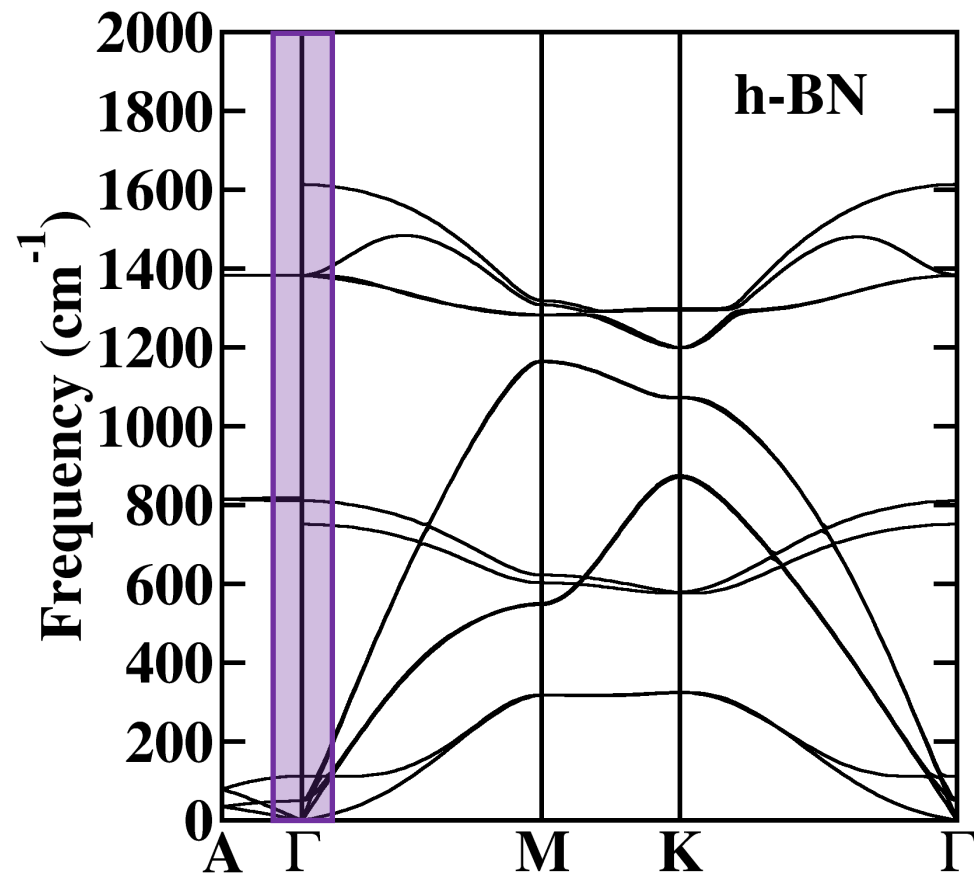
Of the 12 normal modes near  $q = 0$ , only 3 couple with EM waves:

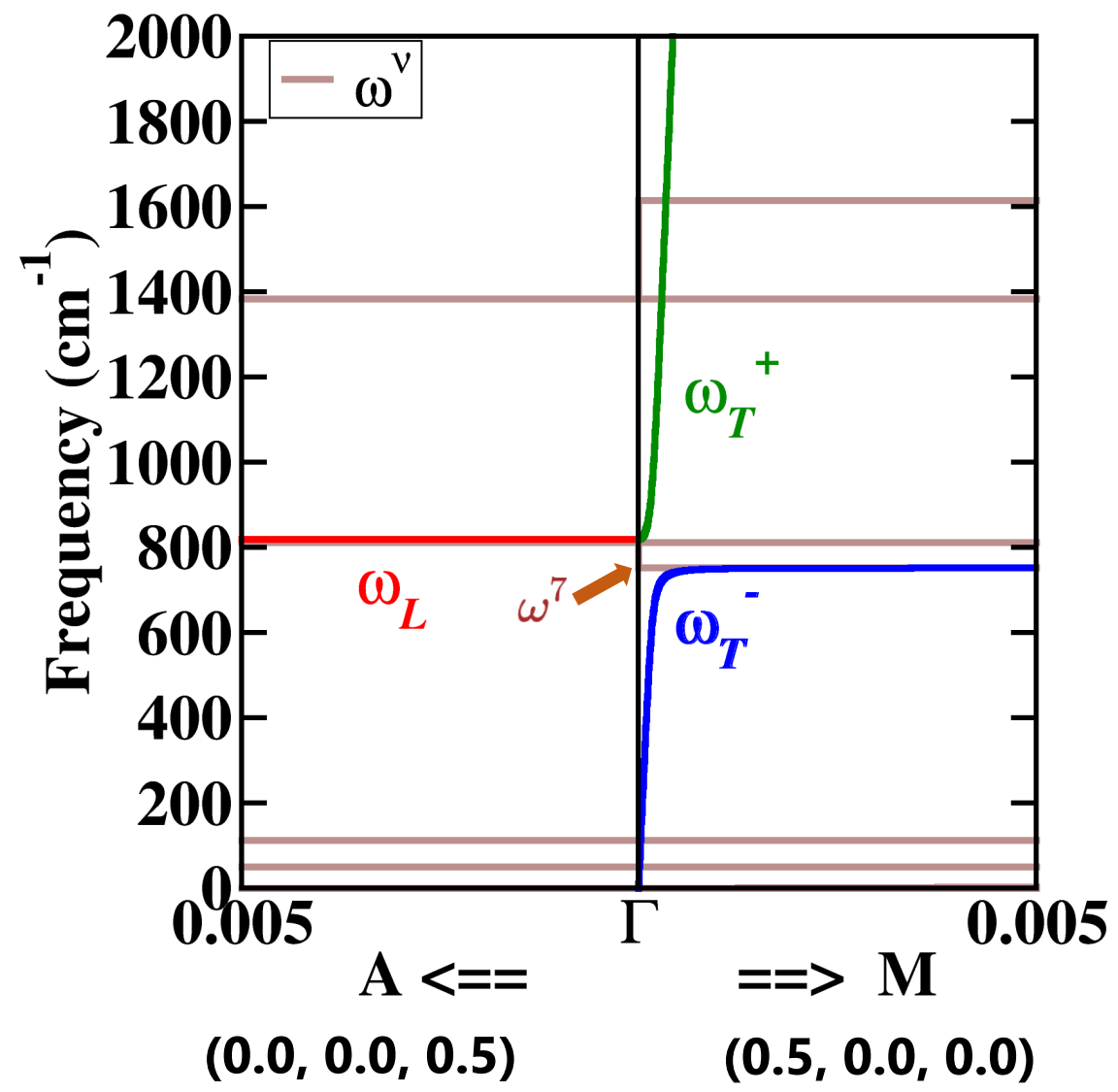


Mode #7 involves displacements along  $z$  ( $c$ ) axis



Modes #11 & #12 involve displacements along  $x, y$  ( $a, b$ ) axes





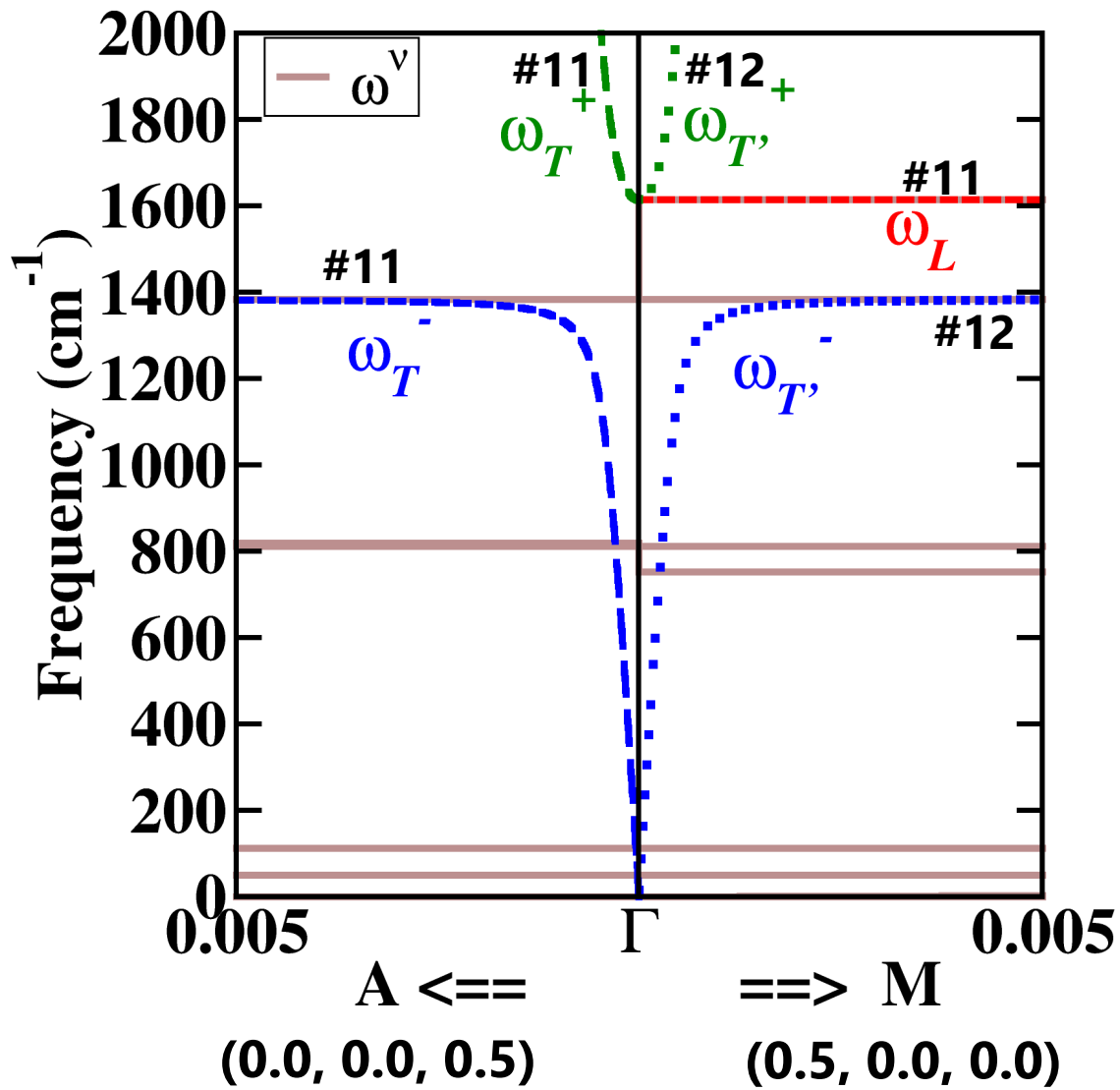
Mode #7 involves displacements along z (c) axis

$$(\mathfrak{z}_L)^2 = (\mathfrak{z}_7)^2 \frac{1}{\omega_{zz}^\infty} \frac{4\pi e^2}{CM^7} \left| \begin{matrix} 7 \\ z \end{matrix} \right|^2$$

$$(\mathfrak{z}_{T^+})^2 \approx \left( \begin{matrix} 7 \\ + \end{matrix} \right)^2 \frac{1}{\omega_{zz}^\infty} \frac{4\pi e^2}{CM^7} \left| \begin{matrix} 7 \\ + \\ z \end{matrix} \right|^2 C_q^2$$

For  $q \rightarrow 0$ :  $\mathfrak{z}_T^- \approx \frac{qc}{\sqrt{\omega_{zz}^\infty}}$

For  $q \gg 0$ :  $\mathfrak{z}_T^- \approx \omega^7$



Modes #11 & #12 involve displacements along x,y (a,b) axes

$$(\mathfrak{Z}_L)^2 = (\mathfrak{Z}^{11})^2 \frac{1}{\omega_{xx}^\infty} \frac{4\epsilon e^2}{\Omega M^{11}} \left| \begin{matrix} 11 \\ x \end{matrix} \right|^2$$

$$(\mathfrak{Z}_{T^+})^2 \approx \left( \begin{matrix} 11 \\ + \end{matrix} \right)^2 \frac{1}{\omega_{xx}^\infty} \frac{4\epsilon e^2}{\Omega M_L^{11}} \left| \begin{matrix} 11 \\ x \\ + \end{matrix} \right|^2 C_q$$

For  $q \rightarrow 0$ :  $\mathfrak{Z}_T^- \approx \frac{qc}{\sqrt{\omega_{xx}^0}}$

For  $q \gg 0$ :  $\mathfrak{Z}_T^- \approx \begin{matrix} 11 \\ + \end{matrix}$

Note that ... ( $\omega_T$ ) curves represent coupling to mode #12 with transverse contributions associated with longitudinal mode along  $\Gamma \rightarrow K$

- ❑ The parameters needed to analyze the phonon-photon coupling can be calculated from first principles using density functional theory (DFT) and density functional perturbation theory (DFPT), available in ABINIT and QUANTUM ESPRESSO, for example. Particularly, the phonon eigenstates evaluated at  $\mathbf{q} = 0$ , the Born effective charge tensors, and the electronic contributions to the dielectric permittivity tensor.
- ❑ Apparent “discontinuities” or mode “disappearances” in the phonon dispersion curves of ionic materials for  $\mathbf{q} \rightarrow 0$  in hexagonal and other anisotropic materials are caused by the directional dependence of the Born effective charge tensor.
- ❑ The full dispersion curves of the phonon–photon system, including both longitudinal and transverse modes, are continuous functions of wavevector, modifying both the longitudinal and transverse dispersions. This was illustrated for hexagonal boron nitride.

**J. Condens. Matter Phys. 32, 055402 (2020)**



- Research background: General motivation and theoretical tools
- **Finished/ongoing projects: Inputs and outcomes**

## **$\text{Na}_4\text{P}_2\text{S}_6$ , $\text{Li}_4\text{P}_2\text{S}_6$ , and possible alloy**

Yan Li, Zachary D. Hood, and N. A. W. Holzwarth  
*Phys. Rev. Mater.* 4, 045406 (2020)

## **Phonon dispersion**

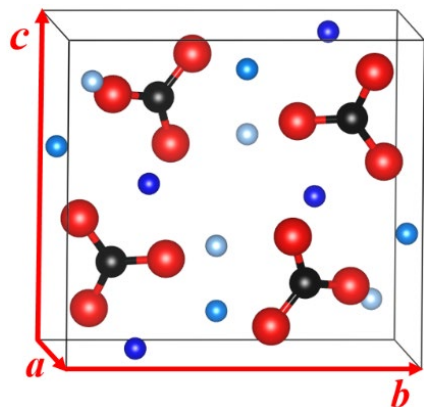
Yan Li, W. C. Kerr, and N. A. W. Holzwarth  
*J. Condens. Matter Phys.* 32, 055402 (2020)

## **$\text{Li}_3\text{BO}_3$ and $\text{Li}_3\text{BN}_2$ (I & II)**

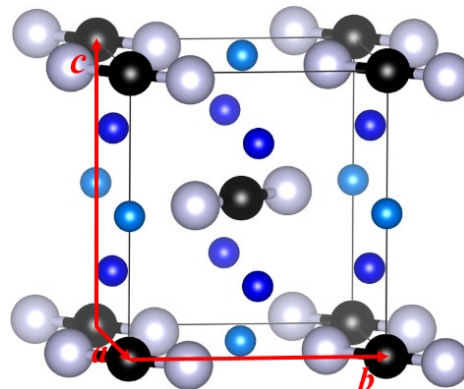
Yan Li, Zachary D. Hood, and N. A. W. Holzwarth  
*Phys. Rev. Mater.* 5, 085402 & 085403 (2021)

## **$\text{Li}_{4+x}\text{B}_7\text{O}_{12+x/2}\text{Cl}$ ( $x = 0, 1$ ) and related**

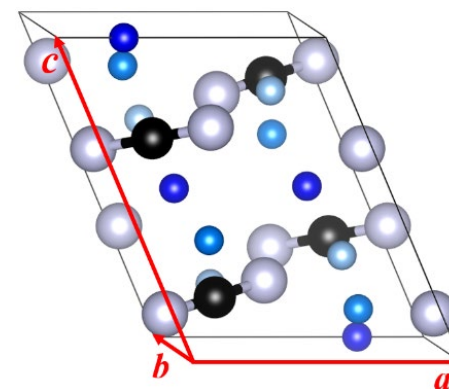
**$\text{Li}_{7.5}\text{B}_{10}\text{O}_{18}\text{X}_{1.5}$  ( $\text{X} = \text{Cl, Br, and I}$ )**



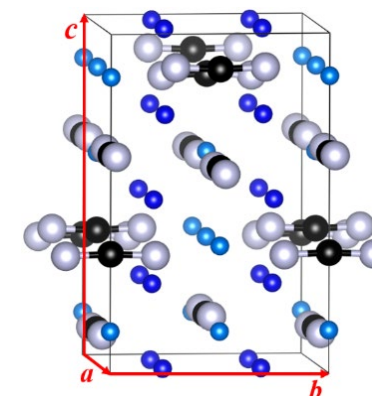
Monoclinic P2<sub>1</sub>/c (#14)<sup>1</sup>  
4 formula units / unit cell



Tetragonal P4<sub>2</sub>/mnm (#136)<sup>2</sup>  
2 formula units / unit cell



Monoclinic P2<sub>1</sub>/c (#14)<sup>2</sup>  
4 formula units / unit cell



Tetragonal I4<sub>1</sub>/amd (#141)<sup>3</sup>  
8 formula units / unit cell

## Focuses of this project:

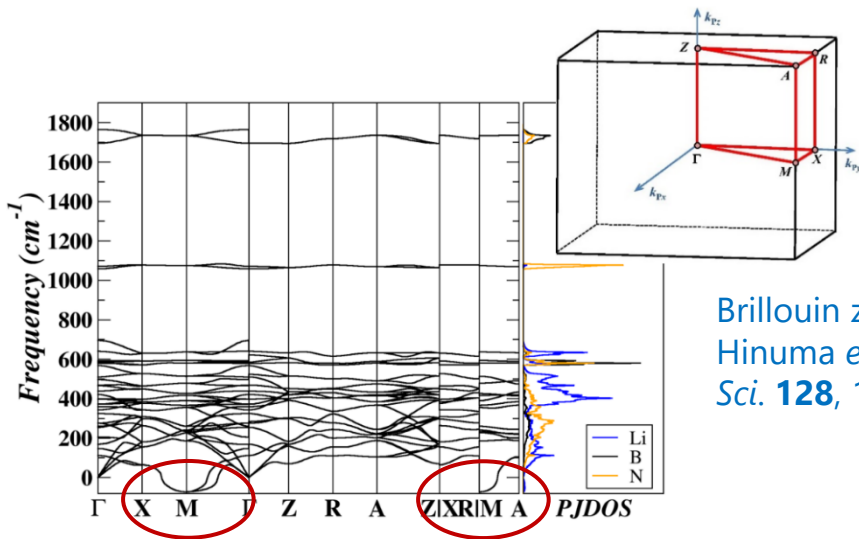
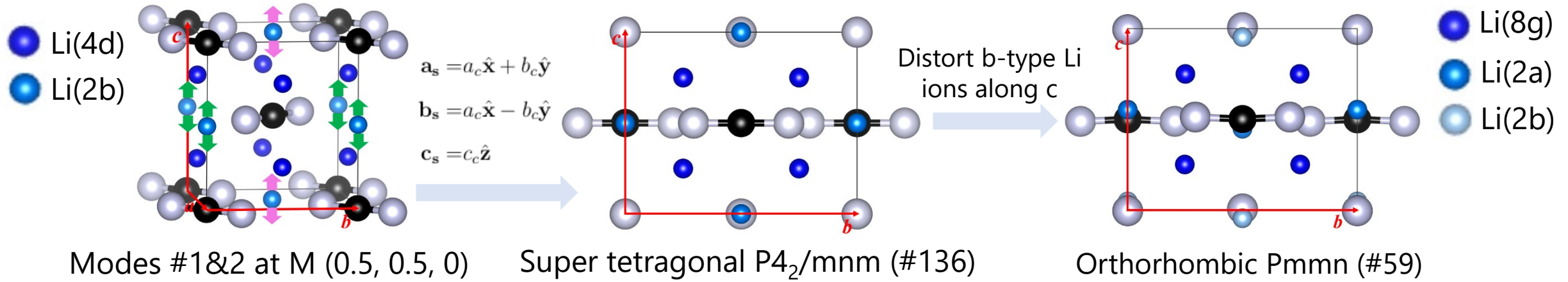
- Structure correction for α-Li<sub>3</sub>BN<sub>2</sub>
- Electrolyte properties of pure and doped Li<sub>3</sub>BO<sub>3</sub> and β-Li<sub>3</sub>BN<sub>2</sub> crystals
- Stability analysis of the ideal interfaces of pure Li<sub>3</sub>BO<sub>3</sub> and β-Li<sub>3</sub>BN<sub>2</sub> with Li metal anode

<sup>1</sup>Stewner, *Acta Crystallogr. section B.* **27**, 904 (1971)

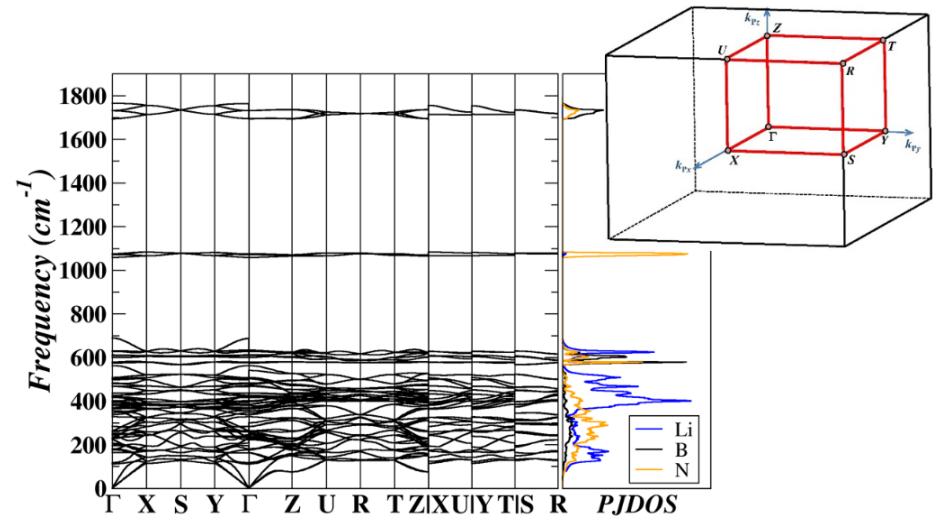
<sup>2</sup>Yamane et al., *J. Solid State Chem.* **71**, 1-11 (1987)

<sup>3</sup>Pinkerton and Herbst, *J. Appl. Phys.* **99**, 113523 (2016)

# Corrected $\alpha$ phase of $\text{Li}_3\text{BN}_2$



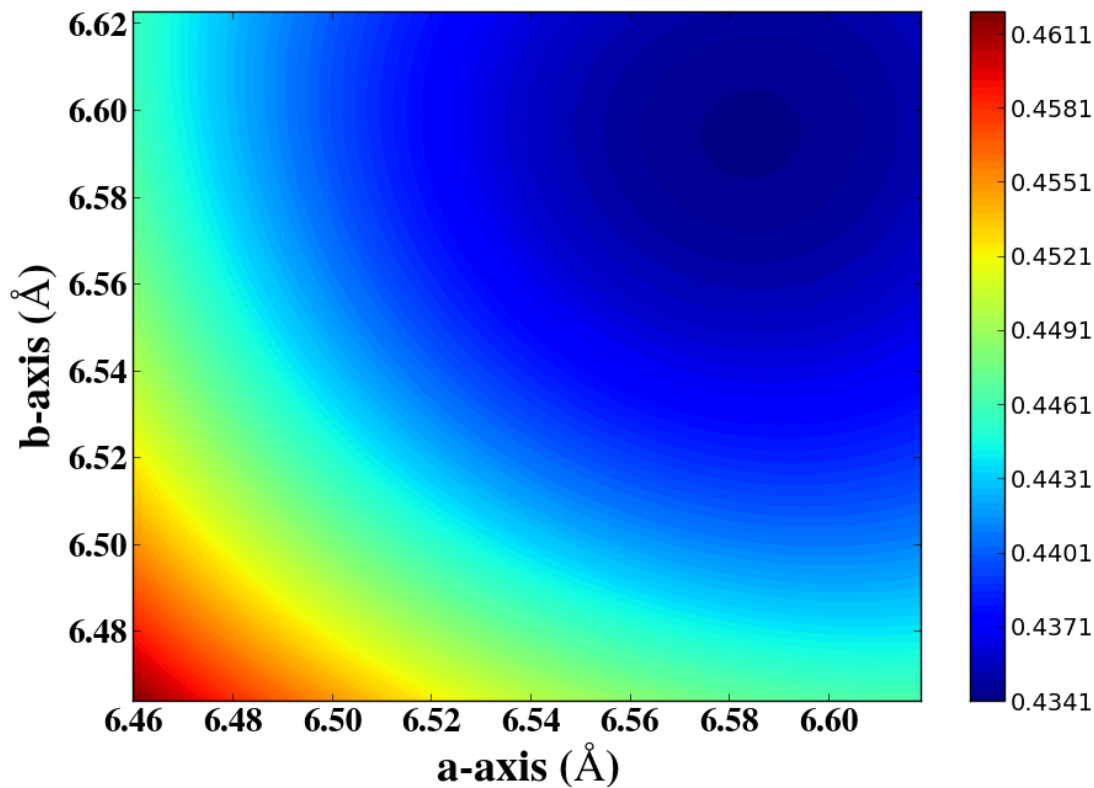
Reported  $\alpha\text{-Li}_3\text{BN}_2$  in the tetragonal  $P4_2/mnm$  structure



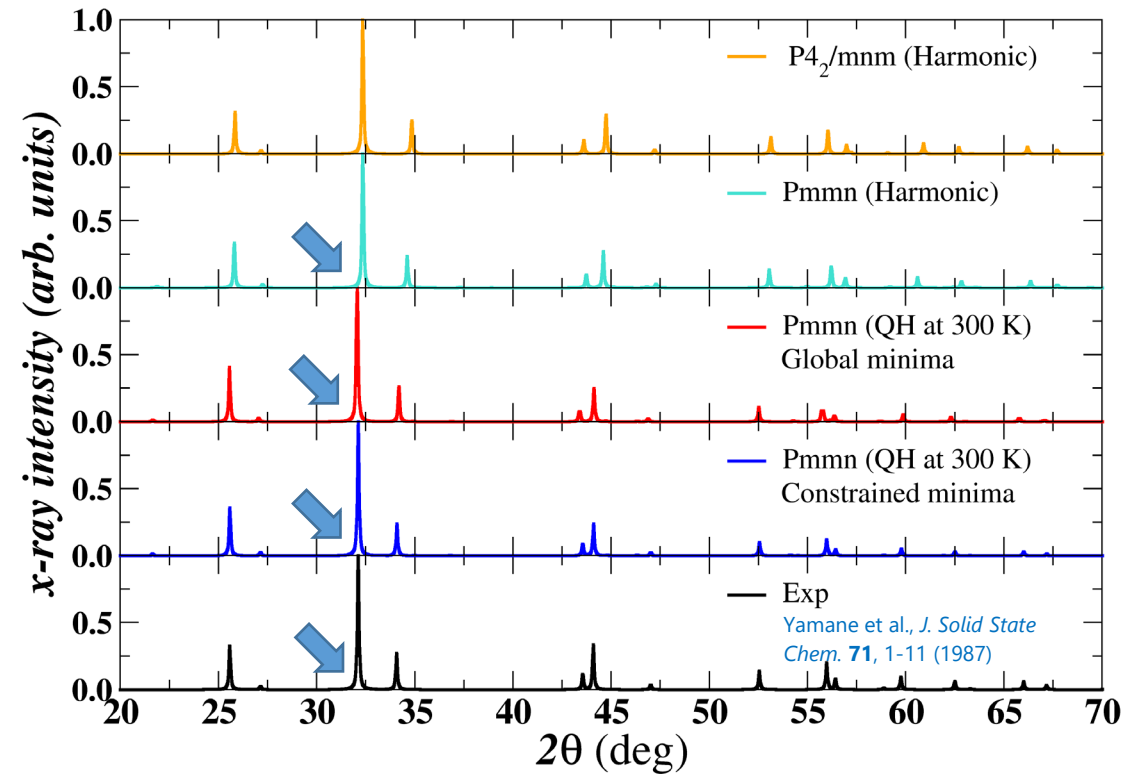
New  $\alpha\text{-Li}_3\text{BN}_2$  in the orthorhombic  $Pmmn$  structure

**Harmonic:**  $F(T) = U_{SL} + F_{vib}(T)$

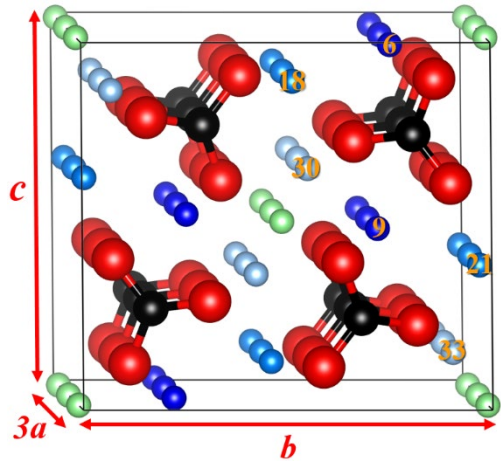
**Quasiharmonic:**  $F^{QH}(T, a, b, c) = U_{SL}(a, b, c) + F_{vib}^{QH}(T, a, b, c); F_{min}^{QH}(T) = \min_{(a,b,c)} F^{QH}(T, a, b, c)$



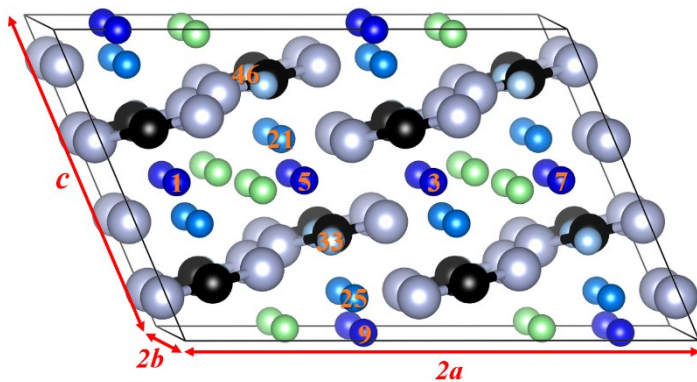
Contour plot of  $F^{QH}$  ( $T = 300$  K,  $a, b, c_{min}$ )



Comparison of simulated and experimental x-ray diffraction ( $\lambda = 1.54056$  Å) patterns.



3x1x1 supercell of  $\text{Li}_3\text{BO}_3$



2x2x1 supercell of  $\beta\text{-Li}_3\text{BN}_2$

## Metastable interstitial defects (green balls):

- $\text{Li}_3\text{BO}_3$ : Wyckoff sites  $2b$  with coordinates  $(0.5, 0.5, 0.5)$ ;  $E_f = 1.25 \text{ eV}$
- $\text{Li}_3\text{BN}_2$ : Wyckoff sites  $4e$  with coordinates  $(0.560, 0.279, 0.978)$ ;  $E_f = 1.23 \text{ eV}$

## Models of Li-deficient structures:

- Pure crystal with an ideal Li vacancy created by removing a Li ion and compensating with a uniform charge of the opposite sign -- **I-vac**
- F-doped crystal with the stoichiometry of  $\text{Li}_{3-x}\text{BO}_{3-x}\text{F}_x$  ( $x = 1/12$ ) -- **F-doped**
- C-doped crystal with the stoichiometry of  $\text{Li}_{3-x}\text{B}_{1-x}\text{C}_x\text{N}_2$  ( $x = 1/16$ ) -- **C-doped**

## Stability analysis:

- $\text{Li}_{3-x}\text{BO}_{3-x}\text{F}_x \rightarrow (1 - 2x) \text{Li}_3\text{BO}_3 + 2x \text{Li}_2\text{O} + x \text{B}_2\text{O}_3 + x \text{LiF} - 0.06 \text{ eV}$
- $\text{Li}_{3-x}\text{B}_{1-x}\text{C}_x\text{N}_2 \rightarrow (1 - x) \text{Li}_3\text{BN}_2 + x \text{Li}_2\text{CN}_2 + 0.05 \text{ eV}$

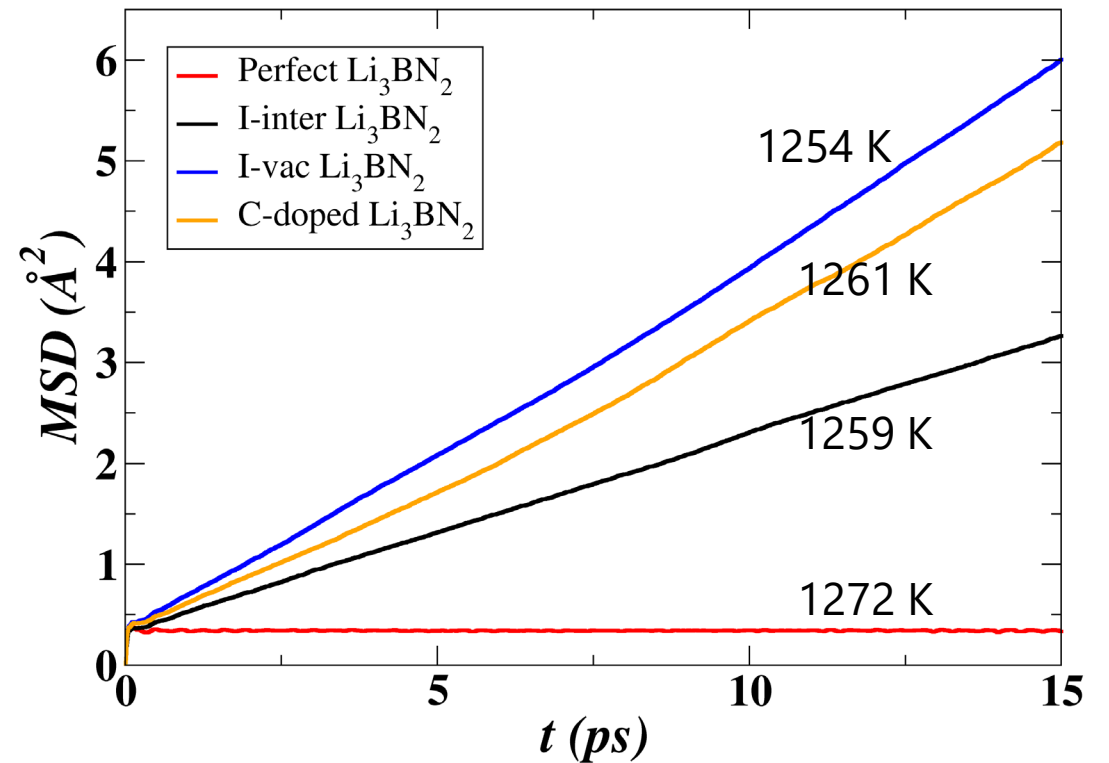
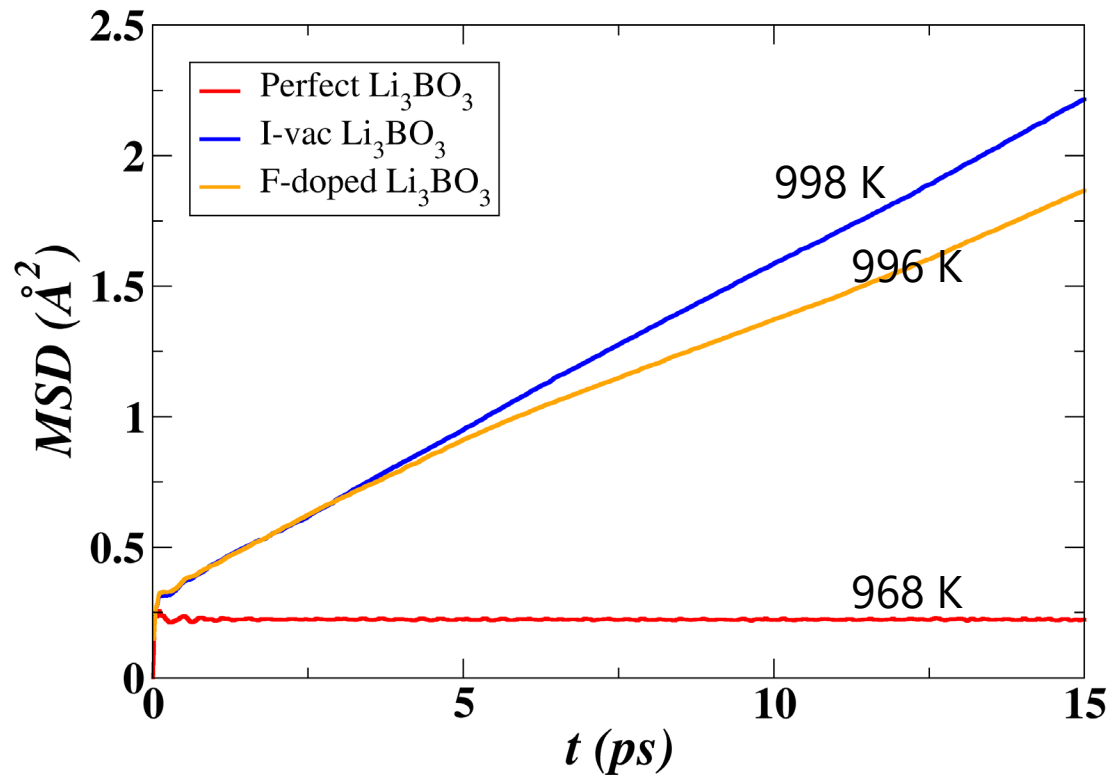


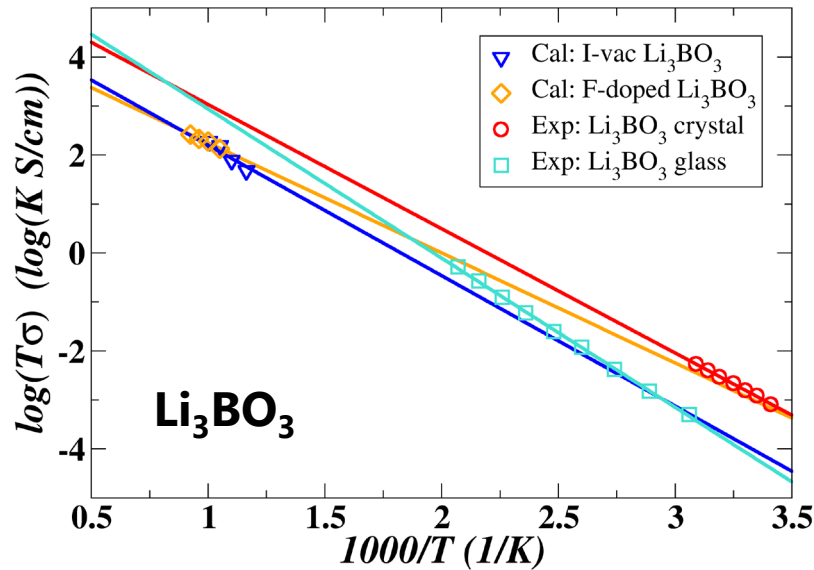
NVE ensemble for MD simulations

$$\langle T \rangle = \frac{2}{3(N_{\text{atom}} - 1)k_B} \frac{1}{(t_{\text{max}} - t_{\text{eq}})} \int_{t_{\text{eq}}}^{t_{\text{max}}} E_{\text{kin}}^{\text{ion}}(t') dt'$$

$$\text{MSD}(t, T) \equiv \frac{1}{N_{\text{Li}}} \left\langle \sum_{i=1}^{N_{\text{Li}}} |\mathbf{R}_i(t) - \mathbf{R}_i(0)|^2 \right\rangle$$

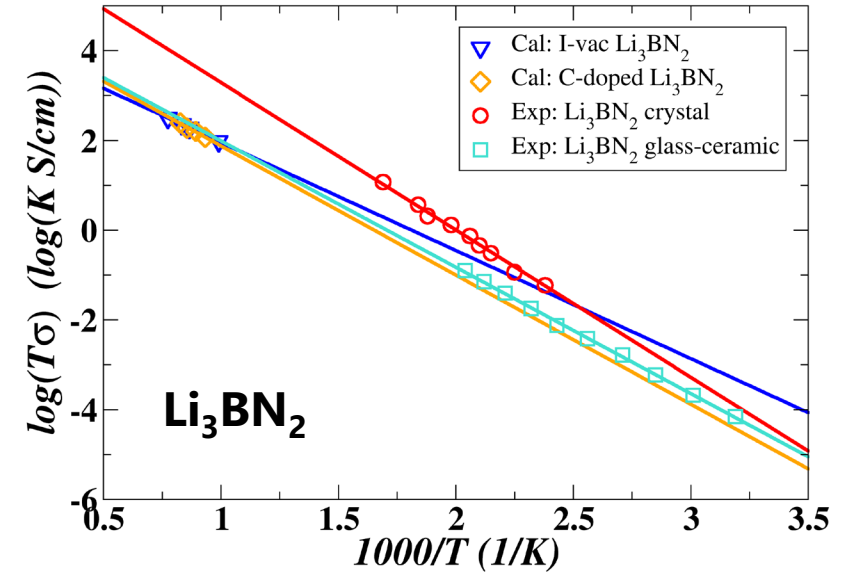
$$D_{\text{tr}}(T) = \frac{1}{6} \lim_{t \rightarrow \infty} \frac{1}{(t - t_{\text{eq}})} \text{MSD}(t - t_{\text{eq}}, T)$$





$$\sigma(T) = \rho q^2 \frac{D_{tr}(T)}{k_B T H_r}$$

$$D_{tr}(T) = D_0 e^{-E_a^{MD}/k_B T}$$



Materials	Analysis	$E_a$	$\sigma$ (T = 300 K)
I-vac $\text{Li}_3\text{BO}_3$	MD	0.53	$3.2 \times 10^{-7}$
	NEB	0.38 (bc)	--
<b>F-doped <math>\text{Li}_3\text{BO}_3</math></b>	MD	0.45	$3.4 \times 10^{-6}$
	<b>NEB</b>	<b>0.72 (bc)</b>	--
Polycrystalline $\text{Li}_3\text{BO}_3$	Exp <sup>1</sup>	0.51	$2.0 \times 10^{-6}$
Glassy $\text{Li}_3\text{BO}_3$	Exp <sup>2</sup>	0.60	$3.4 \times 10^{-7}$

Materials	Analysis	$E_a$	$\sigma$ (T = 300 K)
I-vac $\text{Li}_3\text{BN}_2$	MD	0.48	$7.2 \times 10^{-7}$
	NEB	0.30 (a)/0.81 (bc)	--
C-doped $\text{Li}_3\text{BN}_2$	MD	0.57	$4.8 \times 10^{-8}$
	NEB	0.40 (a)/1.02 (bc)	--
Polycrystalline $\text{Li}_3\text{BN}_2$	Exp <sup>2</sup>	0.66	$1.4 \times 10^{-7}$
Glassy-ceramic $\text{Li}_3\text{BN}_2$	Exp <sup>3</sup>	0.56	$1.1 \times 10^{-7}$

Exp<sup>1</sup>: Ohta *et al.*, *J. of Power Sources* **238**, 53 (2013); Exp<sup>2</sup>: Yamane *et al.*, *J. Solid State Chem.* **71**, 1 (1987); Exp<sup>3</sup>: Shigeno *et al.*, *Solid State Ion.* **339**, 114985 (2019)

## Predicted reactions:

$$\Delta F = \sum_i F_i^P - \sum_j F_j^R$$

Reaction: R → P	$\Delta U_{SL}$	$\Delta F_{vib}$	$\Delta F$
$\text{Li}_3\text{BO}_3 + \frac{3}{4}\text{Li} \rightarrow \frac{3}{4}\text{LiBO}_2 + \frac{1}{4}\text{B} + \frac{3}{2}\text{Li}_2\text{O}$	0.19	0.07	0.26
$\text{Li}_3\text{BO}_3 + \text{Li} \rightarrow 2\text{Li}_2\text{O} + \frac{1}{3}\text{B} + \frac{1}{3}\text{B}_2\text{O}_3$	0.64	0.08	0.72
$\text{Li}_3\text{BN}_2 + 3\text{Li} \rightarrow 2\text{Li}_3\text{N} + \text{B}$	1.91	0.06	1.97
$\text{Li}_3\text{BN}_2 + \frac{3}{2}\text{Li} \rightarrow \frac{3}{2}\text{Li}_3\text{N} + \frac{1}{2}\text{B} + \frac{1}{2}\text{BN}$	1.38	0.07	1.45

## The interface energy:

$$\gamma_{ab}(\Omega, n_b) = \frac{E(\Omega, A, n_a, n_b) - n_a E_a - n_b E_b}{2A_i}$$

$$\gamma_{ab}(\Omega, n_b) = \gamma_{ab}^{\text{lim}}(\Omega) - \sigma n_b$$

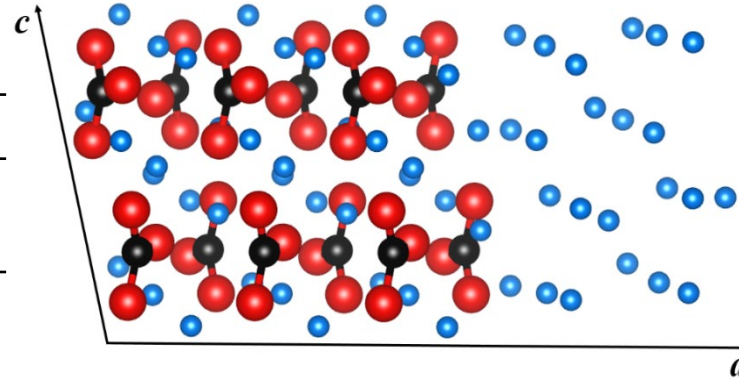
Where  $\sigma$  denotes the strain factor.

a -- electrolyte; b -- Li

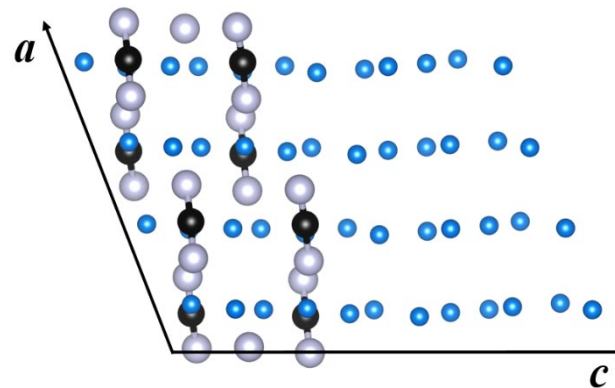
$$\sigma(\text{Li}_3\text{BO}_3/\text{Li}) = 19 \text{ meV}/\text{\AA}^2/\text{Li}$$

$$\sigma(\text{Li}_3\text{BN}_2/\text{Li}) = \mathbf{0.11 \text{ meV}/\text{\AA}^2/\text{Li}}$$

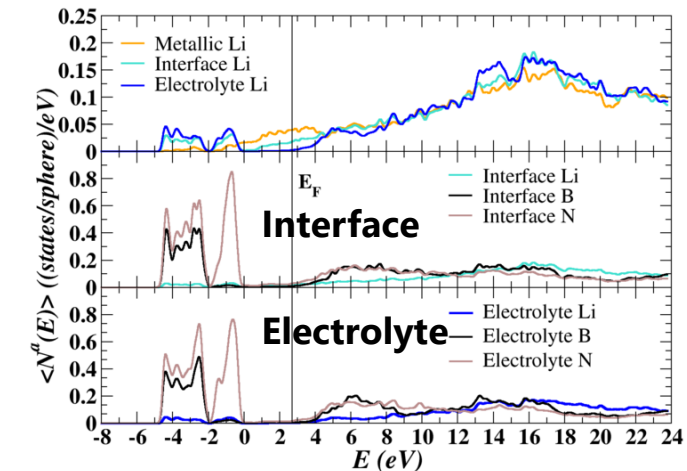
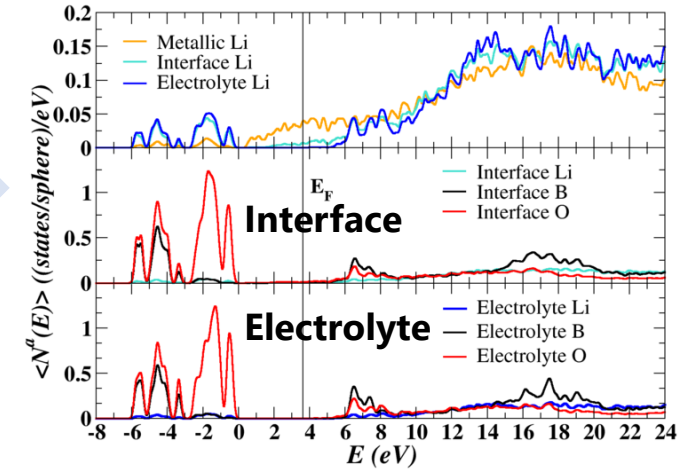
-- good compatibility



3x1x1 supercell of  $\text{Li}_3\text{BO}_3$  and 24 metallic Li ions in [100] direction.



2x1x1 supercell of  $\text{Li}_3\text{BN}_2$  and 24 metallic Li ions in [001] direction.







- ❑ The imaginary phonon modes near the M point of the Brillouin zone suggested the structural instability of the reported tetragonal phase of  $\alpha$ -Li<sub>3</sub>BN<sub>2</sub>.
- ❑ The real  $\alpha$  phase has an orthorhombic structure formed with twice as many formula units and very small adjustments of the fractional coordinates compared with the original analysis. Quasi-harmonic corrections further improve the comparisons with experiment.
- ❑ Both NEB and MD simulations indicate that the Li ion migration in monoclinic crystals of Li<sub>3</sub>BO<sub>3</sub> and  $\beta$ -Li<sub>3</sub>BN<sub>2</sub> most likely proceeds via vacancy mechanisms.
- ❑ To enhance the ionic conductivity, the practical methods include: 1) Varying the structural perfection to intentionally form poor-crystallinity material containing vacancy-interstitial defect pairs; 2) Substituting F for O in Li<sub>3</sub>BO<sub>3</sub> and C for B in  $\beta$ -Li<sub>3</sub>BN<sub>2</sub>.
- ❑ The plausible Li<sub>3</sub>BO<sub>3</sub>/Li and  $\beta$ -Li<sub>3</sub>BN<sub>2</sub>/Li interfaces are found to be physically and chemically stable.

**Phys. Rev. Mater. 5, 085402 & 085403 (2021)**

- Research background: General motivation and theoretical tools
- **Finished/ongoing projects: Inputs and outcomes**

## **Na<sub>4</sub>P<sub>2</sub>S<sub>6</sub>, Li<sub>4</sub>P<sub>2</sub>S<sub>6</sub>, and possible alloy**

Yan Li, Zachary D. Hood, and N. A. W. Holzwarth  
Phys. Rev. Mater. 4, 045406 (2020)

## **Phonon dispersion**

Yan Li, W. C. Kerr, and N. A. W. Holzwarth  
J. Condens. Matter Phys. 32, 055402 (2020)

## **Li<sub>3</sub>BO<sub>3</sub> and Li<sub>3</sub>BN<sub>2</sub> (I & II)**

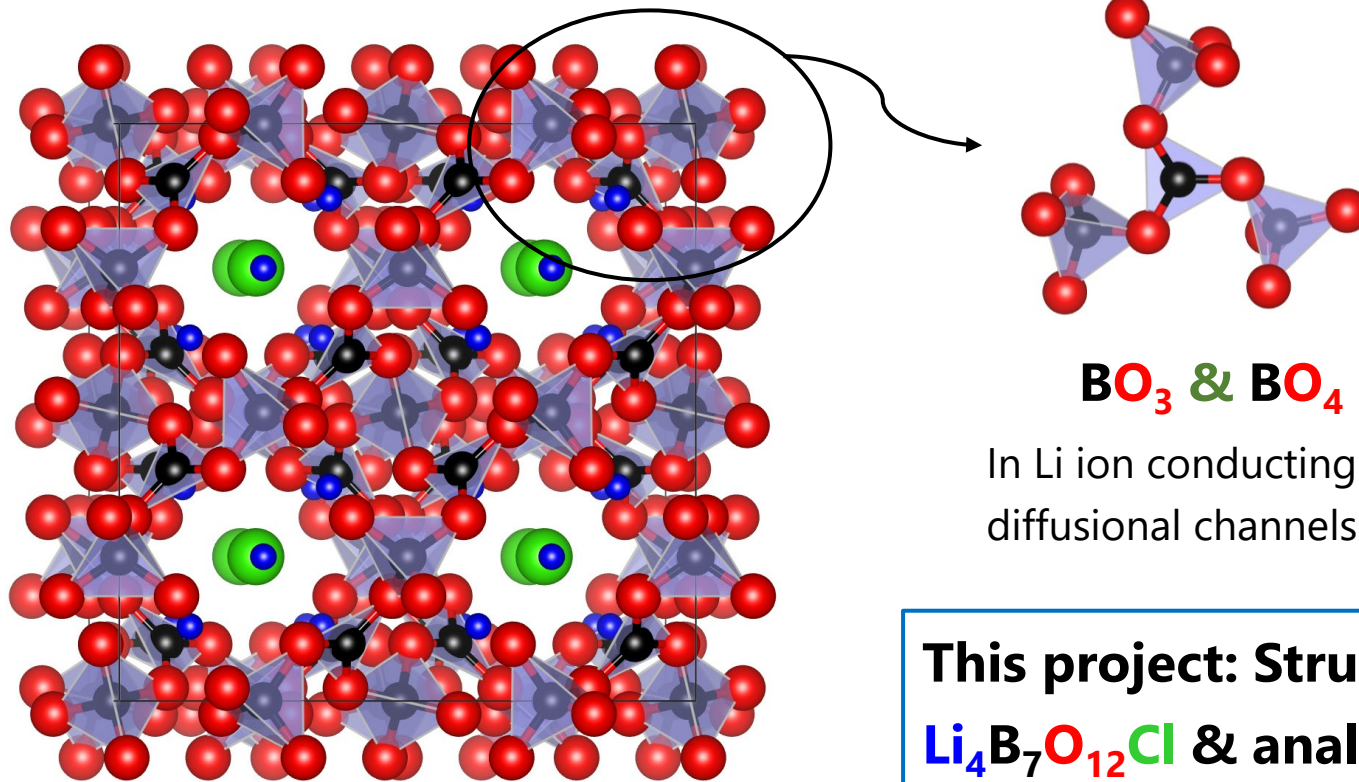
Yan Li, Zachary D. Hood, and N. A. W. Holzwarth  
Phys. Rev. Mater. 5, 085402 & 085403 (2021)

## **Li<sub>4+x</sub>B<sub>7</sub>O<sub>12+x/2</sub>Cl (x = 0, 1) and related**

Li<sub>7.5</sub>B<sub>10</sub>O<sub>18</sub>X<sub>1.5</sub> (X = Cl, Br, and I)

Mineral boracites  $M_3B_7O_{13}X$ , where M = Mg, Cr, Mn, Fe, Co, Ni, Zn or Cd, and X = Cl, Br or I

Li-containing boracites  $Li_{4+x}B_7O_{12+x/2}X$ , where  $0 \leq x \leq 1$ , and X = Cl, Br or I

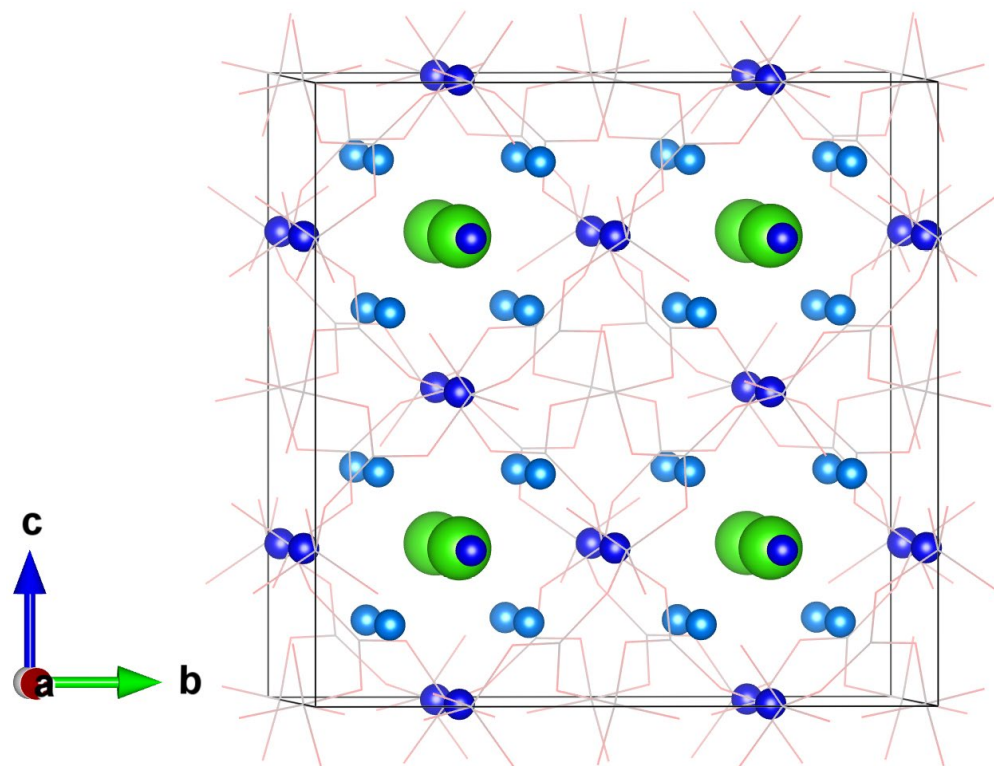


In Li ion conducting compounds, the **Li** ions are arranged in diffusional channels formed by the  $B_7O_{12}$  framework.

**This project: Structural and electrolyte properties of  $Li_4B_7O_{12}Cl$  & analogs obtained by ionic substitutions**

## Three disordered phases

\*Jeitschko *et al.*, *Acta Cryst.* B33, 2767-2775 (1977)



Ideal cubic model  
8 formula units/cell

**Above 348 K**     $\gamma$  phase ( $F\bar{4}3c$ , No. 219)

Li(24c): 93.7% occupied

Li(32e): 31.6% occupied

**310 – 348 K**     $\beta$  phase ( $P\bar{4}3c$ , No. 218)

Ideal  $F\bar{4}3c$  model

Li(24c): 96.7% occupied

Li(32e): 27.8% occupied

**Room T**     $\alpha$  phase (Exp. R3, No. 146)

Ideal  $F\bar{4}3c$  model

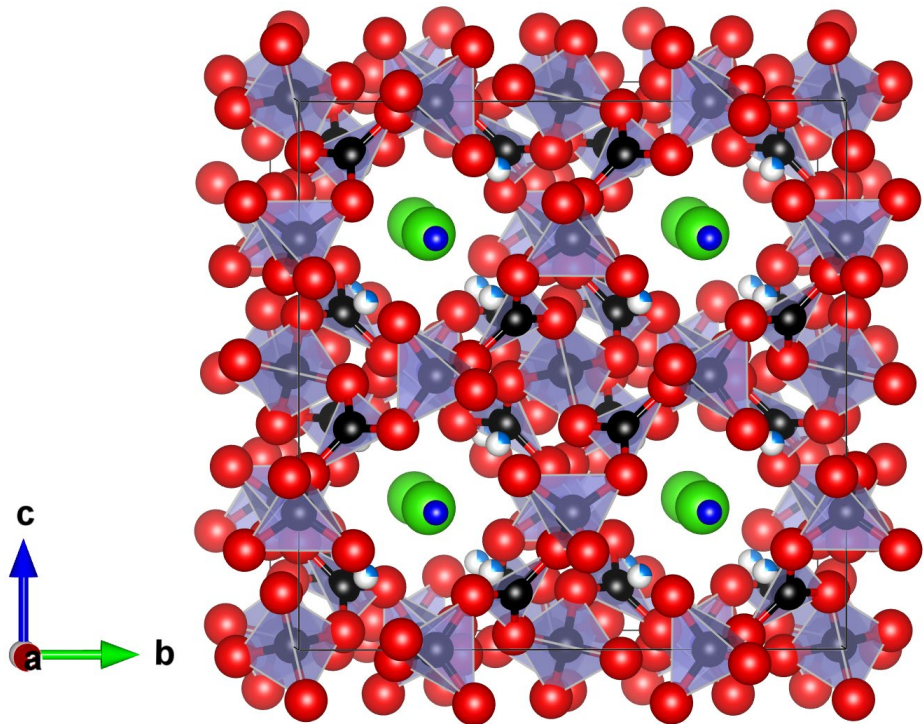
Li(24c): 100% occupied

Li(32e): 25% occupied

\* The real space groups of the  $\alpha$  and  $\beta$  phases are subgroups of  $F\bar{4}3c$ .

\*\* The atomic positions for both  $\alpha$  and  $\beta$  phases are not known in experiment

● Li(24c) 
 ● Li(32e) 
 ● B 
 ● O 
 ● Cl

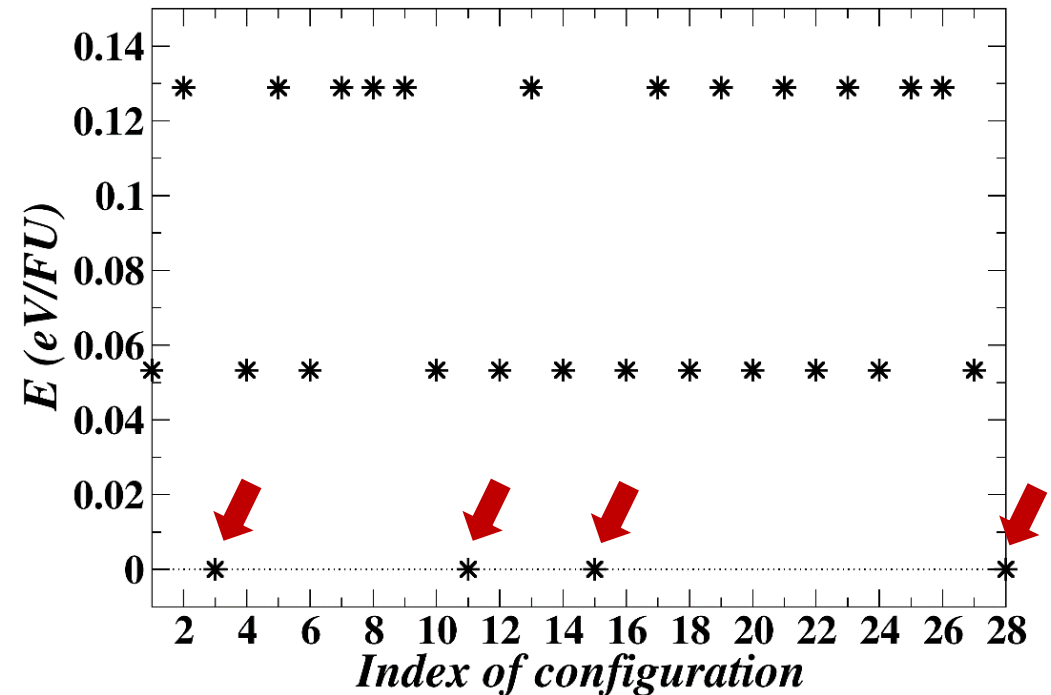


Conventional cell of  $F\bar{4}3c$  model

Li(24c): 100% occupied

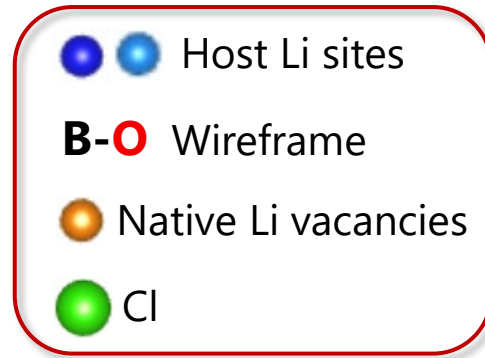
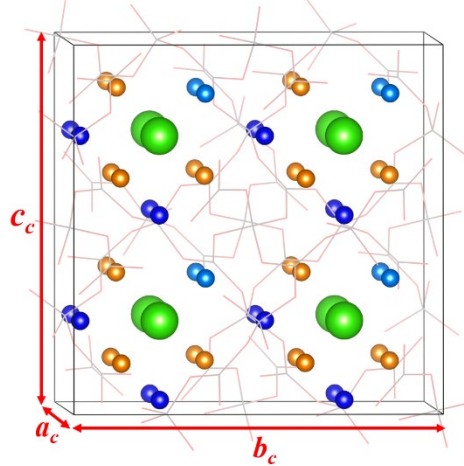
Li(32e): 25% occupied

Perform geometry optimizations for 28 unique configurations in the primitive cell setting

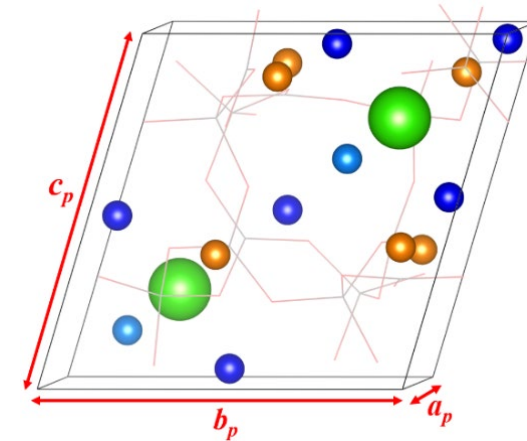


The calculation finds four identical lowest-energy configurations with the **rhombohedral R3c (No. 161)** symmetry

## Conventional cell 8 formula units



## Face-centered primitive cell 2 formula units



$$\mathbf{a}_c = \mathbf{b}_c = \mathbf{c}_c \text{ and } \alpha = \beta = \gamma = \theta_c \approx 90^\circ$$

$$\mathbf{a}_c = a_c(\hat{\mathbf{x}}(\lambda_c + 2\mu_c) + \hat{\mathbf{y}}(\lambda_c - \mu_c) + \hat{\mathbf{z}}(\lambda_c - \mu_c))$$

$$\mathbf{b}_c = a_c(\hat{\mathbf{x}}(\lambda_c - \mu_c) + \hat{\mathbf{y}}(\lambda_c + 2\mu_c) + \hat{\mathbf{z}}(\lambda_c - \mu_c))$$

$$\mathbf{c}_c = a_c(\hat{\mathbf{x}}(\lambda_c - \mu_c) + \hat{\mathbf{y}}(\lambda_c - \mu_c) + \hat{\mathbf{z}}(\lambda_c + 2\mu_c))$$

$$\lambda_c \equiv \frac{\sqrt{1 + 2 \cos \theta_c}}{3} \text{ and } \mu_c \equiv \frac{\sqrt{1 - \cos \theta_c}}{3}$$

$$\cos(\theta_c) = \frac{2 \cos(\theta_p) - 1}{3 - 2 \cos(\theta_p)}$$

$$\mathbf{a}_p = \mathbf{b}_p = \mathbf{c}_p \text{ and } \alpha = \beta = \gamma = \theta_p \approx 60^\circ$$

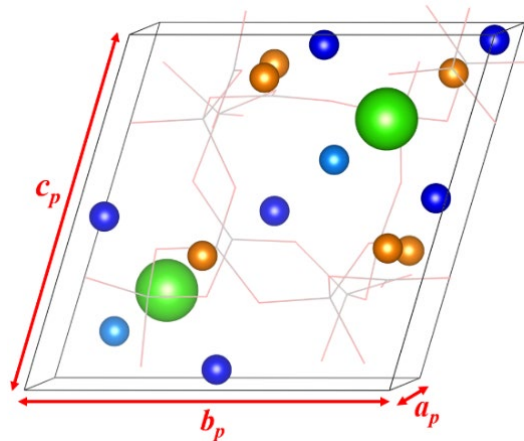
$$\mathbf{a}_p = (\mathbf{a}_c + \mathbf{b}_c)/2 = a_p(\hat{\mathbf{x}}(\lambda_p + \mu_p) + \hat{\mathbf{y}}(\lambda_p + \mu_p) + \hat{\mathbf{z}}(\lambda_p - 2\mu_p))$$

$$\mathbf{b}_p = (\mathbf{b}_c + \mathbf{c}_c)/2 = a_p(\hat{\mathbf{x}}(\lambda_p - 2\mu_p) + \hat{\mathbf{y}}(\lambda_p + \mu_p) + \hat{\mathbf{z}}(\lambda_p + \mu_p))$$

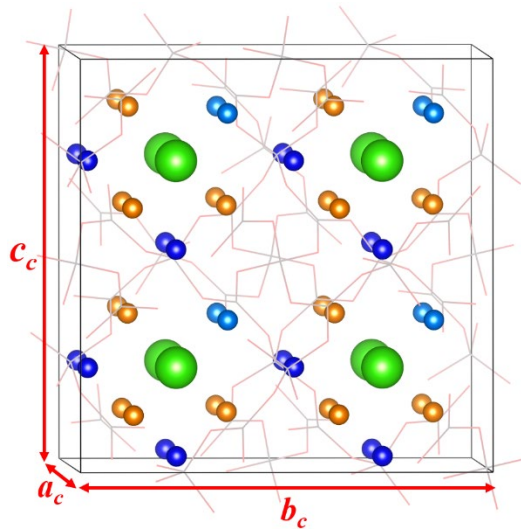
$$\mathbf{c}_p = (\mathbf{a}_c + \mathbf{c}_c)/2 = a_p(\hat{\mathbf{x}}(\lambda_p + \mu_p) + \hat{\mathbf{y}}(\lambda_p - 2\mu_p) + \hat{\mathbf{z}}(\lambda_p + \mu_p))$$

$$\lambda_p \equiv \frac{\sqrt{1 + 2 \cos \theta_p}}{3} \text{ and } \mu_p \equiv \frac{\sqrt{1 - \cos \theta_p}}{3} \text{ and } a_p = \frac{a_c}{\sqrt{3 - 2 \cos(\theta_p)}}$$

$$\cos(\theta_p) = \frac{1 + 3 \cos(\theta_c)}{2(1 + \cos(\theta_c))}$$



Primitive cell model



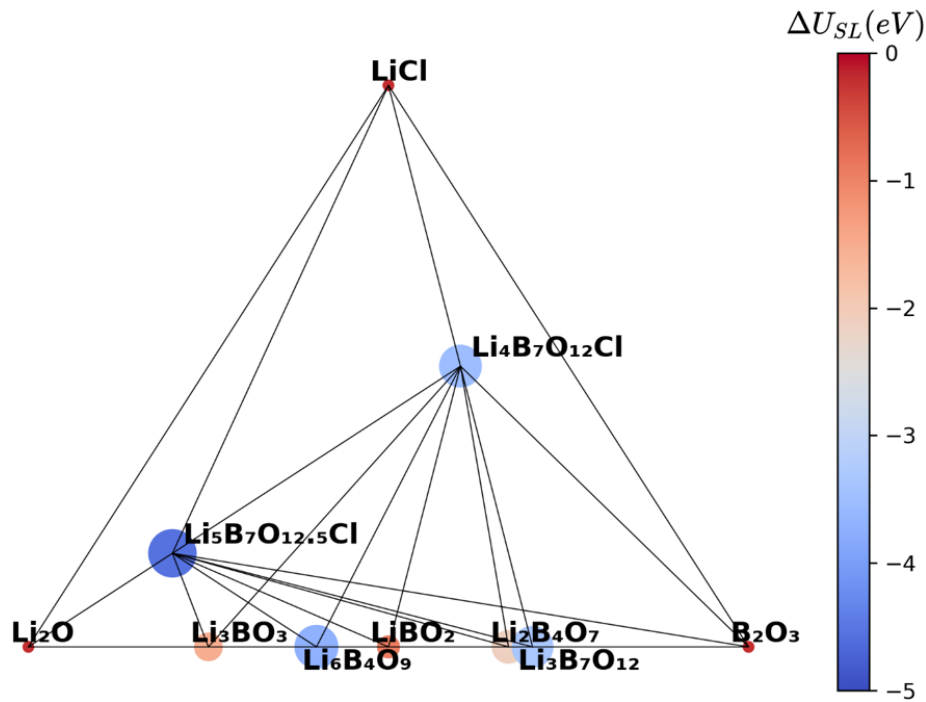
Conventional cell model

**Lattice parameters and Li ion fractional coordinates for the R3c structure of  $\alpha$ -Li<sub>4</sub>B<sub>7</sub>O<sub>12</sub>Cl, comparing calculated results with the experimental measurements.**

Li <sub>4</sub> B <sub>7</sub> O <sub>12</sub> Cl	a = b = c (Å)	$\alpha = \beta = \gamma$ (deg)
Cal. R3c	12.137	90.108
Exp.* R3	12.141	90.084
Exp.* F $\bar{4}$ 3c model	12.141	90.000

Cal. R3c				Exp. F $\bar{4}$ 3c model			
Atom	Wyck	f(x, y, z) (conv.)	Occ.	Atom	Wyck	f(x, y, z)	Occ.
Li(1)	4x6 b	(0.030, 0.245, 0.245)	1.00	Li(1)	24 c	(0.000, 0.250, 0.250)	1.00
Li(2)	4x2 a	(0.865, 0.865, 0.865)	1.00	Li(2)	32 e	(0.871, 0.871, 0.871)	0.25
Vac. Li	4x6 b	(0.633, 0.635, 0.873)	0.00				

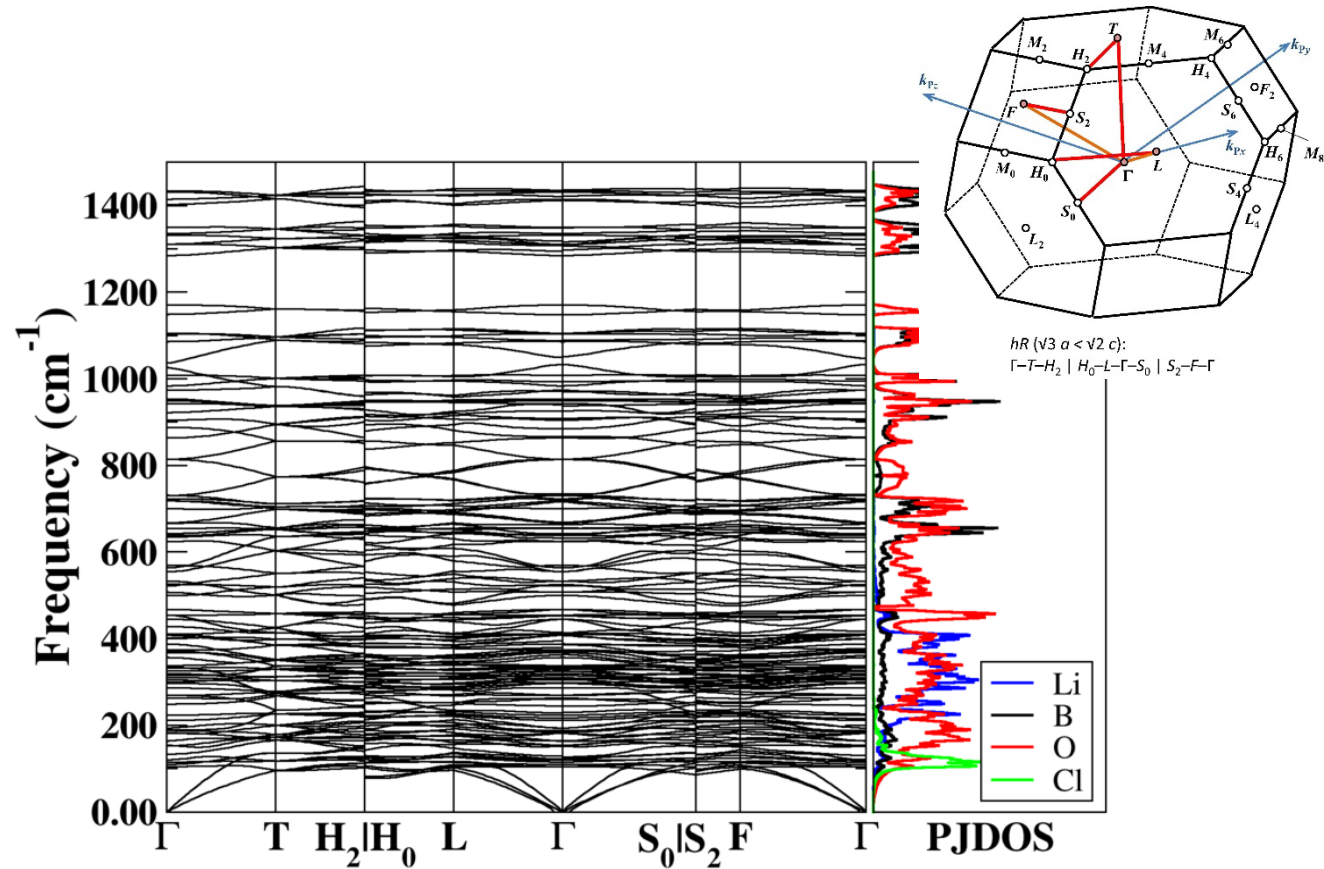
\*Experimental data taken from Jeitschko *et al.*, *Acta Cryst. B.* **33**, 2767-2775 (1977)



$\text{Li}_2\text{O}\text{-B}_2\text{O}_3\text{-LiCl}$  phase diagram at 0 K and 0 atm

$$\text{Reaction energy: } \Delta U_{SL} = U_{SL} - \sum x_i U_{SL}^i$$

Where  $U_{SL}$  is the total static energy per formula unit of a specific compound.  $x_i$  with  $i = \text{Li}_2\text{O}, \text{B}_2\text{O}_3,$  and  $\text{LiCl}$  represents the compositional ratio of each reference phase for which the total static energy per formula unit is denoted by  $U_{SL}^i$ .

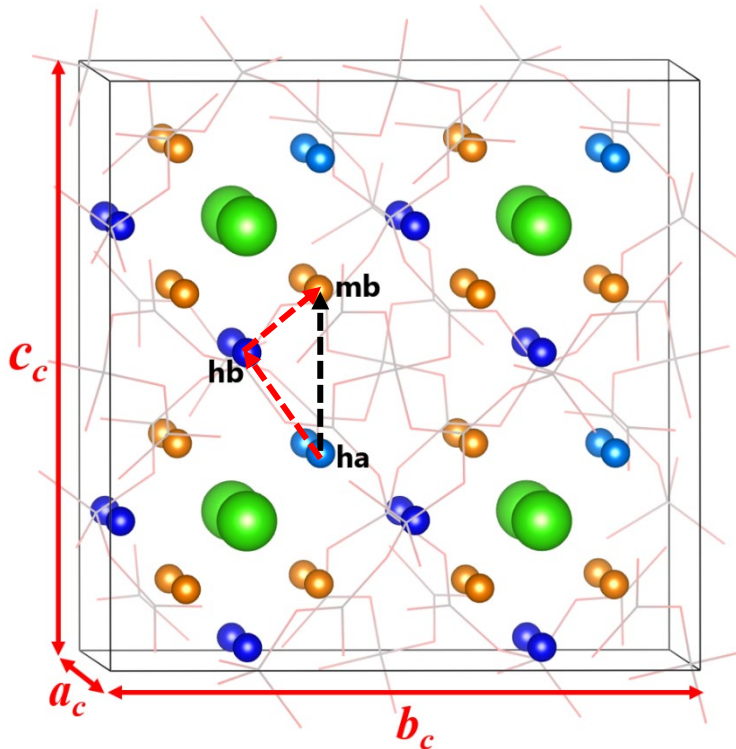


Phonon dispersion curves and projected density states of  $\text{Li}_4\text{B}_7\text{O}_{12}\text{Cl}$  with frequencies ranging from 0 ~ 1440  $\text{cm}^{-1}$ .

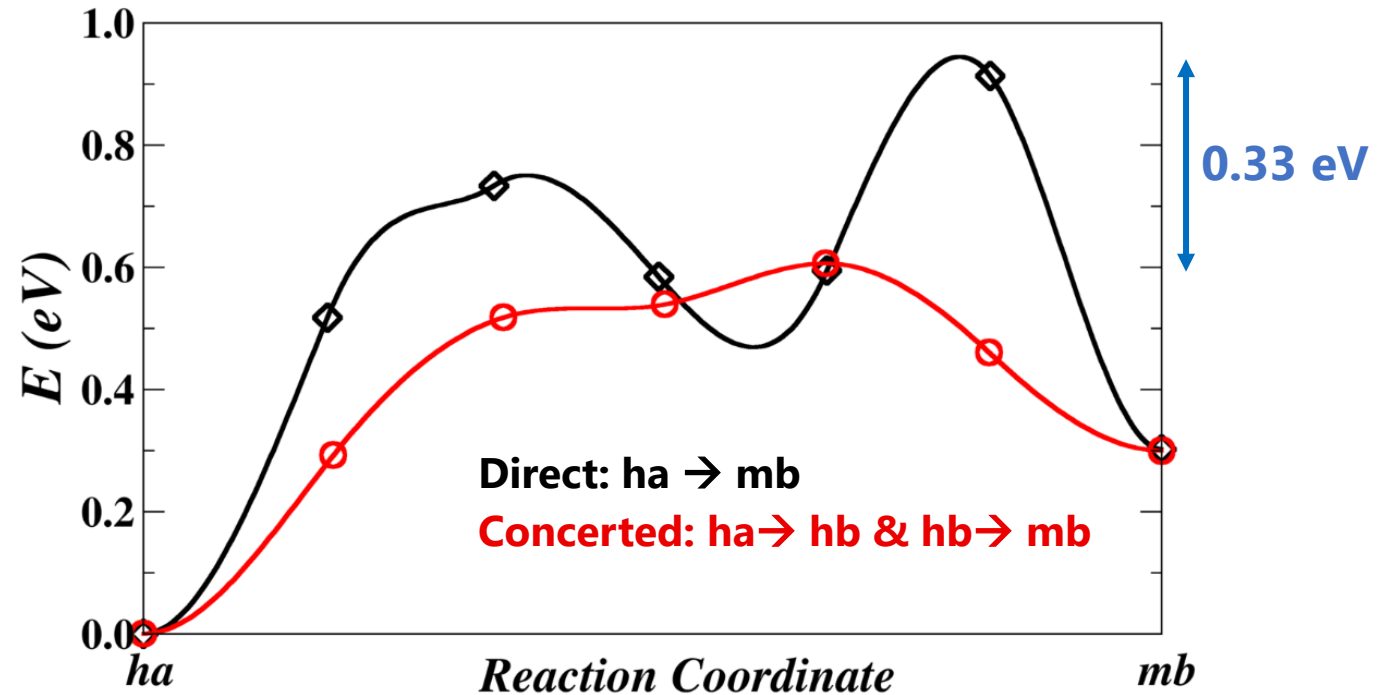
Brillouin zone diagram: Hinuma et al., *Comp. Mat. Sci.* **128**, 140-184 (2017). Note that the rhombohedral lattice is described by an equivalent hexagonal system.



$$E_{hb} < E_{ha} < E_{mb}$$



**hb:** host b-type site; **ha:** host a-type site  
**mb:** metastable b-type site (native vacancy)

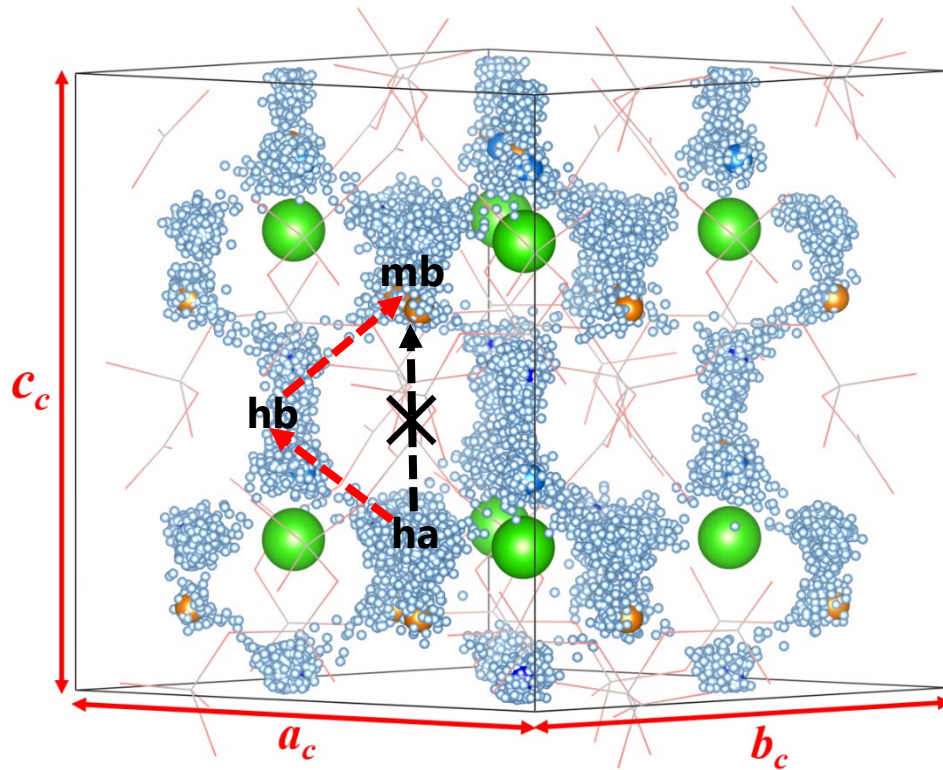


→ The concerted migration mechanism reduces the energy barrier for Li ion conduction in  $\alpha\text{-Li}_4\text{B}_7\text{O}_{12}\text{Cl}$ .

NEB: <sup>1</sup>Jónsson et al., in *Classical and Quantum Dynamics in Condensed Phase Simulations*, World Scientific, Singapore (1998)

<sup>2</sup>Henkelman et al., *J. Chem. Phys.* **113**, 9901-9904 (2000)

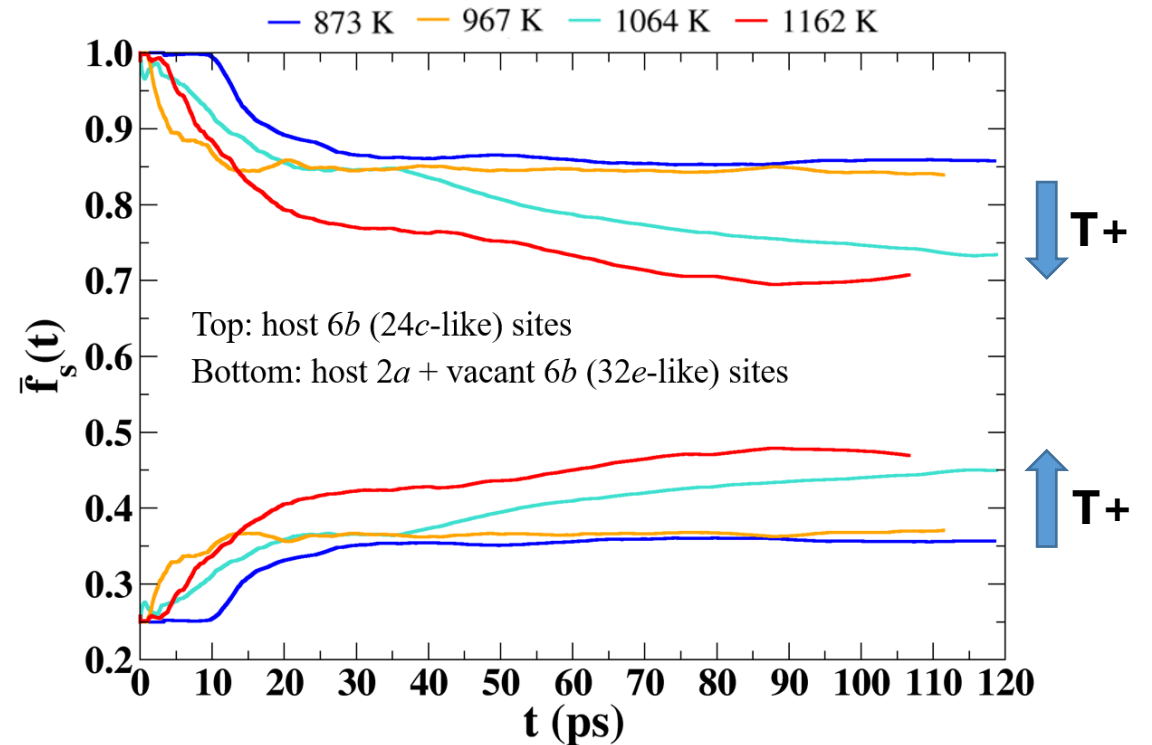
- Li(6b) ● Li(2a) ● Vacant Li(6b)
- Time-dependent positions of Li ions



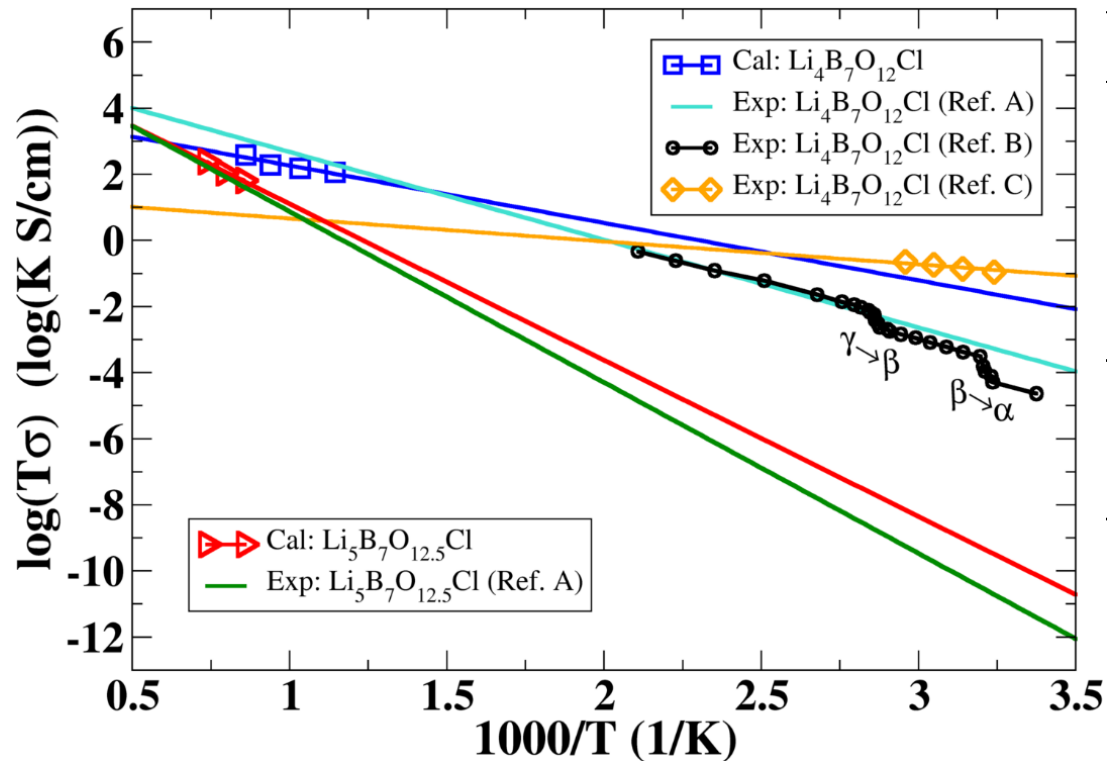
Model of  $\text{Li}_4\text{B}_7\text{O}_{12}\text{Cl}$  crystal cell with superposed Li positions of molecular dynamics simulation at  $\langle T \rangle = 1162 \text{ K}$ .

Site occupancy factor:  $f_s(t) = \frac{1}{N_s^{Li}} \sum_{i=1}^{N_s^{Li}} n_s^i(t), i = 1, 2, \dots, N_s^{Li}$

Time-averaged:  $\bar{f}_s(t) = \frac{1}{t} \int_0^t f_s(t') dt'$



\*Recall: the three reported forms  $\alpha$  ( $T < 310 \text{ K}$ ),  $\beta$  ( $310 \text{ K} < T < 348 \text{ K}$ ),  $\gamma$  ( $T > 348 \text{ K}$ ) mainly differ in lattice site occupancy.



Materials	Analysis	Samples	$E_a$ (eV)	$\sigma$ (T = 300 K, S/cm)
$\text{Li}_4\text{B}_7\text{O}_{12}\text{Cl}$	Cal.	Ideal	0.34	$3.83 \times 10^{-4}$
	Exp: Ref (A)	Polycrystalline	0.53	$1.00 \times 10^{-7}$
	Exp: Ref (B)	Single crystal	0.49	$0.98 \times 10^{-7}$
	Exp: Ref (C)	Polycrystalline	0.14	$3.68 \times 10^{-4}$
$\text{Li}_5\text{B}_7\text{O}_{12.5}\text{Cl}^*$	Cal.	Ideal	0.84	$6.58 \times 10^{-12}$
	Exp: Ref (A)	Polycrystalline	1.03	$2.14 \times 10^{-14}$

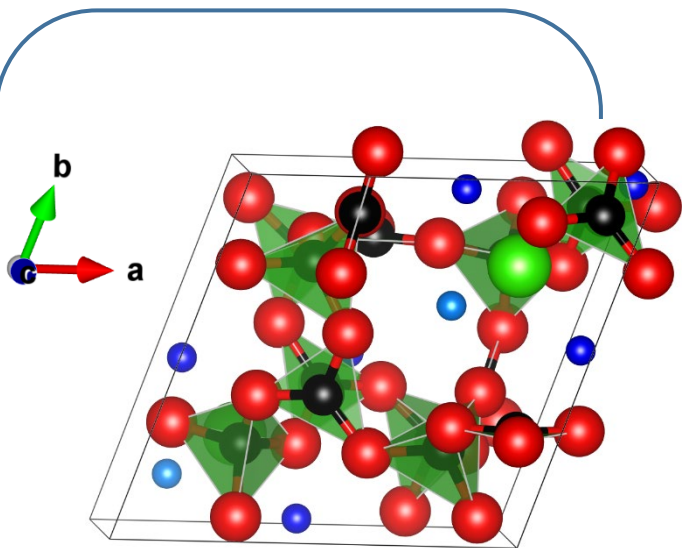
$$\sigma(T) = \rho q^2 \frac{D_{tr}(T)}{k_B T H_r} \quad \text{with } H_r = 1, D_{tr}(T) = D_0 e^{-E_a^{MD}/k_B T}$$

\*The ordered  $\text{Li}_5\text{B}_7\text{O}_{12.5}\text{Cl}$  has a similar B-O framework with  $\text{Li}_4\text{B}_7\text{O}_{12}\text{Cl}$  but a different ordering of Li ions.

Ref. A: Cales *et al.*, *Solid State Commun.* **24**, 323 (1977)

Ref. B: Jeitschko *et al.*, *Acta Cryst. B.* **33**, 2767-2775 (1977)

Ref. C: Tan *et al.*, *ACS Appl. Energy Mater.* **2**, 5140 (2019).

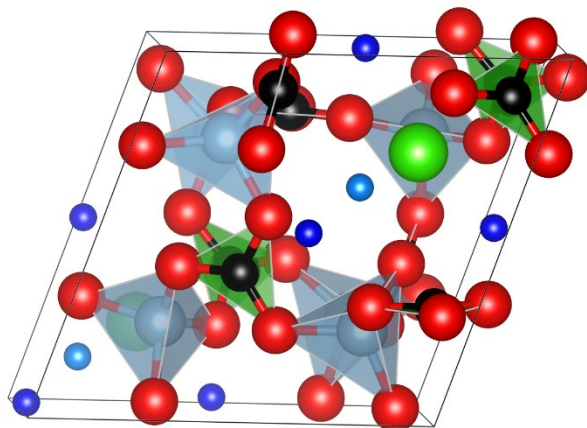


Original material

**Rhombohedral R3c**

$$\begin{aligned} a_p &= b_p = c_p = 8.574 \text{ \AA} \\ \alpha_p &= \beta_p = \gamma_p = 60.124^\circ \\ a_c &= b_c = c_c = 12.137 \text{ \AA} \\ \alpha_c &= \beta_c = \gamma_c = 90.108^\circ \end{aligned}$$

B(1)  $\rightarrow$  Al



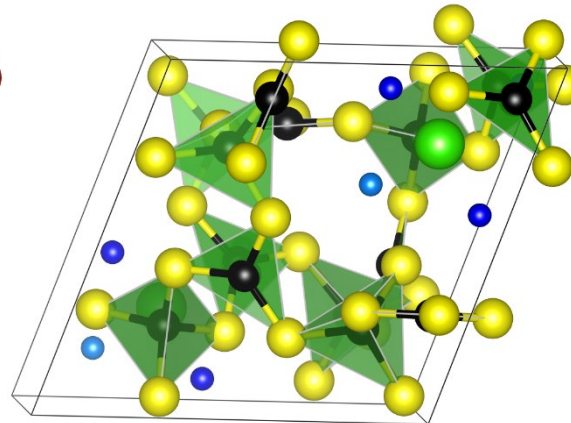
Realized in experiment\*

**Rhombohedral R3c**

$$\begin{aligned} a_p &= b_p = c_p = 9.133 \text{ \AA} \\ \alpha_p &= \beta_p = \gamma_p = 61.194^\circ \\ a_c &= b_c = c_c = 13.033 \text{ \AA} \\ \alpha_c &= \beta_c = \gamma_c = 91.022^\circ \end{aligned}$$

\*Kajihara *et al.*, *Bull. Chem. Soc. Jpn.*  
**90**, 1279–1286 (2017)

O  $\rightarrow$  S

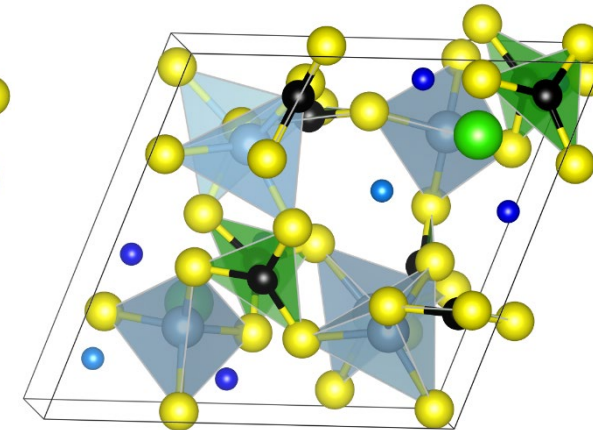


Predicted in this work

**Rhombohedral R3c**

$$\begin{aligned} a_p &= b_p = c_p = 10.584 \text{ \AA} \\ \alpha_p &= \beta_p = \gamma_p = 59.704^\circ \\ a_c &= b_c = c_c = 14.934 \text{ \AA} \\ \alpha_c &= \beta_c = \gamma_c = 89.743^\circ \end{aligned}$$

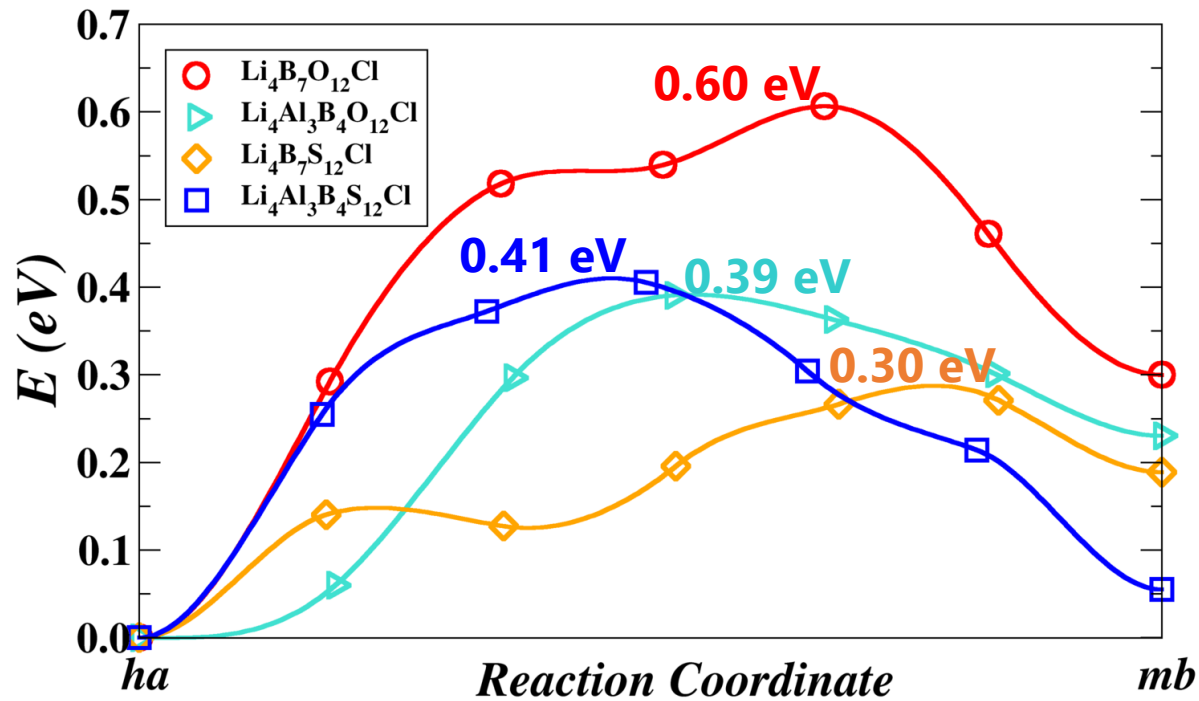
B(1)  $\rightarrow$  Al & O  $\rightarrow$  S



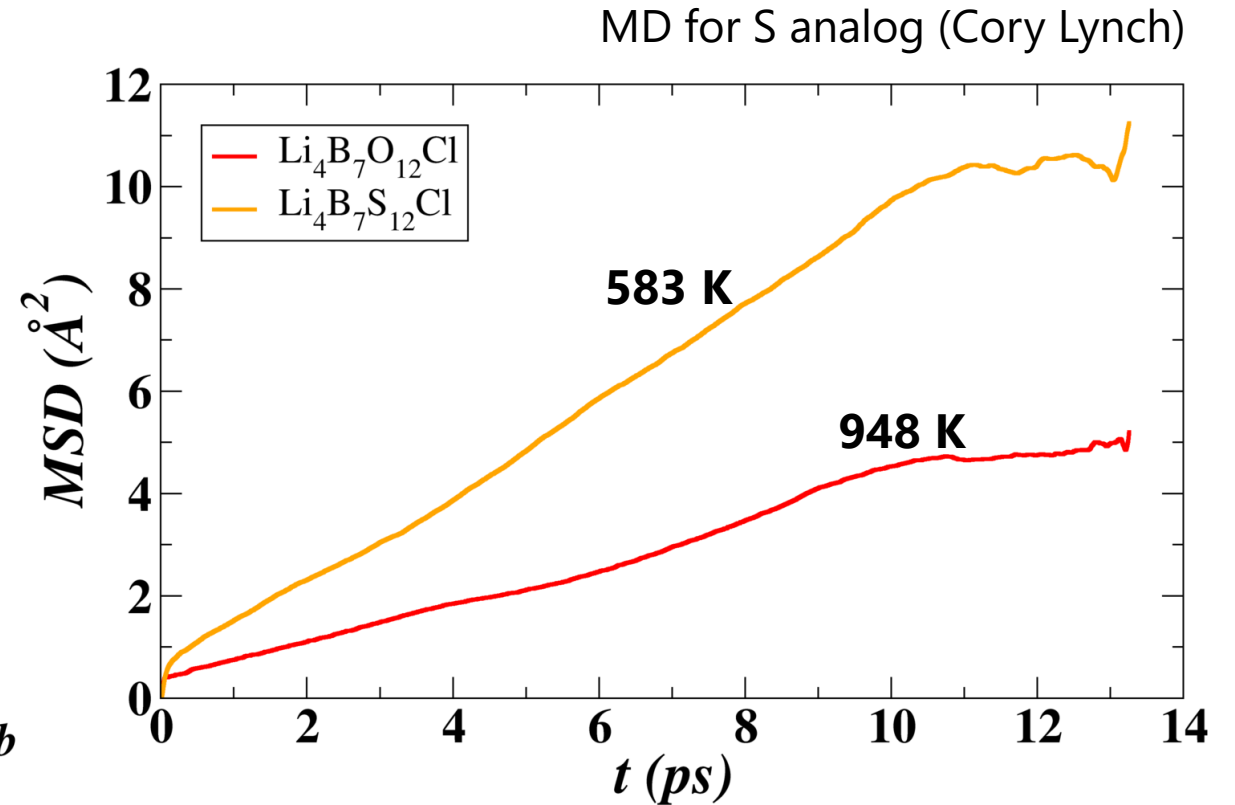
Predicted in this work

**Rhombohedral R3c**

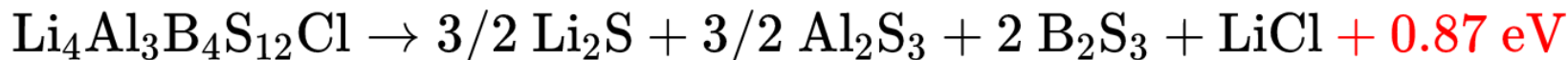
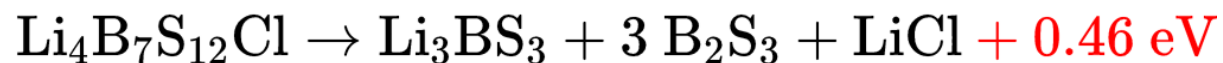
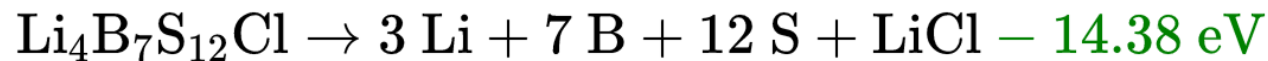
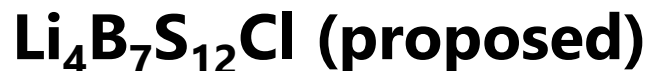
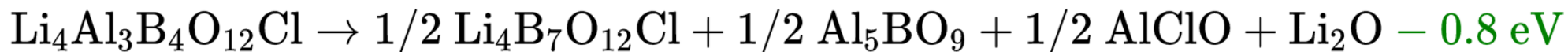
$$\begin{aligned} a_p &= b_p = c_p = 11.386 \text{ \AA} \\ \alpha_p &= \beta_p = \gamma_p = 68.601^\circ \\ a_c &= b_c = c_c = 15.933 \text{ \AA} \\ \alpha_c &= \beta_c = \gamma_c = 88.771^\circ \end{aligned}$$



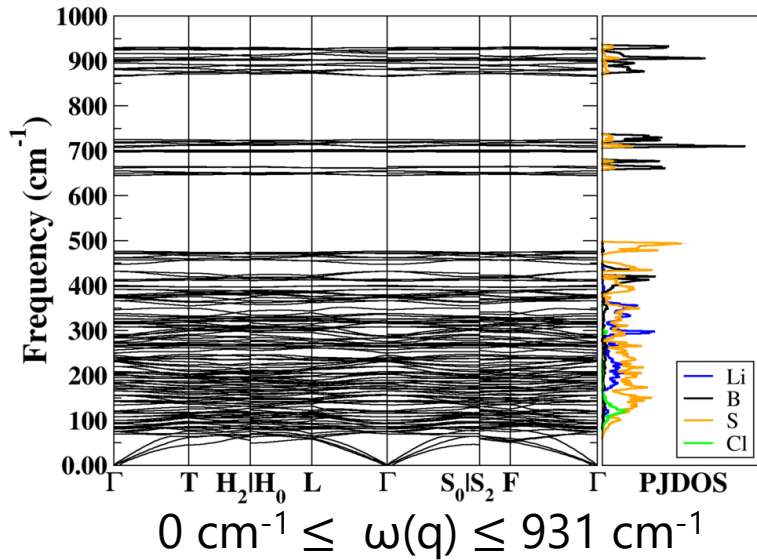
NEB energy diagram of concerted migrations



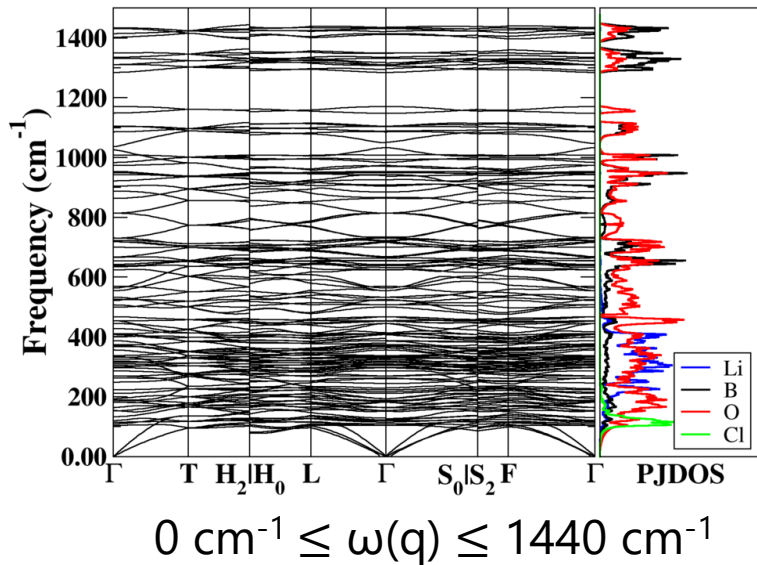
Mean squared displacement vs. time interval



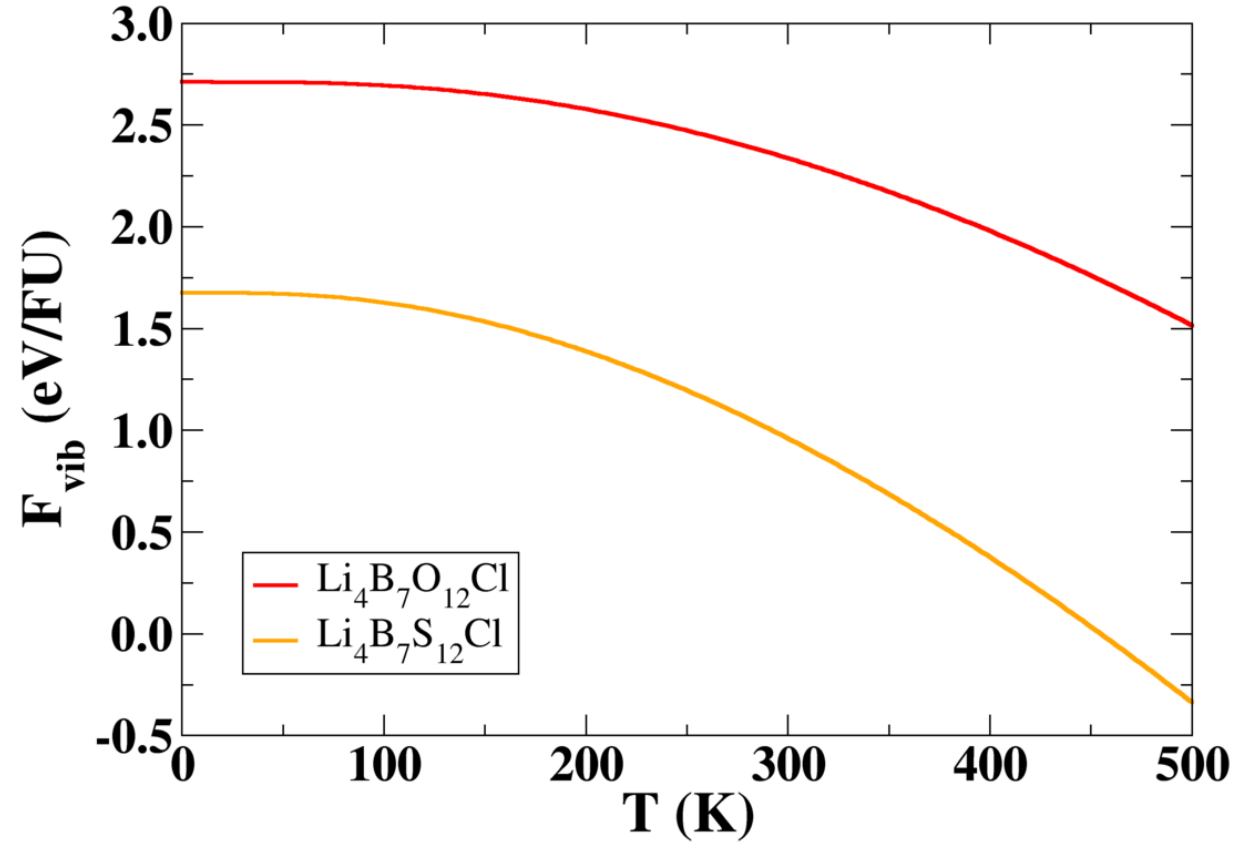
**Predicated**  
**Li<sub>4</sub>B<sub>7</sub>S<sub>12</sub>Cl**



**Known**  
**Li<sub>4</sub>B<sub>7</sub>O<sub>12</sub>Cl**



$$F_{vib}(T) = k_B T \int_0^\infty d\omega \ln \left( 2 \sinh \left( \frac{\hbar\omega}{2k_B T} \right) \right) g(\omega)$$



$$\Delta F_{vib}(T = 300 \text{ K}) = 1.38 \text{ eV/FU}$$



- ❑ The ground state structure of the room-temperature form of  $\text{Li}_4\text{B}_7\text{O}_{12}\text{Cl}$  is identified to have rhombohedral R3c symmetry. The phase is estimated to be stable from the analysis of the convex hull approach and of the phonon spectrum.
- ❑ The NEB calculations indicate that Li ion migration in  $\text{Li}_4\text{B}_7\text{O}_{12}\text{Cl}$  most likely proceeds via concerted migration mechanisms involving two host sites and one natural vacancy.
- ❑ The room-temperature ionic conductivity of  $\text{Li}_4\text{B}_7\text{O}_{12}\text{Cl}$ , calculated from the MD simulation results, is on the order of  $10^{-4}$  S/cm, which is in good agreement with the recent experiment measurement for pure polycrystalline samples.
- ❑ Consistent with the recent experimental results, our preliminary calculations also find reduced Li ion migration barriers in the partially B-replaced compound  $\text{Li}_4\text{Al}_3\text{B}_4\text{O}_{12}\text{Cl}$ . The studies on predicted compounds  $\text{Li}_4\text{B}_7\text{S}_{12}\text{Cl}$  and  $\text{Li}_4\text{Al}_3\text{B}_4\text{S}_{12}\text{Cl}$  also suggest improved Li ion conducting performance compared with  $\text{Li}_4\text{B}_7\text{O}_{12}\text{Cl}$ .
- ❑ The chemical stabilities of the  $\text{Li}_4\text{B}_7\text{S}_{12}\text{Cl}$  and  $\text{Li}_4\text{Al}_3\text{B}_4\text{S}_{12}\text{Cl}$  need further investigation.

**Manuscript in preparation**



□ Research background: General motivation and theoretical tools

□ **Finished/ongoing projects: Inputs and outcomes**

**$\text{Na}_4\text{P}_2\text{S}_6$ ,  $\text{Li}_4\text{P}_2\text{S}_6$ , and possible alloy**

Yan Li, Zachary D. Hood, and N. A. W. Holzwarth

Phys. Rev. Mater. 4, 045406 (2020)

**Phonon dispersion**

Yan Li, W. C. Kerr, and N. A. W. Holzwarth

J. Condens. Matter Phys. 32, 055402 (2020)

**$\text{Li}_3\text{BO}_3$  and  $\text{Li}_3\text{BN}_2$  (I & II)**

Yan Li, Zachary D. Hood, and N. A. W. Holzwarth

Phys. Rev. Mater. 5, 085402 & 085403 (2021)

**$\text{Li}_{4+x}\text{B}_7\text{O}_{12+x/2}\text{Cl}$  ( $x = 0, 1$ ) and related**

**$\text{Li}_{7.5}\text{B}_{10}\text{O}_{18}\text{X}_{1.5}$  ( $\text{X} = \text{Cl}, \text{Br}, \text{and I}$ )**



Monoclinic C2/c (No. 15)

Disordered Li and X sites

Room-T  $\sigma \sim \text{mS/cm}$



Communications



Angewandte  
International Edition  
Chemistry

How to cite: *Angew. Chem. Int. Ed.* 2021, 60, 6975–6980  
International Edition: doi.org/10.1002/anie.202013339  
German Edition: doi.org/10.1002/ange.202013339

VIP Ion Conductivity Very Important Paper

## Fast Li-Ion Conductivity in Superadamantanoid Lithium Thioborate Halides

Kavish Kaup, Abdeljalil Assoud, Jue Liu, and Linda F. Nazar\*

**Kaup et al. 2021**

[\*] K. Kaup, A. Assoud, L. F. Nazar

Department of Chemistry, Department of Chemical Engineering and the Waterloo Institute for Nanotechnology, University of Waterloo  
200 University Ave W, Waterloo, Ontario N2L 3G1 (Canada)  
E-mail: lfnazar@uwaterloo.ca

J. Liu

Neutron Scattering Division, Oak Ridge National Laboratory  
Oak Ridge, TN 37831 (USA)

of supertetrahedral clusters (also antanoid)  $\text{B}_{10}\text{S}_{20}$  structural units. ructures were observed in lithium licates,<sup>[11,12]</sup> lithium nitridophos- per thioborates such as  $\text{Ag}_6\text{B}_{10}\text{S}_{18}$  many other sulfide-based materi- networks are of interest because the d anions to distribute into the void s. For frameworks with a large void akly bonded to the surrounding tion mobility within the structure.

For such materials, the highest reported room-temperature ionic conductivity is only  $4 \times 10^{-4} \text{ S cm}^{-1}$  for sodium phosphido- silicates,<sup>[11]</sup> and  $\approx 10^{-7} \text{ S cm}^{-1}$  for lithium phosphido- silicates.<sup>[21]</sup> An ionic conductivity greater than  $10^{-4} \text{ S cm}^{-1}$  is often considered fast, but at least  $10^{-3} \text{ S cm}^{-1}$  is necessary to achieve practical solid-state batteries.<sup>[22]</sup>

lithium and halide anion disorder. The phases are non- stoichiometric, adopting slightly varying halide contents within the materials. These new superadamantanoid materials exhibit high ionic conductivities up to  $1.4 \text{ mS cm}^{-1}$ , which can be effectively tuned by the polarizability of the halide anion within the channels.

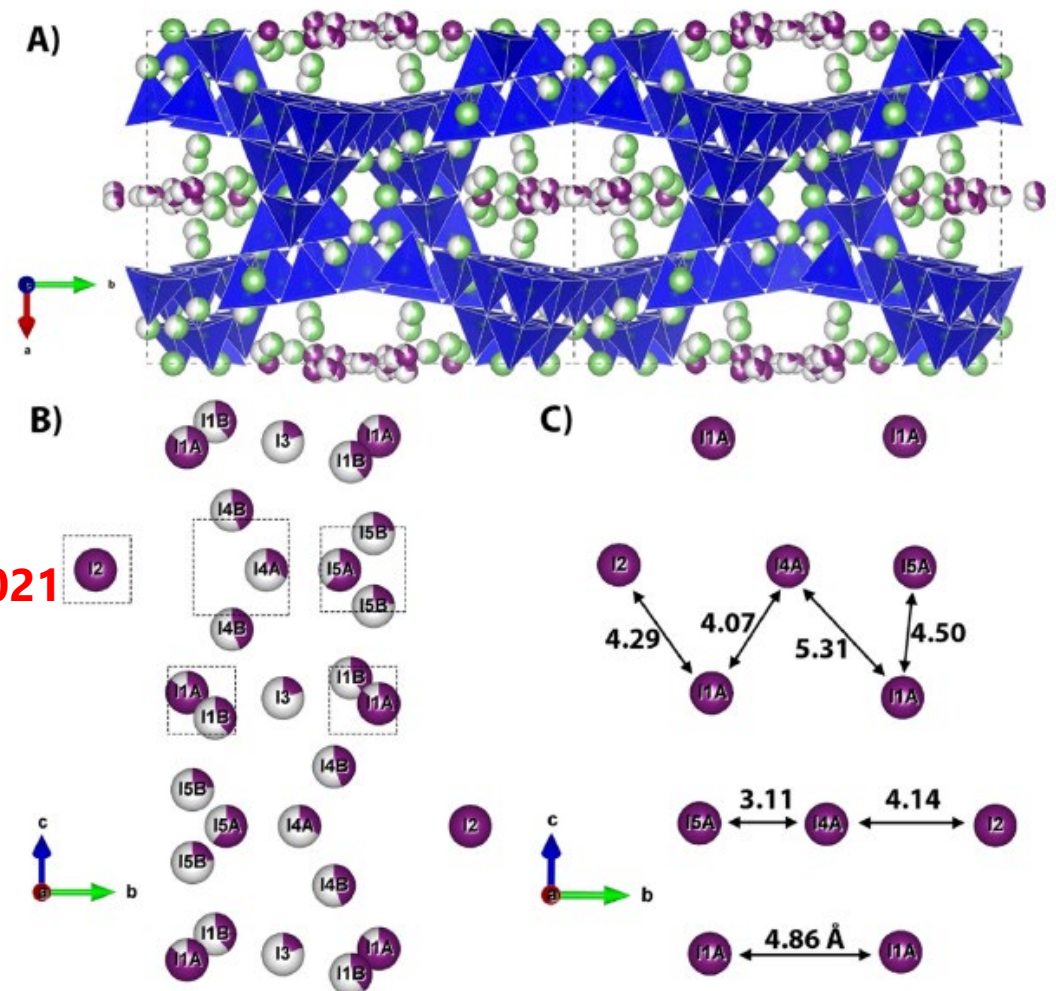


**Figure 3.** A)  $\text{Li}_{7.5}\text{B}_{10}\text{S}_{18}\text{I}_{1.5}$  structure with lithium and iodine in the channels. B) Average structure (refined from NPD at 300 K) and C) local structure (refined from NPDF at 290 K) of iodine in the tunnels. The iodide ions distributed through the channel are positioned in groups, as indicated by the dashed boxes in (B).

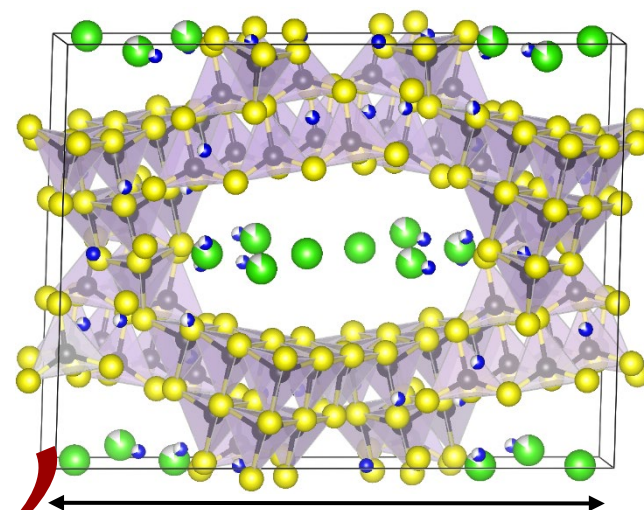
## Similarities –

- Same atomic elements
- B-S framework + large voids for Li and Cl
- Favorable Li ion conductivity

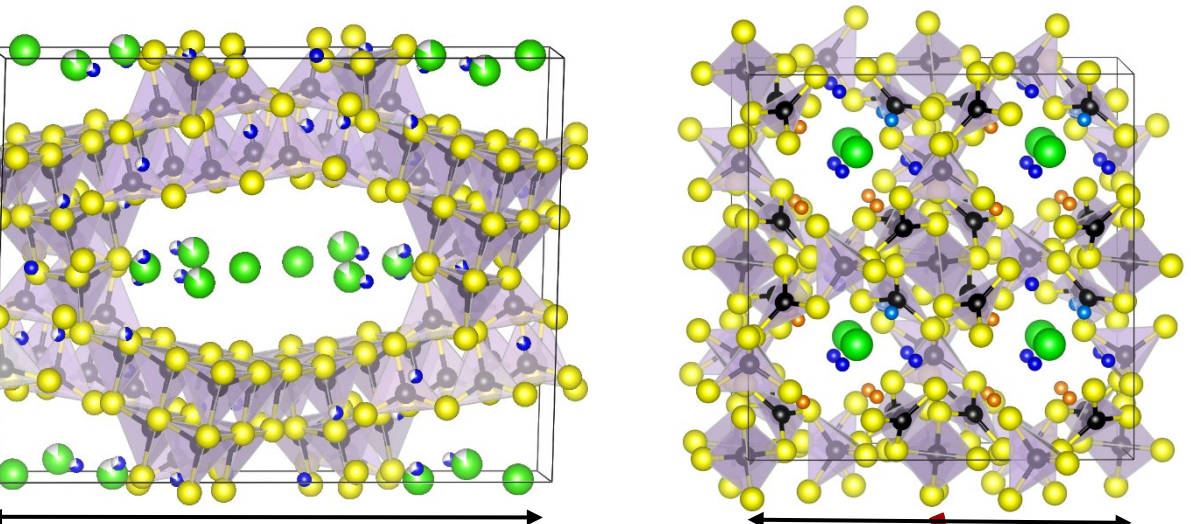
## Differences –



- Experimentally realized; chemically stable
- Framework based on  $\text{BS}_4$  tetrahedra
- Low symmetry structure (monoclinic)
- Large voids without obvious structure
- 148 ions in MD simulation cell (primitive C2/c lattice)



$$b = 21.2 \text{ \AA} > a > c$$



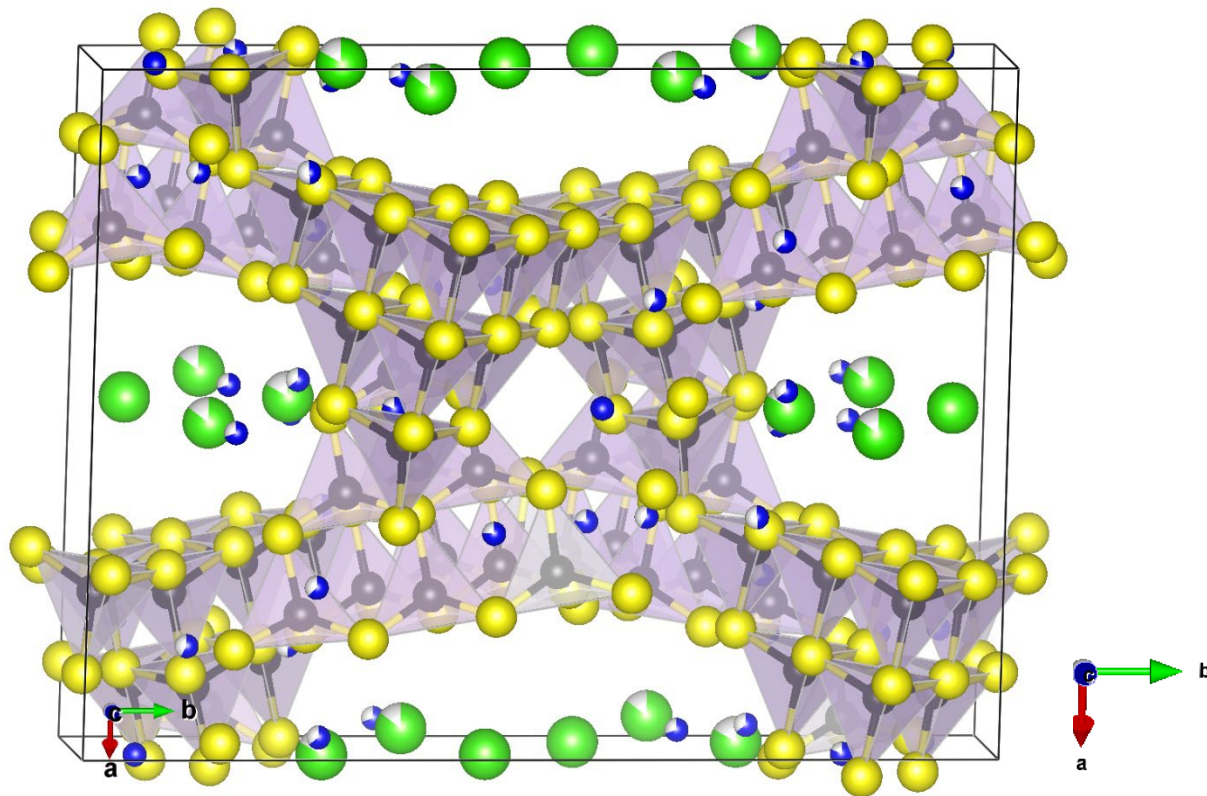
$$a = b = c = 14.9 \text{ \AA}$$

- Not (yet) experimentally realized; chemical reactivity
- Framework based on  $\text{BS}_4 + \text{BS}_3$  units
- Based on ordered rhombohedral structure
- Structured voids
- 196 ions in MD simulation cell (similar to conventional FCC lattice)

## From experiment

$\text{Li}_{7.5}\text{B}_{10}\text{S}_{18}\text{Cl}_{1.5}$  from Kaup *et al.* (2021)

Monoclinic C2/c (No. 15)

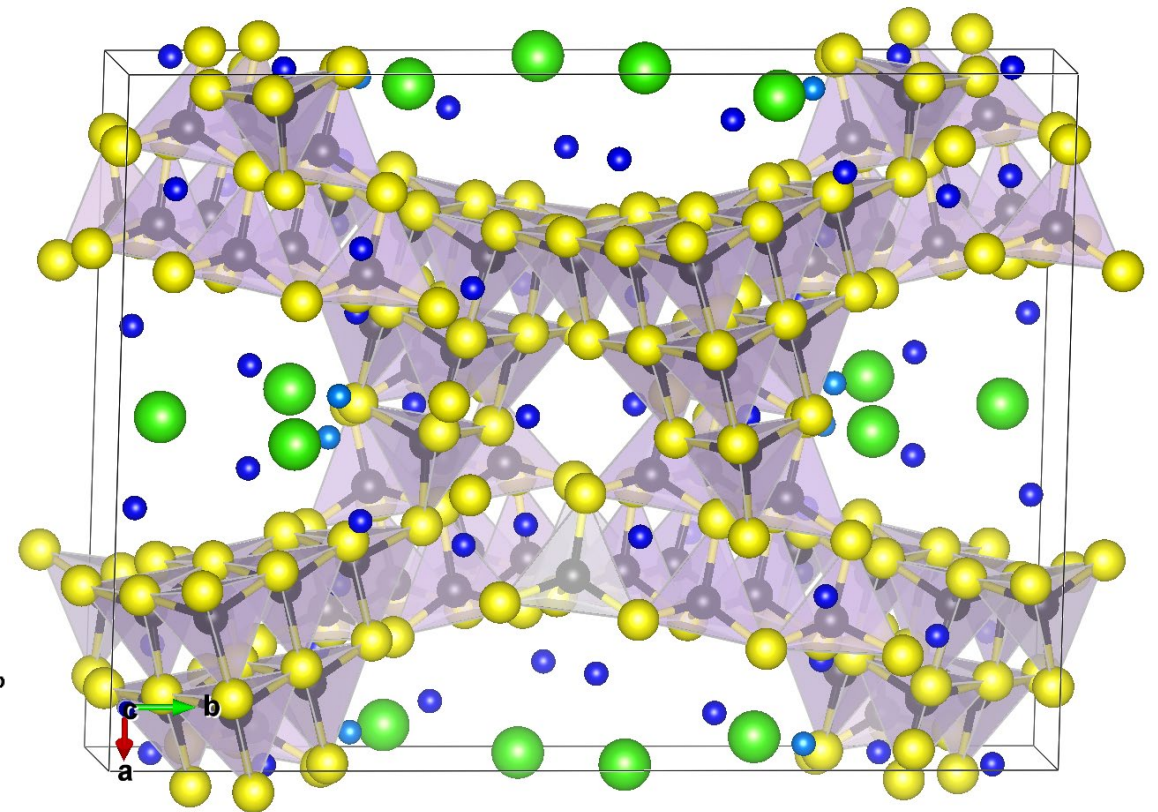


Some Li ions are missing

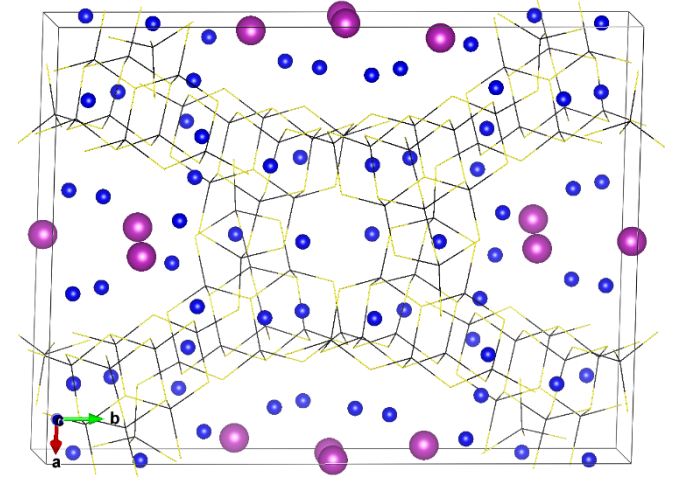
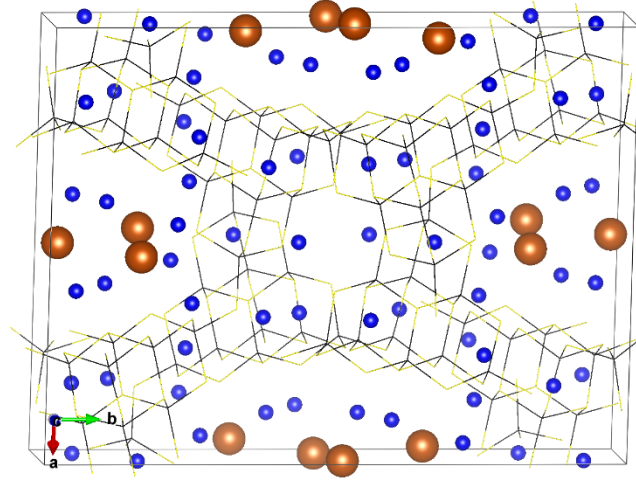
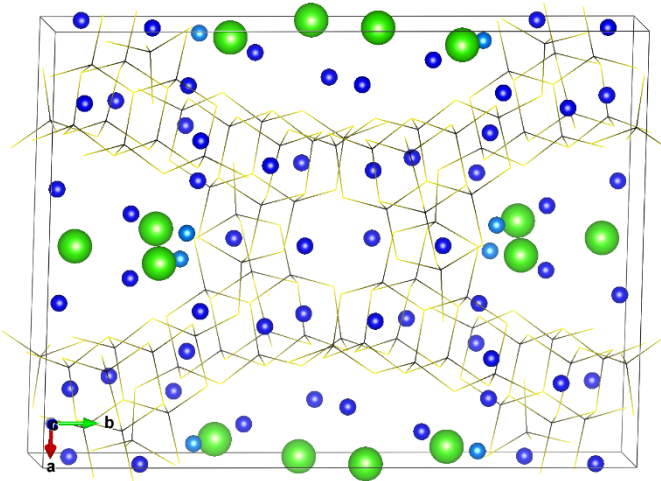
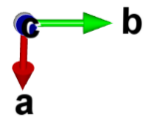
## From computation

$\text{Li}_{7.5}\text{B}_{10}\text{S}_{18}\text{Cl}_{1.5}$  from DFT optimization

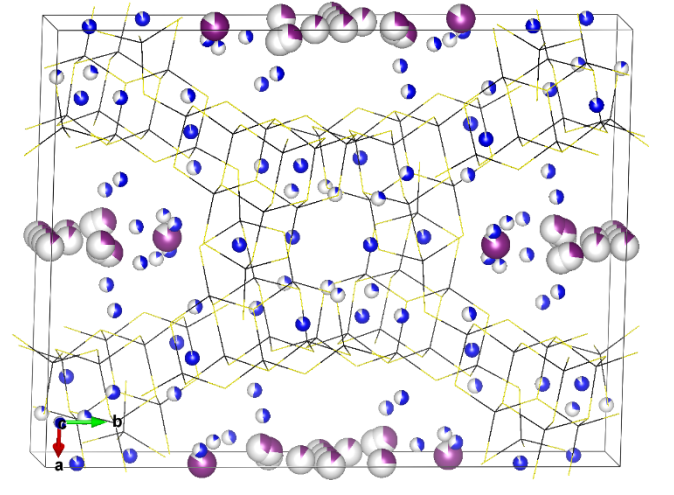
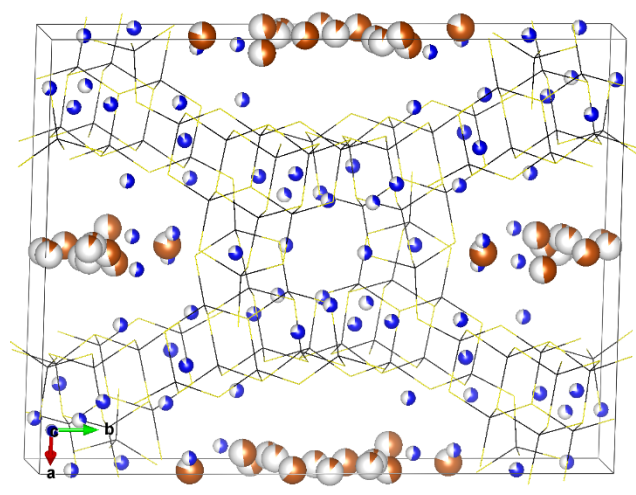
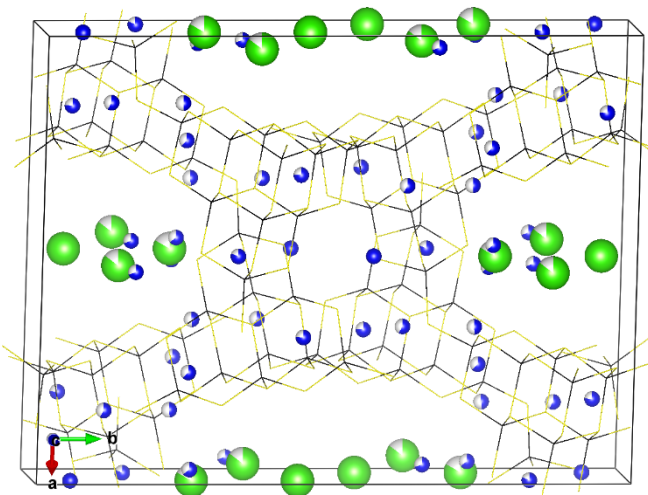
Monoclinic C2/c (No. 15)



From calc →  
DFT opt  
(at 0 K)



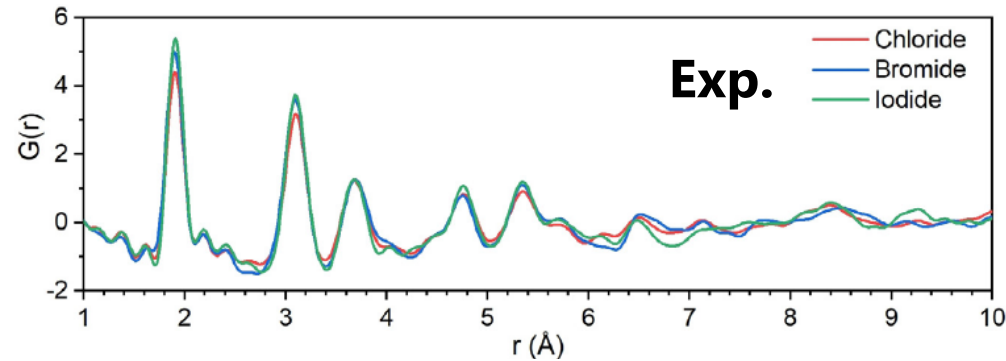
From exp →  
(at 300 K)



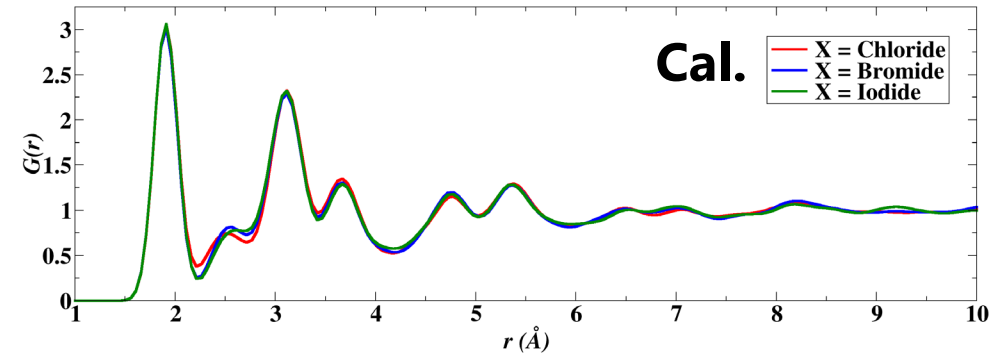
**Numerical comparison of conventional lattice parameters of optimized (“cal”) and experimental (Kaup *et al.*)**  
 $\text{Li}_{7.5}\text{B}_{10}\text{S}_{18}\text{X}_{1.5}$  (X=Cl, Br, I).

	X = Cl (cal. /exp.)	X = Br (cal. /exp.)	X = I (cal. /exp.)
a (Å)	20.96/21.16	20.88/21.21	21.09/21.32
b (Å)	21.66/22.23	21.19/21.25	21.40/21.27
c (Å)	16.02/16.13	16.07/16.26	16.08/16.21
$\alpha = \gamma$ (deg)	90.00/90.00	90.00/90.00	90.00/90.00
B (deg)	128.75/128.92	128.43/128.82	128.70/128.77
Volume (Å <sup>3</sup> )	5672.62/5638.31	5572.37/5708.07	5664.13/5731.36

**Pair distribution analysis: From neutron scattering (Kaup *et al.*)** →

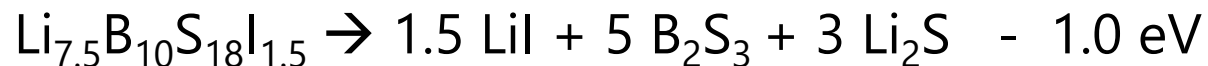
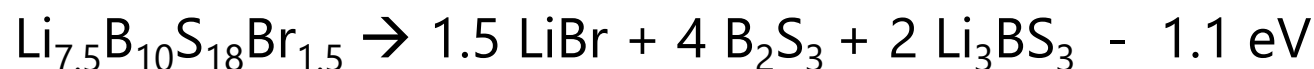
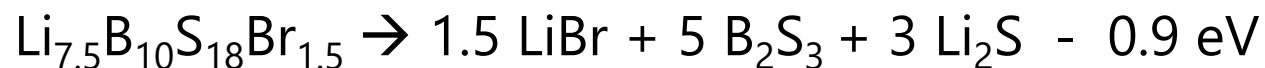
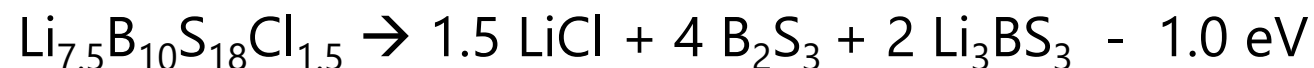
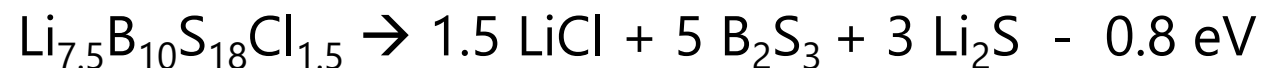


**From molecular dynamics simulations (This work at 400 K over 30 ps)** →





**Based on DFT static lattice calculations, several decomposition pathways indicate endothermic reactions at equilibrium and suggest chemical stability of  $\text{Li}_{7.5}\text{B}_{10}\text{S}_{18}\text{X}_{1.5}$**





Define a probability density\* for the mobile ions

$$p^a(\mathbf{r}) = \frac{1}{k_{\max}} \sum_{k=1}^{k_{\max}} \sum_{i \in a}^{N^a} \delta(\mathbf{r} - \mathbf{R}_i^a(t_k))$$

$N^a$  -- Number of ions of type  $a$  within the simulation cell

$\mathbf{R}_i^a(t_k)$  -- Trajectories of ion  $i$  at sampling time  $t_k$

$k_{\max}$  -- Number of time steps

In practice, the Gaussian shape

$$\delta(\mathbf{s}) \approx \frac{1}{(2\pi\sigma^2)^{3/2}} e^{-s^2/2\sigma^2} \quad \text{with } \sigma \text{ chosen as } 0.2 \text{ \AA}$$

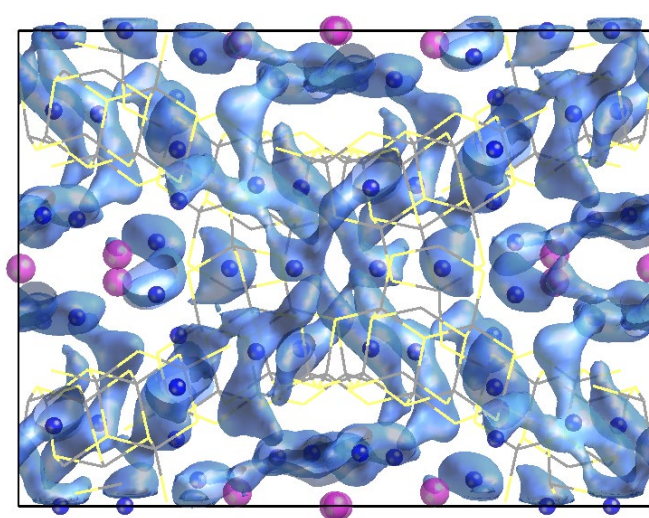
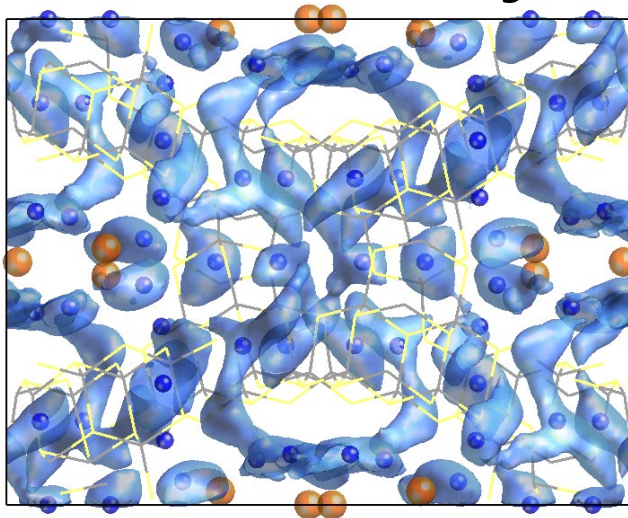
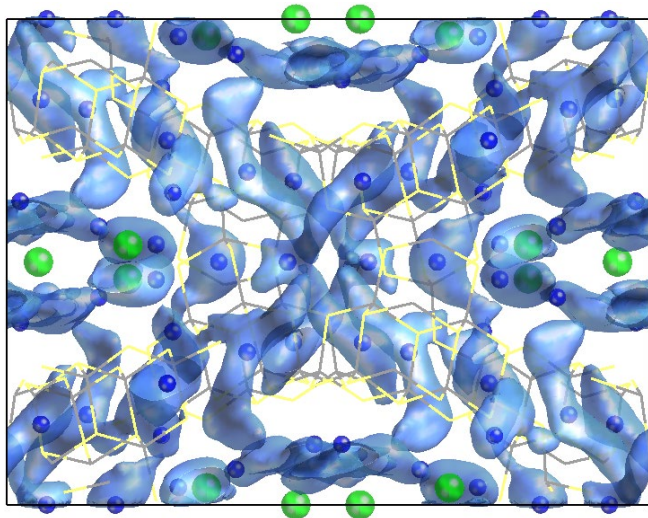
\*He, Zhu, and Mo, *Nat. Comm.* **8**, 15893 (2017)



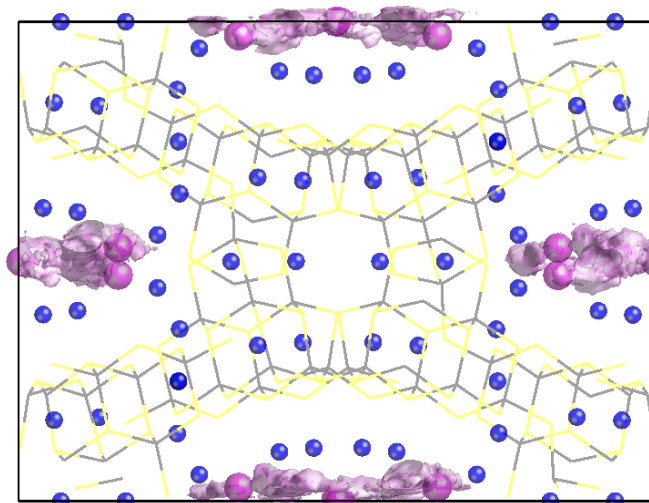
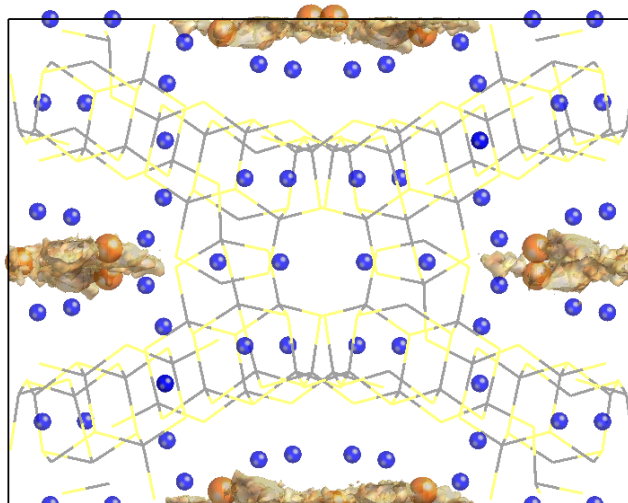
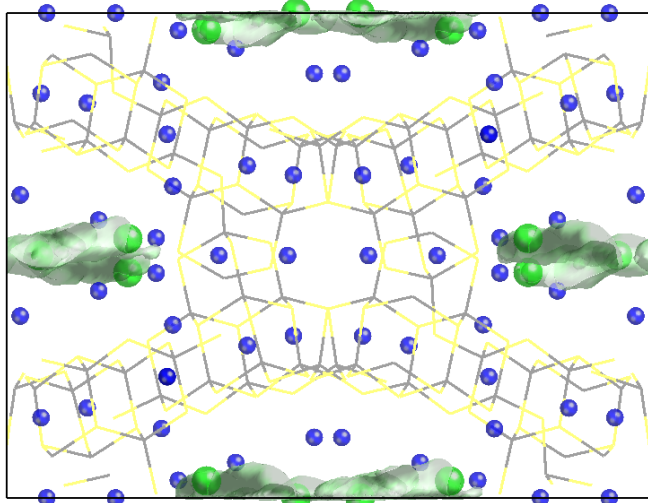
# Isosurface plots of $P^a(r)$

\*Visualized along the c-axis from MD simulations at ~800 K

$P^{Li}(r)$  →



$P^X(r)$  →



For an MD simulation at average temperature  $T$  :

$$\text{MSD}(\tau, T) = \frac{1}{N^{\text{Li}}} \left\langle \sum_{i=1}^{N^{\text{Li}}} \left| \mathbf{R}_i^{\text{Li}}(t + \tau) - \mathbf{R}_i^{\text{Li}}(t) \right|^2 \right\rangle_t$$

which is related to the tracer diffusion:

$$D_{tr}(T) = \lim_{\tau \rightarrow \infty} \left( \frac{1}{6\tau} \text{MSD}(\tau, T) \right). \text{ The Nernst-}$$

Einstein relation then leads to an estimate of

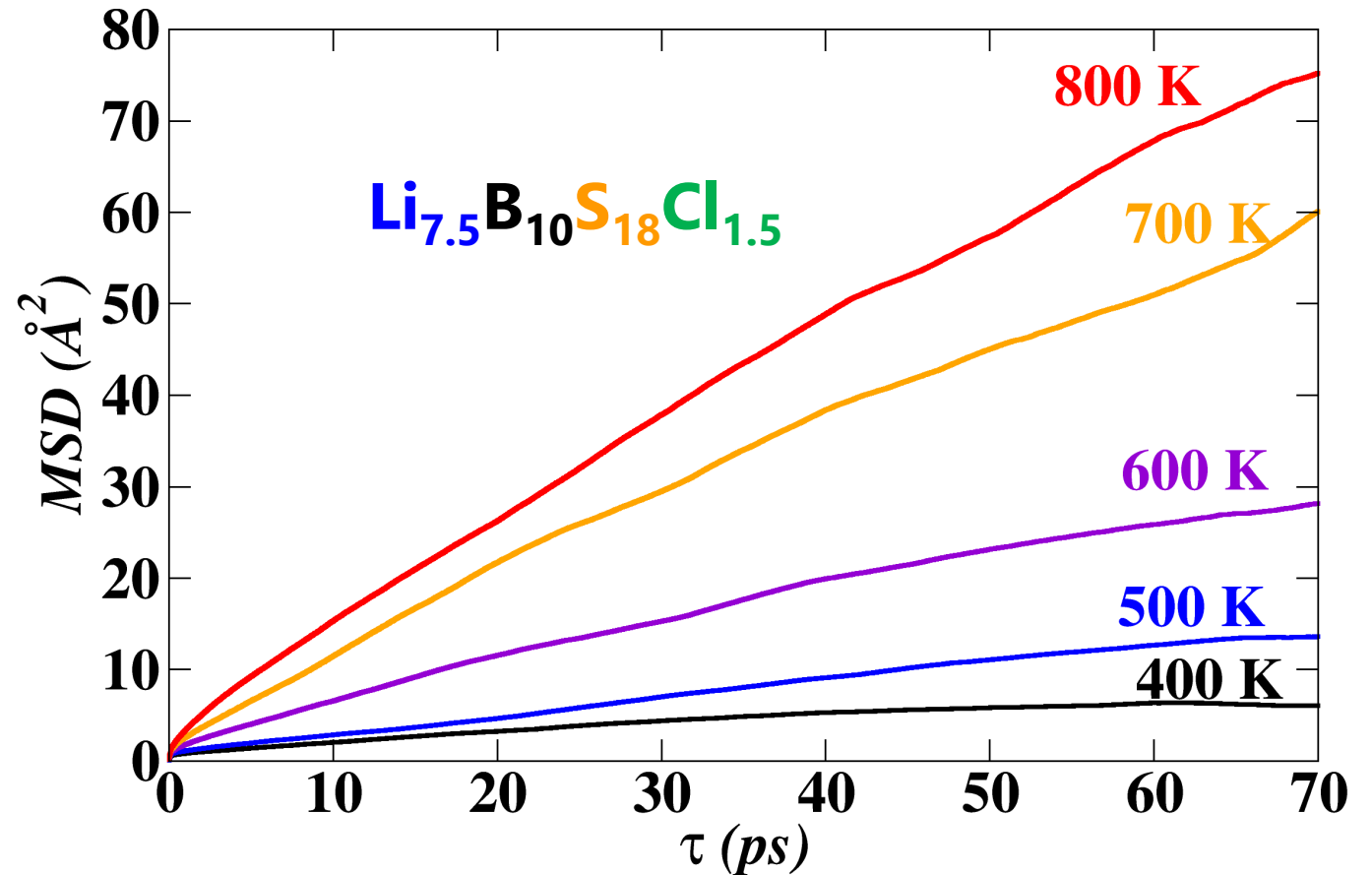
$$\text{the ionic conductivity: } \sigma(T) = \frac{N^{\text{Li}}}{V} \frac{e^2 D_{tr}(T)}{k_B T H_r},$$

where  $V$  = volume,  $k_B$  = Boltzmann constant,

$e$  = elementary charge,  $H_r$  = Haven ratio. It is

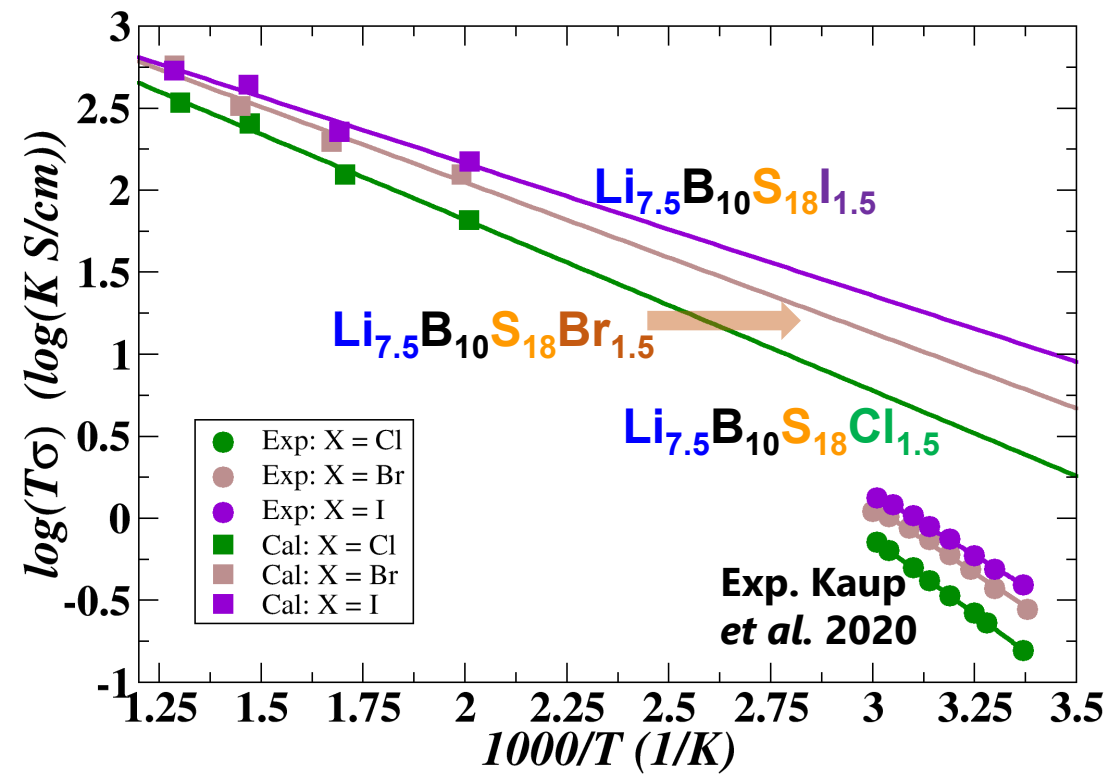
also reasonable to assume an Arrhenius behavior for the tracer diffusion with activation energy  $E_a$  :

$$D_{tr}(T) = D_{ref} e^{-E_a/k_B T}.$$

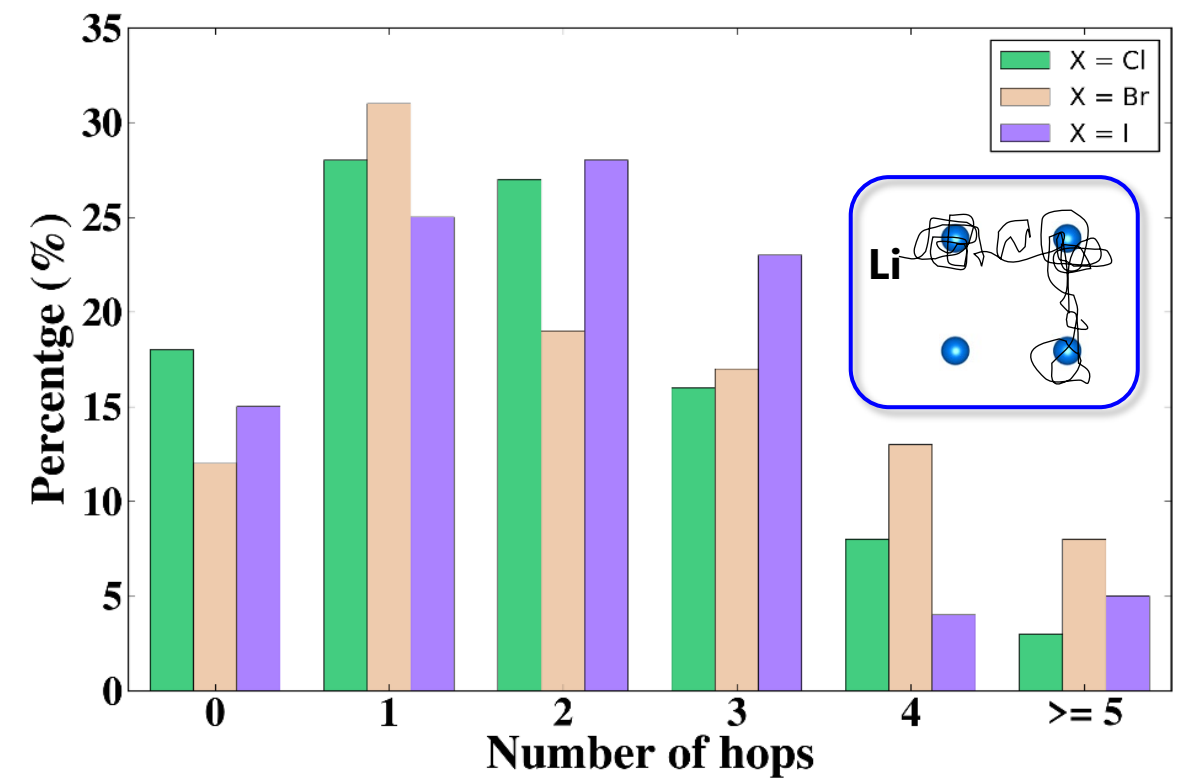


$$\sigma(T) = \frac{N^{\text{Li}}}{V} \frac{e^2 D_{tr}(T)}{k_B T H_r}$$

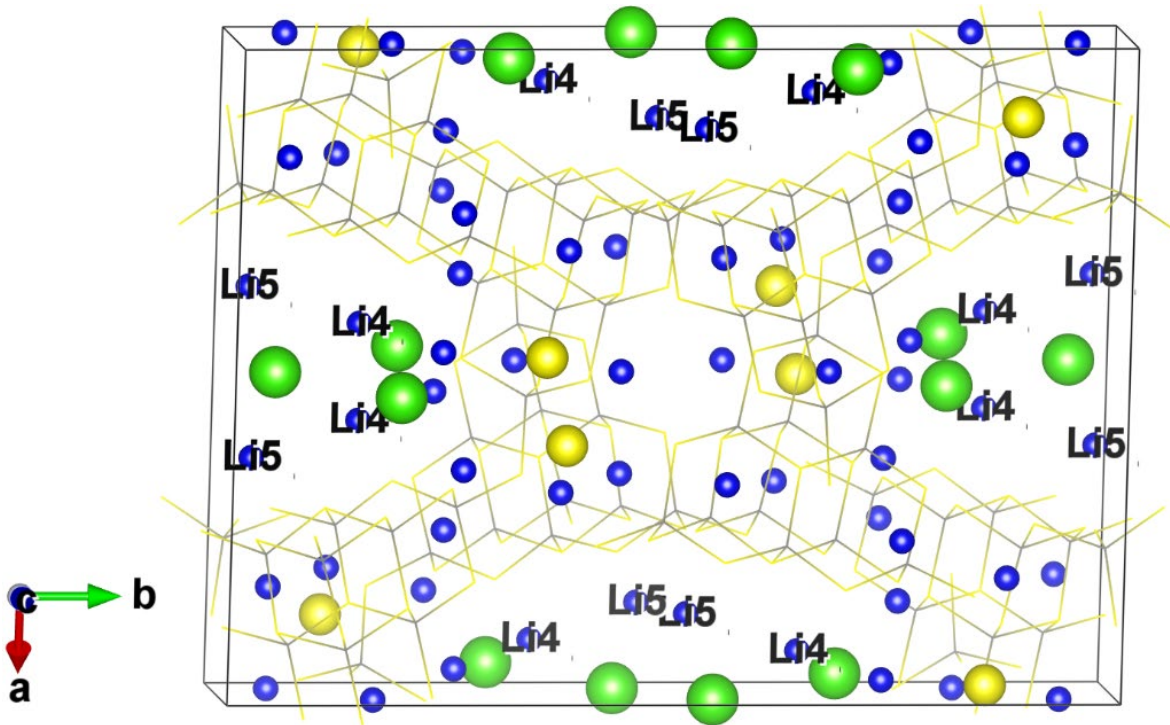
Evaluated for  $H_r = \frac{D_{tr}}{D_{tr} + D_{cross}} = 1$



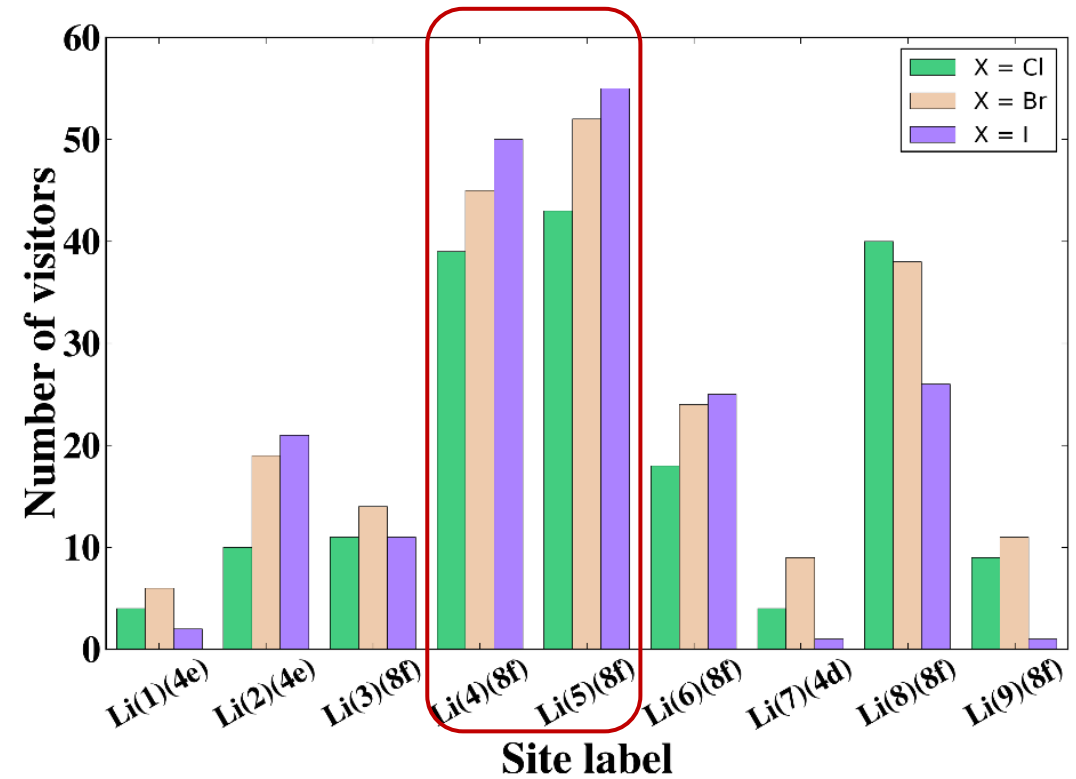
**Histogram of numbers of Li ion hops within 100 time intervals of 0.5 ps each at ~800 K**



Each hopping event was assessed on the basis of the equilibrium sites of the optimized lattice. A hopping event was tabulated at each arrival time of an ion at a new site.



Visualization of active Li sites for  
 $\text{Li}_{7.5}\text{B}_{10}\text{S}_{18}\text{X}_{1.5}$  (X = Cl, Br, I)



Number of visitors of each distinct Li site  
 evaluated from MD simulation trajectories at 800 K

- ❑ Computationally determined plausible idealized structures for the  $\text{Li}_{7.5}\text{B}_{10}\text{S}_{18}\text{X}_{1.5}$  ( $\text{X} = \text{Cl}, \text{Br}, \text{I}$ ) materials developed by Kaup *et al.* (2021), consistent with published X-ray and neutron diffraction analyses.
- ❑ Computed equilibrium total energies suggest chemical stability against decomposition.
- ❑ MD simulations show remarkable 3-dimensional Li ion mobility within the  $\text{B}_{10}\text{S}_{18}$  framework at temperatures close to 400 K and higher.
- ❑ Preliminary analysis of detailed MD trajectories suggests concerted mechanisms for the Li ion motions primarily within the void cavities.

**Manuscript in preparation**

**Details: WFU Physics colloquium on Nov. 4, 2021 from 4:00 pm - 5:00 pm ESD**

1. **Y. Li** and N. A. W. Holzwarth, First principles simulations to understand the structural and electrolyte properties of idealized  $\text{Li}_{7.5}\text{B}_{10}\text{S}_{18}\text{X}_{1.5}$  ( $\text{X} = \text{Cl}, \text{Br}, \text{I}$ ), in preparation.
2. D. Lynch, **Y. Li (co-first)**, and N. A. W. Holzwarth, Computational investigation of the structural and electrolyte properties of the boracite materials related to  $\text{Li}_4\text{B}_7\text{O}_{12}\text{Cl}$ , in preparation.
3. **Y. Li** and N. A. W. Holzwarth, First principles simulations of Li boracites  $\text{Li}_4\text{B}_7\text{O}_{12}\text{Cl}$  and  $\text{Li}_5\text{B}_7\text{O}_{12.5}\text{Cl}$ , to be submitted.
4. **Y. Li**, Z. D. Hood, and N. A. W. Holzwarth, Computational study of  $\text{Li}_3\text{BO}_3$  and  $\text{Li}_3\text{BN}_2$  I: Electrolyte properties of pure and doped crystals, *Physical Review Materials* **5**, 085402 (2021). DOI: <https://doi.org/10.1103/PhysRevMaterials.5.085402>
5. **Y. Li**, Z. D. Hood, and N. A. W. Holzwarth, Computational study of  $\text{Li}_3\text{BO}_3$  and  $\text{Li}_3\text{BN}_2$  II: Stability analysis of pure phases and of model interfaces with Li anodes, *Physical Review Materials* **5**, 085403 (2021). DOI: <https://doi.org/10.1103/PhysRevMaterials.5.085403>
6. **Y. Li**, Z. D. Hood, and N. A. W. Holzwarth, Computational (Re)investigation of the Structural and Electrolyte Properties of  $\text{Li}_4\text{P}_2\text{S}_6$ ,  $\text{Na}_4\text{P}_2\text{S}_6$ , and  $\text{Li}_2\text{Na}_2\text{P}_2\text{S}_6$ , *Physical Review Materials* **4**, 045406 (2020). DOI: <https://doi.org/10.1103/PhysRevMaterials.4.045406>
7. **Y. Li**, W. C. Kerr, and N. A. W. Holzwarth, Continuity of phonon dispersion curves in layered ionic materials, *Journal of Physics: Condensed Matter* **32**, 055402 (2020). DOI: <https://doi.org/10.1088/1361-648X/ab4cc1>



## <http://users.wfu.edu/natalie/recentpubs.html>

### [Link to Google Scholar Profile](#)

[Computational study of  \$\text{Li}\_3\text{BO}\_3\$  and  \$\text{Li}\_3\text{BN}\_2\$ : I: Electrolyte properties of pure and doped crystals and II: Stability analysis of pure phases and of model interfaces with Li anodes](#)

Yan Li, Zachary D. Hood, and N.A.W. Holzwarth

[Physical Review Materials](#) **5**, 085402 (2021)(I) and [Physical Review Materials](#) **5**, 085403 (2021)(II) Local copies: [I](#) and [II](#)

["Computational and experimental \(re\)investigation of the structural and electrolyte properties of  \$\text{Li}\_4\text{P}\_2\text{S}\_6\$ ,  \$\text{Na}\_4\text{P}\_2\text{S}\_6\$ , and  \$\text{Li}\_2\text{Na}\_2\text{P}\_2\text{S}\_6\$ "](#)

Yan Li, Zachary D. Hood, and N.A.W. Holzwarth

[Physical Review Materials](#) **4**, 045406 (2020) [Local copy](#)

["Continuity of phonon dispersion curves in layered ionic materials "](#)

Yan Li, W. C. Kerr, and N. A. W. Holzwarth

[Journal of Physics: Condensed Matter](#) **32** 055402 (2019) [\(local copy\)](#)

["Updated comments on projector augmented wave \(PAW\) implementations within various electronic structure code packages"](#)

N. A. W. Holzwarth

[Computer Physics Communications](#) **234** 25-29 (2019) <https://doi.org/10.1016/j.cpc.2019.05.009> [\(local copy\)](#)

## <http://users.wfu.edu/natalie/presentations.html>

- Presentation by Yan Li at the [240th ECS Meeting](#), Oct 10-14, 2021 -- ["Computational Investigation of Li Boracite  \$\text{Li}\_4\text{B}\_7\text{O}\_{12}\text{Cl}\$  and Related Materials as Solid Electrolytes "](#) ([link to abstract](#))
- Presentation by N. A. W. Holzwarth at the [240th ECS Meeting](#), Oct 10-14, 2021 -- ["First Principles Simulations to Understand the Structural and Electrolyte Properties of Idealized  \$\text{Li}\_{7.5}\text{B}\_{10}\text{S}\_{18}\text{X}\_{1.5}\$  \(X = Cl, Br, I\) -- Li Superionic Conductors Recently Identified in the Experimental Literature."](#) ([link to abstract](#))
- Presentation by N. A. W. Holzwarth at the Electronic Structure Discussion Group at Cambridge University invited by WFU alum Angela Harper -- June 9, 2021 -- [First principles simulations of electrolyte materials with a view toward all solid-state battery technology --  \$\text{Li}\_4\text{P}\_2\text{S}\_6\$ ,  \$\text{Na}\_4\text{P}\_2\text{S}\_6\$ , and possible alloys](#)
- Presentation by N. A. W. Holzwarth at the [10<sup>th</sup> ABINIT International Developer Workshop](#) May 31-June 4, 2021 -- [Progress on self-consistent meta-gga PAW datasets from ATOMPAW](#) ([PP slides](#))
- Presentation by Yan Li at the [March 2021 APS meeting](#) -- [" \$\text{Li}\_3\text{BO}\_3\$  and  \$\text{Li}\_3\text{BN}\_2\$ : Computational study of structural and electrolyte properties of pure and doped crystals"](#) ([link to abstract](#))
- Annotated slides that would have been presented by Yan Li at the cancelled March 2020 APS meeting -- ["Prediction and analysis of a sodium ion electrolyte:  \$\text{Li}\_2\text{Na}\_2\text{P}\_2\text{S}\_6\$ "](#)



Photo taken with → Dr. Hood and Prof. Holzwarth  
at ECS meeting in Atlanta, GA in Oct. 2019



## Advisor:

Prof. Natalie A. W. Holzwarth

## Dissertation committee:

Prof. Abdessadek Lachgar, Prof. William C. Kerr

Dr. Oana Jurchescu, Dr. Timo Thonhauser

## Experimental collaborator:

Dr. Zachary D. Hood (Argonne National Laboratory)

## Former and current graduate students:

Jason Howard, Ahmad Al-Qawasmeh, Cory Lynch

## DEAC team:

Adam Carlson, Cody Stevens, Sean Anderson

## WFU physics community:

Students, faculty, and staff

## Folks in China:

Family, friends, and CUMT physics



**Thank you for your attending!**



Google image